Methylglyoxal content in Southern African Honey: Antibacterial and Cellular Effects

Erika Rabie

UNIVERSITEIT VAN PRETORIA
UNIVERSITY OF PRETORIA
YUNIBESITHI YA PRETORIA

Methylglyoxal content in Southern African Honey: Antibacterial and Cellular Effects

by

Erika Rabie

Submitted in fulfilment of the requirement for the degree

Master of Science

in the

Faculty of Health Science

Department of Anatomy

University of Pretoria

2015

UNIVERSITEIT VAN PRETORIA
UNIVERSITY OF PRETORIA
YUNIBESITHI YA PRETORIA

Methylglyoxal content in Southern African Honey: Antibacterial and Cellular Effects

By

Erika Rabie

Supervisor: Prof. MJ Bester

Co-supervisor: Ms. J Serem

Department: Anatomy

Degree: MSc Cell Biology

Abstract

The clinical benefits of honey based wound dressings have been established. Methylglyoxal (MGO) containing honey, such as Manuka honey does have numerous beneficial effects, however, concern has been expressed related to the safety of this honey in patients with diabetes. In addition Manuka honey is unique to New Zealand and its use in South Africa is limited due to the cost of importation. Southern Africa has a well described floral biodiversity and the possibility exists that an indigenous honey type with similar or greater wound healing properties than Manuka honey can be found.

The aims of this study were to develop a rapid and inexpensive colorimetric method for the quantification MGO in southern Africa honey. Secondly to evaluate the antibacterial and cellular effects of MGO *in vitro* and to determine whether MGO levels that effectively kills bacteria is cytotoxic to several cell lines. The MGO levels as found in southern Africa honey will be extrapolated to the findings of this study related to the antibacterial activity and cellular effects.

Using a newly developed colorimetric method for the quantification of MGO, MGO levels in a selection of southern Africa honey was found to be from 692.59 – 1261.23 mM MGO which is slightly higher than that found in UMF15 honey.

It was determined that MGO had antibacterial effects on both Gram positive and negative bacteria. The IC_{50} range of MGO on *B. subtilis* and *P. aeruginosa* (Gram positive) was between 0.2 – 0.4 mM MGO and its MIC was at 0.4 – 1.2 mM. For *S. aureus* and *E. coli* (Gram negative) the IC_{50} range was from 0.2 – 1.0 mM MGO and the MIC was at 0.8 – 1.2 mM MGO. With scanning electron microscopy (SEM) it was observed that MGO prevented the formation of fimbriae and flagellae and at higher concentrations caused lysis.

Three cell lines were exposed to 0.0003 – 324.7294 mM MGO for 48 hours. A hormetic effect was observed for all cell lines from a MGO concentration of 0.0003 – 3.2473 mM while at concentrations >32.473 mM toxicity was observed. At the bacterial MIC concentrations from 0.4 – 1.2 mM a hormetic effect was observed in RAW 264.7 mouse macrophages and Caco-2 colon carcinoma cells while the SC-1 fibroblast cell line exhibited normal growth. The MGO levels found in southern Africa honey was generally not cytotoxic.

With SEM morphological changes were only observed at 324.7294 mM. At this concentration the RAW 264.7 mouse macrophages showed signs of activation and differentiation. The Caco-2 cells became more compacted and spheroid in shape while the

SC-1 cells were more spindle-shaped and grew extensions and filopodia at higher concentrations and several large cells, probably myofibroblasts, were observed.

In conclusion at the concentration range where MGO was found to effectively kill Gram positive and negative bacteria, MGO was not cytotoxic to cells *in vitro*. Southern Africa honey contains MGO and levels were generally not cytotoxic. In an endeavour to develop local honey based wound healing products the findings of this study provide important preliminary information on the MGO levels in southern Africa honey. The antibacterial activity of MGO was confirmed and this is the first study to describe the hormetic effects of MGO in several cell lines.

Declaration

I, Erika Rabie, declare that the dissertation, which I hereby submit for the degree MSc Cell Biology at the University of Pretoria, is my own work and has not previously been submitted by me for a degree at this or any other tertiary institution.

Signed:

Date:

Department of Anatomy, School of Medicine, Faculty of Health Science, University of Pretoria

South Africa

Acknowledgements

I would like to thank the following people for their contribution throughout this journey:

To my supervisor, Prof. Bester, thank you for being so supportive and encouraging. You taught me how to approach this project; you were patient with me and always willing to help or give advice when I needed it or when I was having trouble. Also, thank you for helping me with the writing and making sure everything was in the correct order and made sense. Your incredible knowledge and experience has taught me so much.

To my co-supervisor, June Serem, thank you for teaching me about cell and bacteria cultures, and for your wiliness to help me and spend time with me in the lab in order to resolve problems. Thank you for always making sure I understood the assays I did throughout this project and also for reading through this thesis to help to make sure every comma, space and full stop was in its proper place. What a tedious job it must have been.

Helena Taute and Chantelle Venter; I really appreciate you taking the time to teach me how to do electron microscopy and for always being willing to answer my questions or show me how something is done.

The microscopy unit on main campus thank you for the use of your facilities and allowing me the opportunity to learn how to use the SEM.

My parents; Mom, dad, without your support, both financial and emotional, this project would not have been possible. Thank you for being supportive of my decision to do this. You made it possible for me to better myself. Thank you from the bottom of my heart.

My family, friends and colleagues, without you doing my Masters would have been incredibly dull and boring. You showed interest in my project and brightened up my days. Thank you for smiles and conversation in the lab, weekends to relax and for just being there when I needed encouragement.

Without all these people this project would never have been possible and despite some frustrations and stressful times, at the end of it all I can truly say that this was a positive experience.

Table of Contents

List of Tables

List of Figures

indicate the flagella; thick white arrows indicate the fimbriae and the green arrow in D indicates a hole in the cell; green arrow in B shows a pilus.

Figure 4.4: SEM micrographs of *E. coli* exposed to increasing concentrations of MGO. (**A**) Control; (**B**) 0.5 mM MGO; (**C**) 1.0 mM MGO; (**D**) 2.0 mM MGO. Thin white arrows indicate the flagella; thick white arrows indicate the fimbriae; green arrow in B shows a pilus.

Figure 5.1: RAW 264.7 cells exposed to increasing concentrations of MGO showing (A) CV assay indicating percent growth and (B) MTT indicating percent viability after 48 h exposure measuered as a percentage of a control with no MGO added. Data is an average of four (MTT assay) and five (CV assay) experiments ± SEM. Means with stars are significantly different, p≤0.005. Bar indicates the MIC range for all bacteria in chapter 4, section 4.4.1.

Figure 5.2: Light microscope images at x4 magnification of RAW 264.7 cells showing differences in cell number using CV staining. (A): Control. (B – H): cells exposed to increasing concentrations of MGO.

Figure 5.3: Summary showing the ratio between cell viability : cell number for RAW 246.7 cells exposed to increasing concentrations of MGO where 1±0.1 indicates normal growth, > 1.1 indicates hormesis and < 0.9 indicates toxicity. Bar indicates the MIC range for all bacteria in Chapter 4, Section 4.4.1.

Figure 5.4: SEM images of RAW 264.7 cells exposed to 3 different MGO concentrations. A: Control group with no MGO added. B: Low MGO concentration (0.000325 mM) showing similar surface formation to that of the control (A). C: Medium MGO concentration (0.324729 mM) showing similar surface formation to that of the control (A). D: High MGO concentration (324.7294 mM) showing pseudopodia and surface ruffels.

Figure 5.5: Caco-2 cells exposed to incresing concentrations of MGO showing (A) CV assay indicating percent growth and (B) MTT indicating percent viability after 48 h exposure measuered as a percentage of a control with no MGO added.Data is an average of four (MTT assay) and four (CV assay) experiments ± SEM. Means with stars are significantly different, p≤0.005. Bar indicates the MIC range for all bacteria in chapter 4, section 4.4.1.

Figure 5.6: Light microscope images at x4 magnification showing differences in cell number and increase in colonies Caco-2 cells. (A): Control with no MGO and (B – H) exposed to increasing concentrations of MGO. Arrows indicate colonies.

Figure 5.7: The ratio between cell viability and cell number for Caco-2 cells exposed to increasing concentrations of MGO where 1±0.1 indicates normal growth, > 1.1 indicates hormesis and < 0.9 indicates toxicity. Bar indicates the MIC range for all bacteria in chapter 4, Section 4.4.1.

Figure 5.8: SEM images of Caco-2 cells exposed to 3 different MGO concentrations. A: Control group with no MGO added. B: Low MGO concentration (0.0003 mM) showing blebbing on the cell's surface C: Medium MGO concentration (0.3247 mM) showing multiple nuclei and some blebbing on the cell surface. D: High MGO concentration (324.7294 mM) showing multiple compact cells with extensions.

Figure 5.9: SC-1 cells exposed to incresing concnetrations of MGO showing (A) CV assay indicating percent growth and (B) MTT indicating percent viability after 48 h exposure measuered as a percentage of a control with no MGO added. Data is an average of four (MTT assay) and four (CV assay) experiments ± SEM. Means with stars are significantly different, p≤0.005. Bar indicates the MIC range for all bacteria in chapter 4, Section 4.4.1.

List of abbreviations

α	Alpha
β	Beta
°C	Degrees Celcius
%	Percent
µl	Microliter
µM	Micromolar

A

A549	Adult *Homo sapiens* (human) epithelial lung carcinoma
AGE	Advanced glycation end product
Atk1	Alpha serine/threonine-protein kinase 1
Arg	Argenine

B

BC	Before Christ
BGum	Blue Gum honey

C

Ca^{2+}	Calcium ion
Caco-2	Adult *Homo sapiens* (human) epithelial colorectal adenocarcenoma
$C_2H_2O_2$	Glyoxal
$C_3H_4O_2$	Methylglyoxal
$C_5H_9NO_2S$	N-acetylcysteine
$C_{10}H_{17}N_3O_6S$	Gluthathione
$C_{14}H_8N_2O_8S_2$	5,5-Dithiobis-2-nitrobenzoic acid
cm	Centimeter
CO_2	Carbon dioxide
CRS	Chronic Rhinosinitis
CSC	Cancer stem cells
Cys	Cystine
CV	Crystal Violet

D

DC	Dendritic cells
ddH_2O	Double distilled de-ionized water
$dddH_2O$	Triple distilled de-ionized water
3-DG	3-Deoxyglucosone
DHA	Dihydroxyacetone

DMEM	Dulbecco's Modified Essential Medium
DMSO	Dimethyl sulphoxide
DNA	Deoxyriboneucleic acid
DTNB	5,5-Dithiobis-2-nitrobenzoic acid
Dps12	DNA binding protein 12

E

ECM	Extra cellular matrix
EDTA	Ethylenediaminetetraacetic acid
EMEM	Eagles Minimum Essential Medium
ELISA	Enzyme-linked immunosorbent assay
EtOH	Ethanol

F

FB	Fynbos
FB4	Fynbos 4 honey
FB6	Fynbos 6 honey
FB15	Fynbos 15 honey
FB WW	Fynbos honey from Woolworths
FCS	Fetal calf serum

G

G_0	G zero growth phase
G_1	Growth phase 1
Glu	Glutamic acid
Gly	Glycine
GO	Glyoxal
GSH	Glutathione

H

h	Hour
H446	Adult *Homo sapiens* (human) epithelial lung carcinoma
HCl	Hydrogen chloride
HDMS	Hexamethyldisilazane
HMF	Hydroxymethylfurfural
H_2O	Water
H_2O_2	Hydrochloric acid
HPLC	High performance liquid chromatography
HT1080	Adult *Homo sapiens* (human) epithelial fibrosarcoma
HTA	Hemithioacetal

HaCaT	Adult *Homo sapiens* (human) skin keratinocytes

I

IC_{50}	Half maximal inhibitory concentration
IRS	Insulin receptor substrate

K

K^+	Potassium ion

L

LB	Luria Bertani
LPS	Lipopolysaccharide
Lys	Lysine

M

M	Molar
Man	Manuka
Mal	Malgas
Mal FB	Malgas Fynbos honey
MCF-7	Adult *Homo sapiens* (human) epithelial mammary adenocarcinoma
MG63	Adult *Homo sapiens* (human) fibroblastic osteosarcoma
MGO	Methylglyoxal
mg	Milligrams
mg/kg	Milligrams per kilogram
MIC	Minimum inhibitory concentration
Min	Minute
ml	Milliliter
mM	Millimolar
MozmSemb	South Eastern Mozambique honey
MTT	3-(4,5-Dimethylthiazol-2-yl)-2,5-diphenyltetrazolium bromide

N

NAC	N-acetylcysteine
NaCl	Sodium chloride
Na_2HPO_4	Disodium phosphate
$Na_2HPO_4 \cdot 2H_2O$	Sodium phosphate monobasic dihydrate
NaOH	Sodium hydroxide
NZ	New Zealand
NO	Nitric oxide
nm	Nanometer

O

OBloss	Orange Blossom honey
Oct-4	Octamer-binding transcription factor 4
OD	Optical density
OH	Hydroxide
OsO_4	Osmium tetroxide
OvFB	Overberg Fynbos honey

P

PBS	Phosphate-buffered saline
PC12	Adult *Rattusnorvegicus* (rat) adrenal gland pheochromocytoma
PDGF	Platelet derived growth factor
PI3-kinase	Phsophatidyl-ionstiol-3-OH kinase
pH	Measure of hydrogen ion concentration (acidity/alkalinity) of a solution

R

RAW 264.7	Adult *Musmusculus* (mouse) monocyte/macrophage cells
Raw Ac	Raw Acacia honey
RB	Rose benagal
RINm5F	Adult *Rattus norvegicus* (rat) insulin secreting cells
RivGum	Rivergum honey
RNA	Ribonucleic Acid
ROS	Reactive Oxygen Species
RKO	*Homo sapiens* (human) epithelial colon carcinoma
rpm	Revolutions per minute
RpoS	RNA polymerase, sigma S
RS	Revamil^{TM} source
RT4	Adult *Rattus norvegicus*, rat schwannoma

S

SA	South Africa
SC-1	Embryonic *Mus musculus* (mouse) fibroblast cell
SEM	Standard error of means
Sox2	Sex determining region Y (also known as SRY)
SpGum	Spidergum honey
S phase	Synthesis phase of cell cycle
SSI	Surgical site infection

T

TB	Tuberculosis

Thr	Threonine
TNB^{2-}	2-nitro-5-thiobenzoate anion
TRP	Transient receptor potential
TRPA1	Transient receptor potential cation channel member A1

U

UMF	Unique Manuka Factor
U87	*Homo sapiens* (human) epithelial brain glioblastoma/astrocytoma

V

Vs.	Versus
v/v	Volume/Volume

W

W6CH	Western Cape honey of unknown origin
WBloss	Wild Blossom honey
w/v	Weight/Volume

Chapter 1: Introduction

Honey is produced from plant nectar of certain plants by honeybees from the genus *Apis* and *Meliponinae*. The nectar itself consists of glucose, sucrose and fructose and as it is processed by bees enzymes such as invertase and glucose oxidase are also added. The invertase converts sucrose to glucose and fructose and the glucose oxidase oxidises glucose into glucuronic acid, which is responsible for the formation of the hydrogen peroxide (H_2O_2) present in honey (Pieper 2009). The water content of the honey is reduced by the heat of the hive and also from fanning by the bees. The end product is a hyperosmolar, hygroscopic sugar solution that consists of water, sucrose, fructose, glucose, amino acids, enzymes, minerals, wax, pollen and pigments (Pieper 2009; Stewart *et al.* 2014).

Honey has been used from as early as 1600 BC for treating wounds by soaking linen in a honey-oil solution and then applying it to the wound (Stewart *et al.* 2014). During the 19th century honey was popular as a medical product due to identified antibacterial properties. It fell out of favour with the discovery of antibiotics but regained popularity when it was discovered that certain types of honey are effective against antibiotic resistant bacteria (Stewart *et al.* 2014). Various wound healing products have since been produced from honey and these include gels, dressings and ointments (Stewart *et al.* 2014).

The effectiveness of medical honey has been tested on several wound types (Table 1.1). Several studies compare the effectiveness of honey treatment with known antibacterial and wound healing agents such as silver sulfadiazine (topical antibacterial cream), polyurethrane film (waterproof also providing a bacterial barrier), boiled potato peels, sterile linen dressing, petroleum treated gauze and framycetin/gramicidin (antibiotic/sofradex) dressings. The honey accelerated epithelial repair and helped to decrease the perception of pain. Burn wounds, when dressed with honey, did not require any grafting whereas the wounds treated with silver sulfadiazine required a graft. These wound healing properties of honey are multifactorial and is due to the antioxidant, anti-inflammatory and antimicrobial activity of honey. The effectiveness of treatment also depends on the type of wound and how it was obtained (Stewart *et al.* 2014).

Table 1.1: Types of wounds successfully treated with honey dressings (Pieper 2009)
Skin graft
Infected skin-graft donor sites
Infected trauma wounds
Necrotizing fasciitis (Fournier's gangrene)
Abscesses
Pilonidal sinuses
Pressure ulcers
Leg and foot ulcers (diabetic, tropical/Naga sores, leprosy/Hansen's disease, sickle cell, etc.)
Laceration to leg
Traumatic wound
Tropical ulcers (Naga sores)
Malignant ulcers
Burns and scalds
Hidradenitis suppurativa
Meningococcal septicaemia skin lesions
Surgical wounds/infection (Caesarean section, abdominal hysterectomy, amputations, etc.)
Herpetic lesions
Atopic dermatitis
Animal bite wound

Honey has several physical properties that can also aid in wound healing. The high viscosity of honey creates a barrier that helps to keep microbes and foreign particles out of the wound. It reduces the adherence of dressings to wounds making removal of bandages easier. This barrier also prevents the wound from drying out and it's hygroscopic and hyperosmotic nature dehydrates bacteria. The osmotic nature of honey also helps to draw out osmotic fluid that has accumulated in the wound (Stewart *et al.* 2014), thereby alleviating the pressure exerted by edema and pain caused due to pressure. As a consequence there is less pressure exerted on surrounding blood vessels, microcirculation to the area is improved and more oxygen and nutrients are available for healing (Pieper 2009). Rossiter *et al.* (2010) found that honey also stimulates angiogenesis.

Other factors, such as glucose in honey, provide macrophages and other immune cells with fuel to phagocytise foreign microbes (Stewart *et al.* 2014). Polyphenols in honey decrease the number of inflammatory cells in the wound site and reduces the levels of free radicals. Not only can free radicals such as reactive oxygen species (ROS) cause cellular damage but can also stimulate excessive fibroblast growth and subsequent collagen production resulting in abnormal scar formation. Honey based wound dressings effectively reduces ROS formation and improves wound healing (Pieper 2009).

The four main antibacterial components of honey are bee defensin-1, H_2O_2, the acidity of honey as well as the methyglyoxal (MGO) content (Kwakman *et al.* 2010). H_2O_2 is produced from glucuronic acid in honey and in this process hydrogen ions form that lowers the pH of honey to around 3.2 – 5.5. This acidic environment is not favourable for bacterial growth (Stewart *et al.* 2014). The acidic nature of honey also helps to promote wound healing by inhibiting proteases that normally inhibit growth factors and the formation of protein fibres (Stewart *et al.* 2014). H_2O_2 at high levels has a well described antiseptic/antibacterial activity but at low concentrations H_2O_2 stimulates fibroblasts migration and epithelial function (Pieper 2009).

Manuka honey is from the monofloral *Leptospermum* species indigenous to New Zealand (Allen *et al.* 1991; Mavric *et al.* 2008; Kwakman *et al.* 2010; Stewart *et al.* 2014). Comvita UMF® Manuka honey (Adams *et al.* 2009) is widely used as a wound healing product. Mavric *et al.* (2008) identified MGO as the major antibacterial component of this honey ranging between 38.4 – 761 mg/kg MGO. This 'non-peroxide' antibacterial activity is referred to as the Unique Manuka Factor (UMF) which is the term used to classify Manuka based on the presence of three distinct compounds, namely dihydroxyacetone (DHA), leptosperin and MGO (NZ-ManukaNatural 2015; UMFHA 2015).

Manuka honey is a well characterised and an effective method for the treating of wounds and killing or preventing infections. However concern has been raised with regards to the use of Manuka honey with high MGO levels in patients with hyperglycemia and diabetes. In these patients levels of both glyoxal (GO) and MGO are elevated (Thornalley 1996; Kim *et al.* 2004; Han *et al.* 2007). Both GO and MGO are formed through enzymatic and non-enzymatic degradation of glucose (Han *et al.* 2007) and cause the formation of advanced glycosylation end products (AGE) (Lo *et al.* 1994; Jensen *et al.* 2015). Increased AGE levels alter protein structure and function resulting in changes in cellular and tissue function (Jensen *et al.* 2015). Increased levels of MGO are believed to contribute to the formation of cataracts via MGO-mediated formation of AGEs (Kim *et al.* 2004). It has also been suggested that the formation and accumulation of AGEs contributes to the stiffness of the heart muscle due to cross-linking, increased collagen formation or reduced nitric oxide (NO) production contributing to the development of cardiomyopathy (Oguri *et al.* 2014). In addition it has been shown that MGO accumulation causes the apoptosis of RINm5F insulin-secreting cells as well as rat pancreatic β-cells (Sheader *et al.* 2001), hypertension (Chang *et al.* 2011), increased accumulation of adipocytes (Jia *et al.* 2012) and formation of ROS (Rosca *et al.* 2005).

Although MGO containing honey does have numerous beneficial effects concern has been expressed related to the safety of this honey in patients with diabetes. In addition Manuka honey is unique to New Zealand and its use in southern Africa is limited due to the cost of importation. Southern Africa has a well described floral biodiversity and the possibility exists that an indigenous honey type with similar or greater wound healing properties than Manuka honey can be found.

The aims of this study were to develop a rapid and inexpensive colorimetric method for the quantification MGO in southern Africa honey. Secondly to evaluate the antibacterial and cellular effects of MGO *in vitro* and to determine whether MGO levels that effectively kills bacteria is cytotoxic to several cell lines. The MGO levels as found in southern Africa honey will be extrapolated to the findings of this study related to the antibacterial activity and cellular effects. This study will provide preliminary data on MGO levels in a selection of southern Africa honey and important information on MGO toxicity.

Chapter 2: Literature review

2.1 Introduction

The treatment options for certain wounds such as chronic wounds are limited since the healing process has become disrupted due to the infection that has occurred within the wound. Treating such a wound can become expensive since the treatment is more complex and would require treatment over a longer period of time. Medical grade Manuka honey, such as UMF® 25+ (Comvita®) honey, is a well characterised treatment option for wounds, since it has antibacterial activity against wound-associated pathogens strains that have become resistant to other antibiotics such as methicillin-resistant *Staphylocous aureus* (Mavric *et al.* 2008; Pieper 2009).

For effective wound healing the infection first needs to be eradicated before cellular regrowth can be re-stimulated. The main antibacterial component of Manuka honey is MGO (Mavric *et al.* 2008; Kwakman *et al.* 2010; Stewart *et al.* 2014). Manuka honey is graded according to a UMF value which is directly related to the MGO content of this honey. This honey has been effectively used to treat many types of wounds including the treatment of leg and foot ulcers of diabetic patients (Pieper 2009).

There is however some controversy with regards to the safety of MGO due to the fact that that MGO mediates the formation of advanced glycation end products (AGEs). Special concern has been raised with regards to diabetic patients with already high serum levels of MGO (Vaca *et al.* 1997; Daglia *et al.* 2013), therefore the additional application of MGO-containing honey could potentially cause more harm than good. Protein modification via the reversible reaction of MGO with Arg, Lys and Cys residues leads to a loss of function of the protein due to structural changes that occur as a result of the reaction (Lo *et al.* 1994; Thornalley 1996). There is however a MGO detoxification system present in cells, the glutathione (GSH) dependent glyoxalase I-II system which uses the enzymes glyoxalase I and II to convert excess MGO into S-D-lactoyl-glutathione and D-lactate which is harmless to cells. Only when this system is inhibited due to excess MGO binding to GSH, cells undergo apoptosis (Kim *et al.* 2004).

Manuka honey is derived from *Leptospermum scoparium* indigenous to New Zealand (Stewart *et al.* 2014). Southern Africa has a well described floral biodiversity with the possibility of an indigenous honey type being discovered with similar or greater wound healing properties than Manuka honey.

The purpose of this study was to collect 29 honey samples within the southern African region and to quantify the MGO content of these samples using a newly developed colorimetric assay. MGO was also evaluated for its antibacterial activity and the MIC of MGO was determined using Gram positive and Gram negative bacteria. The cellular effect at this MIC was also determined. These findings were correlated back to the MGO content as found in the SA honey samples in order to determine if the MGO concentration in these honeys are high enough in order to have antibacterial activity and whether these concentrations are toxic to cells.

2.1.1 Antibacterial properties of honey

Honey also has antimicrobial action which is attributed to several physical properties and molecules found in honey. As a first line of defence the viscosity of honey creates a barrier which prevents microbes from entering into the wound. The hygroscopic and hyperosmotic nature of honey dehydrates its surrounding environment which is not favourable for bacterial growth. This dehydration also helps to prevent oedema thereby lowering the pressure and helping to increase blood circulation to the affected area. Increased blood flow can help to speed up the healing process. Honey's low pH (3.2 – 4.5), due to the presence of glucuronic acid and the production of H_2O_2, inhibits bacterial growth. The acidity of honey also helps to promote wound healing because the low pH inhibits proteases thereby promoting collagen formation which is associated with increased fibroblast activity. Fibroblast formation is essential for the healing of a wound (Mavric *et al.* 2008; Stewart *et al.* 2014). While directly influencing the environment and making it unfavourable for bacteria to grow in, honey also provides macrophages and other immune cells with extra glucose in order to perform phagocytosis on foreign microbes that might have entered the wound (Stewart *et al.* 2014).

Honey has been found to be effective in killing a wide range of Gram positive and negative bacteria as well as several antibiotic resistant strains as listed in Table 2.1 (Pieper 2009) and biofilms formed by certain bacteria such as methicillin-resistant *S. aureus* and *P. aeruginosa* (Kilty *et al.* 2011). In a study done by Kwakman *et al.* (2010) the antibacterial effects of honey were attributed to more than one component. By neutralizing different contributing factors a combination of four main compounds that all contribute to honey's antibacterial effect were identified. These compounds included peptide bee defensin-1, H_2O_2, the honey's acidity as well as MGO content of the honey. Some of these compounds have a higher potency than others. MGO was identified as one of the components with the highest contribution towards the antibacterial effect of honey (Kwakman *et al.* 2010). The properties and pharmacological activity of honey varies based on type of honey, floral origin, season of harvesting as well as processing and storage.

Table 2.1: Gram positive and negative antibacterial activity of honey (Pieper 2009)	
Gram positive bacteria	**Gram negative bacteria**
Staphylococcus aureus (various)	*Escherichia coli*
Methicillin-resistant *Staphylococcus aureus*	*Salmonella California*
Staphylococcus simulans	*Salmonella enteritidis*
Staphylococcus capitis	*Salmonella typhimurium*
Staphylococcus epidermidis	*Pseudomonas aeruginosa*
Staphylococcus haemolyticus	*Shigella sonnei*
Vancomycin-resistant *enterococci*	*Alcaligenes faecalis*
Vancomycin-sensitive *enterococci* (various isolates)	*Citrobacter freundii*
Beta-hemolytic*streptococci*(various isolates)	*Shigella sonnei*
	Enterobacter aerogenes
	Klebsiella pneumonia
	Serratia marcescens
Other:	
Mycobacterium phlei	

Manuka has been widely evaluated for its antibacterial properties as it has been proven to be one of the most effective treatments for wounds in comparison to other honey types. It has previously been thought that the antibacterial properties of honey was due to its H_2O_2 content but Manuka exhibits 'non-peroxide' antibacterial activity. This was demonstrated by Allen *et al.* (1991) when it was found that Manuka and vipers bugloss (*Boraginaceae* family) honey were the only two honey types amongst the 345 samples (26 floral sources) in their study that exhibited significant non-peroxide antibacterial activity. It was also later confirmed by Kwakman *et al.* (2010) that when H_2O_2 was neutralised with catalase it was found that this honey still retained some of its antibacterial activity. Although there may be several other compounds present in Manuka that also contribute to its non-peroxide antibacterial activity (Russell *et al.* 1990), Mavric *et al.* (2008) identified MGO as the major antibacterial component of honey, especially of Manuka honey. The MGO content of Manuka was found to be from 38.4 – 761 mg/kg MGO. The 'non-peroxide' antibacterial activity of Manuka honey is referred to as the 'Unique Manuka Factor' (UMF) and it is used to classify the honeys based on the presence of three distinct compounds, namely dihydroxyacetone (DHA), leptosperin and MGO. Although three compounds need to be present in order to classify honey as a UMF honey the UMF factor is directly linked to the honey's MGO content (Table 2.2).

Table 2.2: MGO content of different UMF Manuka honeys (UMFHA 2015)	
UMF Grade	**MGO (mg/kg)**
5	≥83
10	≥263
15	≥514
16	≥573
18	≥696
20	≥829
25	≥1200
28	≥1449

2.2 Methylglyoxal

MGO is part of a group of chemicals known as 1,2-dicarbonyls. This group includes MGO, glyoxal (GO) and 3-deoxyglucosulose (3-DG) (Figure 2.1). All three of these compounds can be found in honey (Weigel *et al.* 2004; Mavric *et al.* 2008).

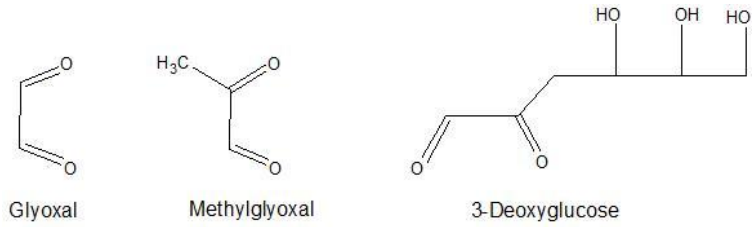

Figure 2.1:1,2-Dicabonyls found in Manuka honey (Weigel *et al.* 2004)

The concentration of GO, MGO and 3-DG varies considerably between honey types. Mavric *et al.* (2008) determined the GO, MGO and 3-DG content of various types of Manuka honeys and the concentrations of these compounds in the different samples varied considerably (Table 2.3).

Table 2.3: Concentration (mg/kg) 1,2-dicarbonyl compounds found in honey (Mavric *et al.* 2008)

Sample	3-DG	GO	MGO	HMF
Commercial honey	342	1.7	3.1	3.9
samples (n = 50)	(119–1451)	(n.d. -4.6)	(n.d. -5.7)	(1.0–75)
Manuka 1 “active 5”	1060 ± 54	0.7 ± 0.2	38.4 ± 5.0	3.0 ± 0.2
Manuka 2 “active”	668 ± 30	3.0 ± 1.0	347 ± 20	22.6 ± 0.5
Manuka 3 “active”	563 ± 26	3.9 ± 1.0	411 ± 24	17.6 ± 0.6
Manuka 4 “UMF 10”	747 ± 40	1.2 ± 0.5	416 ± 35	21.3 ± 1.1
Manuka 5 “UMF 20”	807 ± 39	4.2 ± 1.1	743 ± 40	43.9 ± 2.0
Manuka 6 “UMF 25”	697 ± 44	7.0 ± 1.0	761 ± 25	n.a.
Antibacterial wound gel	n.a.	n.a.	n.a.	n.a.

UMF = Unique Manuka Factor
n.d. – not detected below 0.2 mg/kg
n.a. – not analysed

MGO is the main component responsible for the antibacterial activity of honey with an MIC for both *S. aureus* and *E. coli* at 1.1 mM MGO. GO requires a higher concentration in order to have antibacterial activity with a minimum inhibitory concentration (MIC) of 6.9 mM for *E. coli* and 4.3 mM for *S. aureus*. 3-DG showed no antibacterial activity in this study (Table 2.4). In the same study by Mavric *et al.* (2008) Manuka honey still exhibited antibacterial activity when diluted to 15 – 30% dilutions whereas no antibacterial activity was seen for commercial honey diluted past 80%.

Table 2.4: MIC of 1,2-dicarbonyls or diluted honey samples and MGO concentrations of dilutions required to achieve respective MIC (Mavric *et al.* 2008)

Sample	MIC for *E. coli*	MIC for *S. aureus*
3-DG	No inhibition observed up to 60 mM	
GO	6.9 mM	4.3 mM
MGO	1.1 mM	
Honey samples	>80%	
Manuka honeys 2–6	15–30%	
MGO at MIC dilution	1.1–1.8 mM	

2.2.1 Chemical formation, properties and metabolism of methylglyoxal

Relatively little is known about the origin of MGO in Manuka honey (Mavric *et al.* 2008). With regards to other foods that also contain dicarbonyls, these compounds are normally formed via Maillard reactions, through the process of caramelisation. This occurs during heat treatment when reducing sugars such as glucose react non-enzymatically with lipids, free

amino acids or amino acid residues such as Lys, Arg and Cys. This results in the formation of Schiff bases and unstable intermediates called Amadori products (Singh *et al.* 2001; Weigel *et al.* 2004) that then degrade to form dicarbonyls (Figure 2.2) (Weigel *et al.* 2004). Both 3-DG and MGO can form at various stages of Maillard reactions (Singh *et al.* 2001). 3-DG also forms as an intermediate during heat treatment from the loss of water from glucose and fructose under acidic conditions. Hydroxymethylfurfural (HMF) forms during this reaction with 3-DG as an intermediate. HMF can be used as an indicator to determine whether a product has undergone heat treatment or not (Weigel *et al.* 2004). An increase in 3-DG occurs during heat treatment of different honey samples (stored at 35°C and 45°C for 70 days) but no significant increase in MGO and GO amounts (Weigel *et al.* 2004).

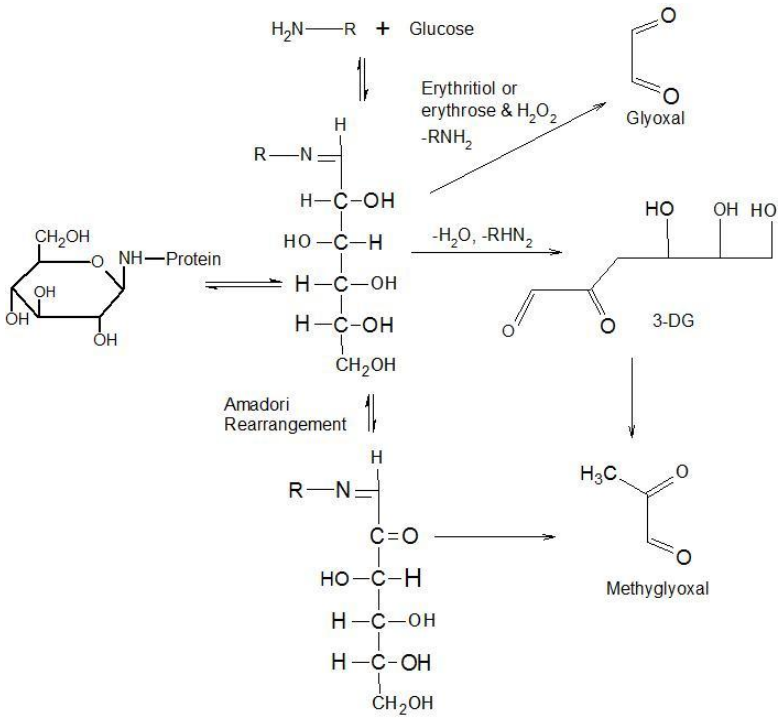

Figure 2.2: Formation of MGO and GO in the Maillard reaction (Wang and Ho 2012)

MGO can also form as a result of the oxidation of glucose (Figure 2.3).

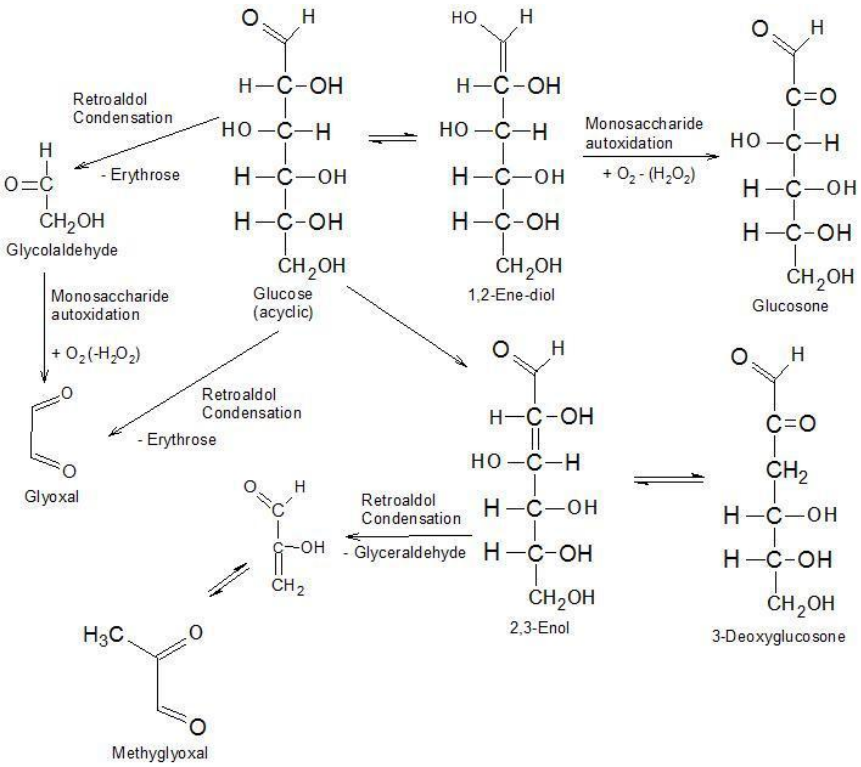

Figure 2.3: Oxidative formation of MGO, GO and 3-DG from glucose (Wang and Ho 2012)

In physiological systems MGO forms enzymatically or non-enzymatically via the elimination of phosphates from the triose phosphates: glycerine phosphate and glyceraldehydes 3-phosphate (Phillips and Thornalley 1993). However, the method of formation in honey is still unclear. According to Mavric *et al.* (2008) and Weigel *et al.* (2004) MGO content of honey was not affected by storage conditions (Weigel *et al.* 2004; Mavric *et al.* 2008). Maillard or carmelization reactions can also be excluded as a source of MGO in honey since the amounts of HMF (Indicator for heat treatment) found in the honeys was very low. The authors suggest that a possible source of MGO could be from bacterial activity since MGO is formed as a by product of glycolysis from bacteria (Mavric *et al.* 2008).

There have been studies that suggest that the formation of MGO is due to the presence of dihydroxyacetone (DHA) (Adams *et al.* 2009; Atrott *et al.* 2012). It is a degradation product of carbohydrates during Maillard reactions. It occurs in aged wines and is also associated with fermentation process of microorganisms. In addition it is used as food additive to enhance browning or as a preservative as well as being used as the functional ingredient in certain cosmetic products such as self tanning creams (Atrott *et al.* 2012).

In a study done by Adams *et al.* (2009) the authors suggest that MGO is formed non-enzymatically as an intermediate in the reaction between DHA and glycine as well as enzymatically via methylglyoxal synthase from DHA-phosphate. The researchers noticed that freshly produced Manuka honey had high levels of DHA but low levels of MGO. Upon

storage at 37°C the levels of DHA decreased as the levels of MGO increased. Similar results were observed when DHA was added to other types of honey and stored at 37°C where a decrease in DHA occurred as MGO levels increased (Adams *et al.* 2009). It is believed that the high levels of DHA in the honey are derived from the nectar from which the honey is produced however, the origin of DHA in the nectar is still unknown (Atrott *et al.* 2012).

2.3 Methylglyoxal and bacteria

2.3.1 Bacterial metabolism of methylglyoxal

Bacteria, like many other organisms, possess biochemical pathways that produce and detoxify MGO. Many bacteria possess the enzyme methyglyoxal synthetase that produces MGO as well as the highly conserved glutathione GSH dependant glyoxylase I-II system that detoxifies MGO. This system is found in bacteria as well as many other organisms including humans, which implies that most organisms have come into contact with MGO at some point during evolution and required a way to detoxify or metabolise MGO (Ferguson *et al.* 1998).

Under normal physiological conditions MGO production and detoxification is in equilibrium, however, if it accumulates it becomes toxic. Despite its toxicity MGO plays an important biochemical role in the regulation of growth, D-lactate production, the uncoupling of anabolism and catabolism and its formation also helps to prevent the accumulation of phosphorylated intermediates which has a direct effect on bacterial growth (Ferguson *et al.* 1998).

The main reason for bacteria to produce MGO is the regulation of carbon flux (Ferguson *et al.* 1998; Booth *et al.* 2003). In an environment of a high carbon supply or high levels of sugar phosphates there is an increase in the production of phosphorylated metabolites of sugar metabolism such as DHA-phosphate and glyceraldehyde-3-phosphate (Ferguson *et al.* 1998) which inhibit the growth of bacteria. MGO is formed from DHA-phosphate and this temporarily relieves the bacteria from the stress caused by the build-up of phosphorylated intermediates (Ferguson *et al.* 1998). The bacteria are then able to survive for longer periods of time until the carbon levels of the environment have returned to normal or the stress causes death. With normalization of carbon levels the bacteria are able to re-colonise their environment. However, if MGO is continuously being produced, high MGO levels are toxic and cause bacterial death (Ferguson *et al.* 1998).

There are three ways in which bacteria regulate the accumulation of MGO and detoxify it in order to prevent build up. These are: the GSH dependent glyoxylase I-II system, the GSH independent glyoxalase III system and the MGO reductase and the dehydrogenase systems

(Ferguson *et al.* 1998). The GSH dependant glyoxylase I-II system is the most well described process of MGO detoxification and it converts MGO into D-lactate and MGO derivatives to corresponding α-hydroxyacids (Ferguson *et al.* 1998; Booth *et al.* 2003). This process is GSH dependant and GSH is present in a wide variety of organisms including most eukaryotes except those that do not have mitochondria or chloroplasts. In prokaryotes it is produced by cyanobacteria, proteobacteria as well as a few strains of gram negative bacteria. Its physiological concentrations in bacteria rage from 0.1 – 10 mM (Masip *et al.* 2006). In *E. coli* GSH plays a major role in protection against different types of stress and toxicity which includes osmotic stress, low pH, oxidative stress as well as MGO toxicity (Masip *et al.* 2006).

The GSH independent glyoxalase III system converts MGO directly into D-lactate. This system does not require the presence of GSH in order to react with MGO and therefore does not convert MGO via the production of S-lactoylglutathione. It does however seem to require thiol containing compounds since thiol blocking agents can interfere with the reaction (Ferguson *et al.* 1998). MGO reductase reduces 2-oxoaldehydes into corresponding 2-hydroxyaldehydes and also catalyses the conversion of aldehydes into alcohols. This enzyme seems to be more significant in eukaryotic cells. A NADP/NADPH dependent version of this enzyme has however been isolated from *E. coli.* It reduces MGO directly to acetol however, its affinity for MGO is poor (Ferguson *et al.* 1998).

Relatively little is known about the mechanism by which Gram positive bacteria detoxify MGO. Genes encoding for glyoxylase I has mainly been identified in Gram negative bacteria and it is generally considered that Gram positive bacteria do not synthesis GSH and therefore cannot make use of the GSH dependant glyoxylase I-II system. However, *B. subtilis* is believed to have a homolog for this enzyme. *S. aureus* does not metabolize MGO in the presence of GSH; in fact it becomes more sensitive to MGO exposure if it is grown in the presence of GSH (Ferguson *et al.* 1998).

2.3.2 Antibacterial effects of methylglyoxal

Of the dicarbonyls present in honey, MGO had the highest antibacterial activity with a MIC of 1.1 mM when tested against both *E. coli* and *S. aureus*. 3-DG showed no inhibition of either bacteria even at concentrations up to 60 mM and the MIC for GO was 6.9 mM for *E. coli* and 4.3 mM for *S. aureus*. Honey with high MGO levels was found to have a higher antibacterial activity than honey with less or no MGO (Mavric *et al.* 2008). Studies have also shown that MGO is effective against *S. aureus* that has become resistant to methicillin and oxacillin (Pieper 2009) (Table 2.1).

The sensitivity of bacteria to MGO is dependent on a number of parameters including cell density, nature and composition of the growth medium and growth phase. As cell density increases sensitivity decreases due to an increase in the detoxification capacity of more cells. This is however not a direct relationship. Cells grown in a Tris-based medium are more sensitive than cells grown in phosphate buffered medium due to the interaction of MGO with the amino groups of Tris. In a study by Ferguson *et al* (1998), ten times more MGO is required to inhibit the growth of *E. coli* grown in Tris-based medium as opposed to *E. coli* grown in phosphate-buffered medium. Potassium content of the growth medium also influences sensitivity with higher K^+ concentrations leading to greater sensitivity. *E. coli* however, possesses KefB and KefC systems that are responsible for the potassium efflux. These systems are activated by GSH conjugates that result in the removal of excess potassium which decreases sensitivity to MGO (Ferguson *et al.* 1998).

During the exponential growth phase bacteria are more sensitive to MGO than bacteria in the stationary phase. This is because during the stationary phase, *E. coli* expresses the gene RpoS which helps in the regulation of the Dps 12 protein. Dps plays a major role in protecting DNA against oxidative stress. The level of expression of the RpoS gene and consequent production of the Dps protein in the exponential phase is lower and therefore is less protected against the damage that may occur to DNA due to MGO exposure (Ferguson *et al.* 1998).

The mechanism by which MGO kills bacteria is still unclear; however it is believed that MGO interferes with protein synthesis, consequently preventing DNA replication (Ferguson *et al.* 1998; Booth *et al.* 2003). MGO is also known to be mutagenic and causes alterations to bacterial DNA (Booth *et al.* 2003). Plasmid DNA extracted from *E. coli* that has been exposed to MGO shows reduced transformation efficiency which suggests that it has been damaged (Ferguson *et al.* 1998). Another way in which MGO inhibits growth is by reacting with Cys residues within specific proteins. This causes changes in the protein structure affecting activity and consequently inhibiting bacterial growth (Ferguson *et al.* 1998; Booth *et al.* 2003).

MGO has also been found to be effective against certain biofilms (Jervis-Bardy and Tan 2011; Kilty *et al.* 2011). This has an important implication in the treatment of chronic rhinosinitis (CRS) (Jervis-Bardy and Tan 2011), nosocomial surgical site infections (nosocomial SSI) (Mangram *et al.* 1999) and chronic wounds (James *et al.* 2008) all of which can occur due to poor post surgical disease control. The most common bacteria found in nosocomial infections are *S. aureus, S. enterococcus, E. coli and* methicillin-resistant *S. aureus* (Mangram *et al.* 1999, Sassi-Gaha *et al.* 2010). Such an infection can be the result of

a biofilm that has formed in the wound. The treatment of a chronic wound is also more complicated than that of a normal wound since the infection has disrupted the normal healing process and it first needs to be eradicated before cellular regrowth can be stimulated. The prolonged nature of such treatment means that it is also a lot more costly than treating normal acute wounds (James *et al.* 2008, Sassi-Gaha *et al.* 2010).

Patients receiving immune suppressing medication, such as in the case of an organ transplant or patients that have a compromised immunity due to illness are also more at risk of becoming infected while hospitalised. It is therefore very important that any bacterial infections in these patients are prevented before they occur (Rubin 1993).

As previously mentioned the mechanism by which MGO kills bacteria is still poorly understood. In a study done by Roberts *et al.* (2014) it was reported that exposure of *P. aeruginosa* to Manuka honey reduced the bacteria's motility due to de-flagellation. In this study the expression of the major structural protein flagellin was reduced after exposure as well as flagellin-associated genes, fliA, fliC, flhF, fleN, fleQ and fleR. The ability to grow fimbrae and flagella are important in order for bacteria to colonise a certain area as well as express virulence (Post *et al.* 2007). De-flagellation of bacteria by Manuka honey would limit bacteria mobility, reduce bacterial adhesion and prevent biofilm formation. It is however unknown whether de-flagellation occurs due to a direct effect of MGO or if it is due to in interplay between more than one compound that this occurs (Roberts *et al.* 2014).

2.4 Cellular effects of methylglyoxal

2.4.1 Formation, detoxification and cellular toxicity of methylglyoxal

MGO is not only present in honey and bacteria but it is also produced in mammalian cells. Generally MGO is formed from the enzymatic as well as non-enzymatic removal of phosphate from glycerone phosphate, DHA phosphate and glyceraldehyde-3-phosphate. Enzymatic formation occurs when MGO leaks from phospho-ene-diolate bound to the active site of phosphate isomerise or methyglyoxal synthase as well as the enzymatic conversion of acetol to MGO by acetole dehydrogenase (Phillips and Thornalley 1993; Thornalley 1996; Ferguson *et al.* 1998). It is also formed from the catabolism of Thr via aminoacetone as well as the metabolism of acetone by cytochrome P450. This results in the formation of DHA and MGO (Phillips and Thornalley 1993; Thornalley 1996). MGO can also form spontaneously as a side chain reaction of DHA-phosphate with triosphosphate isomerise, as a by-product from a mixture of DHA-phosphate and glyceraldehyde-3-phosphate (Ferguson *et al.* 1998) or via the non-enzymatic fragmentation of triosephosphates. These processes occur in all cells in organisms (Phillips and Thornalley 1993; Thornalley 1996).

Under normal glycemic conditions the non-enzymatic fragmentation of triosephosphates is the main source of MGO formation *in vitro*. When metabolites that increase the flux of triosphosphates, such as glucose, fructose, DHA, D-glyceraldehyde, acetone and hydroxyacetone are added however, MGO formation increases. (Phillips and Thornalley 1993; Thornalley 1996). Similarly MGO synthesis increases in a state of hyperglycemia associated with diabetes (Jensen *et al.* 2015).

Plant cells also produce MGO and levels of MGO are usually increased if plants are under salt, drought or cold stress or in order to deal with an increase in carbon flux (Ferguson *et al.* 1998; Yadav *et al.* 2005). The GSH dependant glyoxylase I-II system is important in order to detoxify plant and animal cells from MGO since it converts MGO to D-lactate. In plants where levels of glyoxylase are reduced, germination does not occur due to high MGO levels (Yadav *et al.* 2005). It is unknown if MGO accumulates in nectar and through bee activity, accumulates in the honey.

2.4.2 Cellular detoxification of methylglyoxal

The GSH dependant glyoxylase I-II system is a highly conserved system since it is present in many organisms including plant and bacterial cells as well as mammalian cells. This suggests that most organisms are exposed to MGO at some stage during life. In animal species this pathway is mostly found in the epithelial cells of the gut to protect against the MGO produced by gut associated bacteria (Ferguson *et al.* 1998). High levels of MGO are toxic and can cause disruption of normal cellular pathways and cell death. Therefore effective MGO detoxification is essential (Thornalley 1996).

The GSH dependent glyoxalase I-II system is the main pathway for MGO detoxification in mammalian cells (Ferguson *et al.* 1998). Along the course of this pathway MGO is converted by glyoxalase I and II into D-lactate (Ferguson *et al.* 1998; Yadav *et al.* 2005). In the cytosol MGO reacts spontaneously with the sulphydryl group of GSH to form hemithioacetal (HTA). This compound then undergoes an isomerisation reaction, catalysed by glyoxylase I, to form S-lactyol-glutathione. S-lactyol-glutathione is substrate to glyoxylase II which converts this substrate to D-lactate (Thornalley 1996; Ferguson *et al.* 1998; Yadav *et al.* 2005) (Figure 2.4). MGO derivatives get converted to corresponding α-hydroxyacids (Ferguson *et al.* 1998). In mammalian cells D-lactate is further converted into pyruvate by mitochondrial 2-hydroxyacid dehydrogenase (Thornalley 1996).

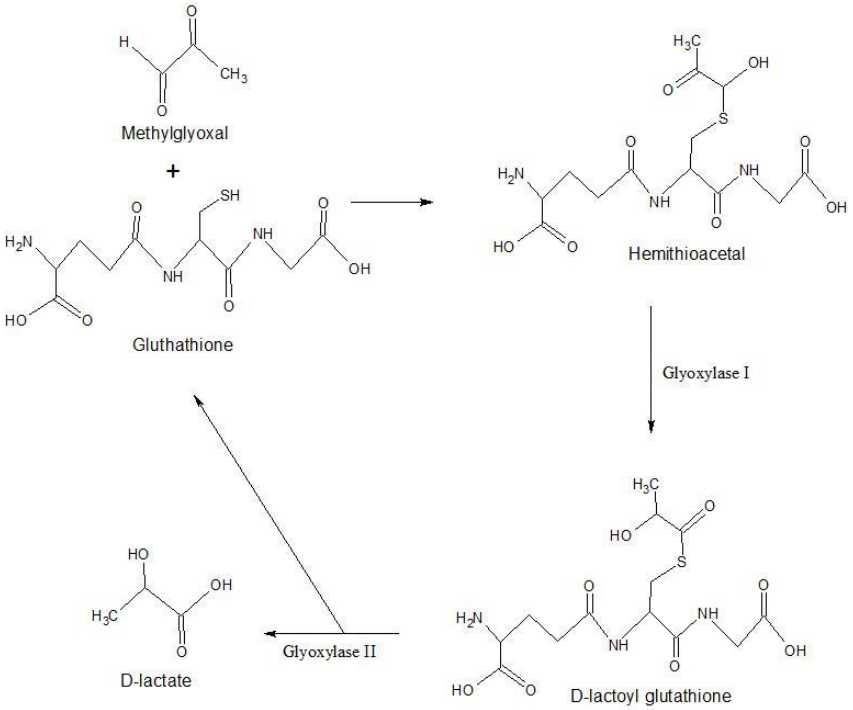

Figure 2.4: The GSH-dependent glyoxalase I-II systems for detoxifying MGO (Sukedo *et al.* 2004)

MGO can also be metabolized by aldose reductase. This is an NADPH-dependant aldehyde reductase that detoxifies aldehydes and is involved in osmoregulation. During this process 95% of the MGO gets converted into hydroxyacetone and the remaining 5% gets converted into D-lactaldehyde (Ferguson *et al.* 1998).

2.4.3 Cellular toxicity of methylglyoxal

There have been several studies identifying MGO toxicity (Suzuki *et al.* 1997; Vaca *et al.* 1997; Paul and Bailey 1999; Sheader *et al.* 2001; Kim *et al.* 2004; Cantero *et al.* 2007; Ota *et al.* 2007; Lee *et al.* 2009). In addition it may also be tumoricidal as it has been shown to have the ability to kill several different types of cancer cells (Talukdar *et al.* 2009). The fact that it influences and interacts with cellular functioning is because MGO is a highly reactive electrophilic molecule that can react with DNA and protein (Ferguson *et al.* 1998). MGO accumulation can result in mutations, protein degradation and eventually cell death (Thornalley 1996).

The toxic effect of MGO is primarily thought to be due to its electrophillic nature which enables it to interact with neucleophillic molecules such as DNA and RNA (Figure 2.5) as well as with proteins (Figure 2.6) (Thornalley 1996; Ferguson *et al.* 1998). In DNA, MGO reacts with the nitrogenous base guanine and to a lesser extent with adenine and cytosine (Ferguson *et al.* 1998) where as in proteins MGO reacts with the amino acids Arg, Lys and Cys (Thornalley 1996; Ferguson *et al.* 1998; Yadav *et al.* 2005). MGO also binds to and modifies bovine serum albumin, ribonuclease A, lysozymes, glycolytic proteins, erythrocyte

membrane proteins, microtubular proteins and collagen. Enzymes bound by MGO become inactivated and the functioning of structural proteins change. Some proteins modified by MGO form non-sulfhydryl cross-links (Lo *et al.* 1994). Simulated gastrointestinal digestion of Manuka honey, the MGO content of the digests decreased and this was due to MGO-mediated carbonylation of the digestive enzymes. However, these structural changes did not cause a loss in enzymatic activity (Daglia *et al.* 2013).

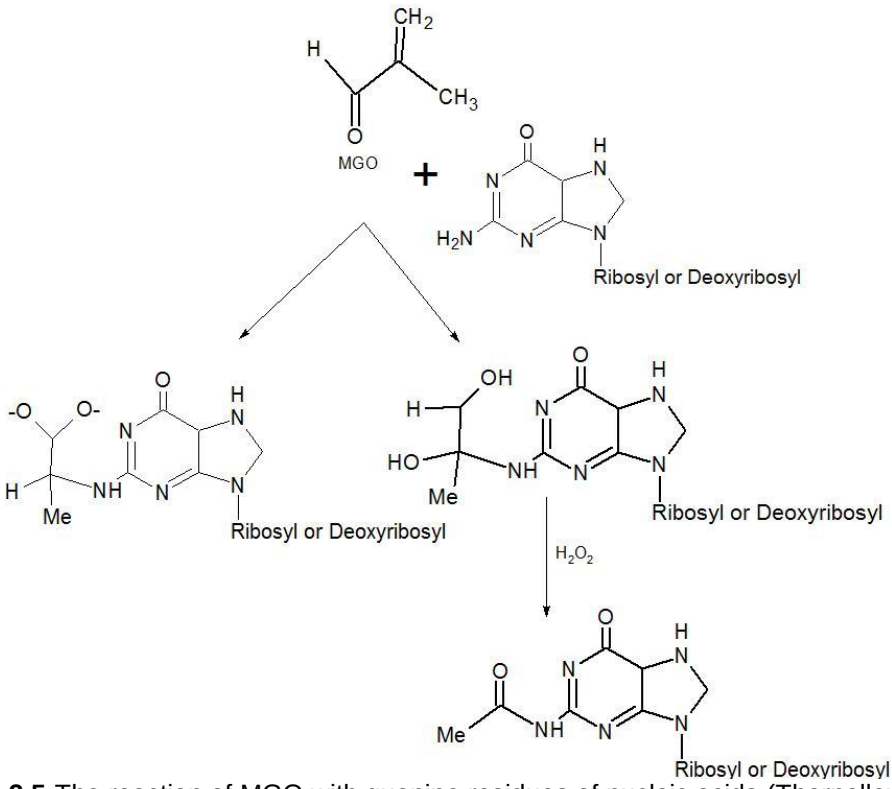

Figure 2.5: The reaction of MGO with guanine residues of nucleic acids (Thornalley 1996)

MGO also inactivates antioxidant systems. Accumulation of MGO results in GSH depletion and increases the rate of protein degradation since less GSH is available to provide protection against oxidative damage (Yadav *et al.* 2005). MGO binding does seem to act as a signal for degradation since serum albumin modified by MGO binds to surface receptors of macrophages and is internalised and degraded (Lo *et al.* 1994).

There has been lots of controversy with regards to MGO and its benefits vs. toxicity. Several studies have been done that suggest it regulates growth and is able to destroy pathogenic microorganisms and viruses (Pavlovic-Djuranovica *et al.* 2006; Rachman *et al.* 2006). It has also been found to destroy cancerous cells without causing harm to the host (Talukdar *et al.* 2009) and in other cases enhance cellular growth in a beneficial manner (Rossiter *et al.* 2010; Chang *et al.* 2011). In contrast, MGO is also believed to be toxic. Its toxicity is mainly thought to be due to the formation of AGEs through its reaction with the amino groups on Arg, and Lys via its carbonyl group. It has also been suggested that MGO and the resultant

formation of AGEs plays a role in diseases such as diabetes, diabetic cataracts, hypertension and uraemia (Talukdar *et al.* 2009). As Manuka honey is used for wound healing these effects will be discussed in greater detail in the following section.

2.4.3.1 Formation of advanced glycation end products

Many studies have linked the toxicity of MGO with the formation of AGEs which is a product that forms when MGO reacts with the amino groups of Arg and Lys and to a lesser extent Cys as well as with terminal end amine groups (Singh *et al.* 2001; Rachman *et al.* 2006). AGE formation has also been found to be closely associated with diseases like diabetes, cataracts, hypertension and uremia (Singh *et al.* 2001; Nomi *et al.* 2009). The formation of AGEs is a non-enzymatic reaction between carbohydrates and proteins in the plasma and forms part of the chain of reactions known as Malliard reactions as shown in Figure 2.2 (Thornalley 1996; Nomi *et al.* 2009). It occurs over a period of weeks therefore affecting long-lived proteins and is concentration dependent. This process is enhanced in diabetes since there is more glucose available to form MGO which then reacts with amino acids, lipids and nucleic acids (Singh *et al.* 2001). Different forms of reducing sugars also form AGEs at different rates. Glucose-6-phosphate and fructose form AGEs at a faster rate where as glucose has the slowest rate of formation (Singh *et al.* 2001). It is not only the reactions of MGO with certain molecules that result in the formation of AGEs but that of GO and other reactive α-dicarbonyls (Nomi *et al.* 2009).

The reaction between MGO and Arg, Lys and Cys residues is reversible however, further irreversible reactions then occur with Arg and Lys. At physiological MGO concentrations (<5 μM) most of the irreversible reactions that occur involve Arg (Thornalley 1996) (Figure 2.6). AGE formation in proteins and components of the extracellular matrix results in cross-links forming within their structure. This cross-linking results in the structure becoming altered and more rigid and less elastic (Bierhaus *et al.* 1998; Singh *et al.* 2001) This stiffness leads to an increased resistance to removal via proteolysis and a resultant impairment in tissue remodelling (Singh *et al.* 2001). The impaired remodelling may result in sclerosis. If this occurs in the kidneys it may contribute to the development of renal disease. In blood vessels, if the matrix of the blood vessel walls becomes more rigid it results in lipoproteins becoming trapped. This impairs cholesterol efflux which leads to cholesterol build up inside the wall of the blood vessel (Singh *et al.* 2001). These structural and resultant functional changes are thought to be the main cause of damage and pathology to proteins (Bierhaus *et al.* 1998; Uchida 2000; Stitt 2001). The process of AGE formation appears to be closely related to, and accelerated in hypertension, diabetes and age (Singh *et al.* 2001).

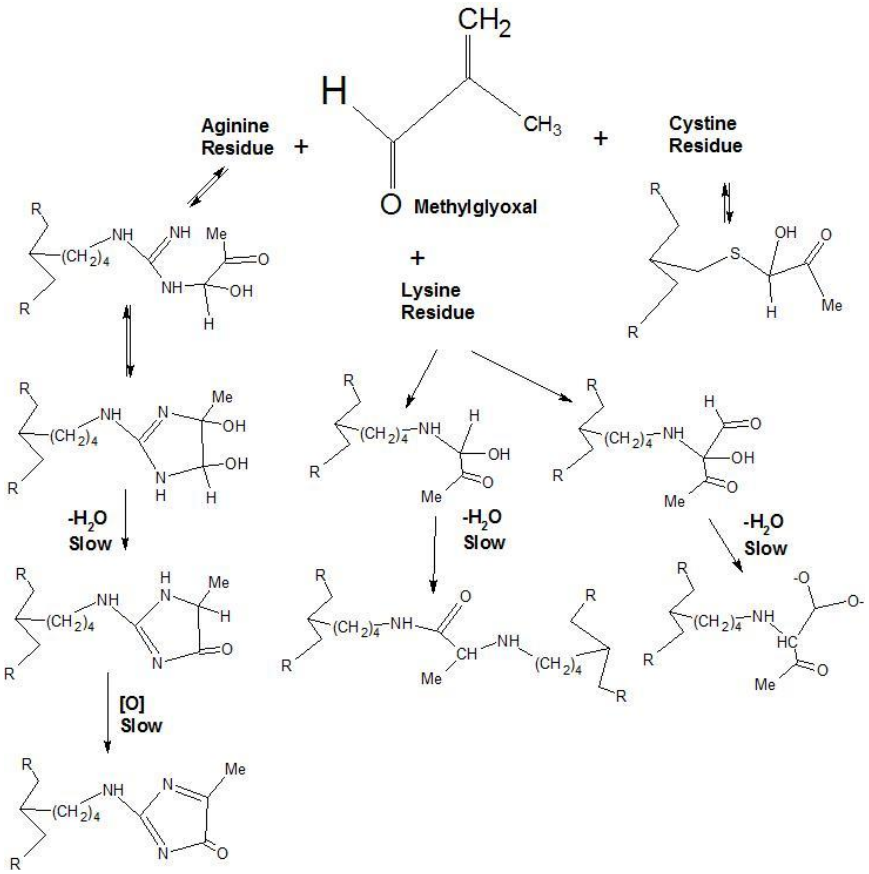

Figure 2.6: The formation of AGEs when MGO reacts with Arg, Lys and Cys (Thornalley 1996)

There are however ways in which AGEs can be metabolised and eliminated. Macrophages and monocytes receptors that can bind to MGO- modified proteins. These then undergo receptor-mediated endocytosis and lysosomal degradation (Thornalley 1996; Singh *et al.* 2001). Liver sinusoidal cells have scavenger receptors such as Kupffer and endothelial cells that aid in AGE endocytosis and it has also been suggested that insulin contributes to AGE elimination via the insulin receptor substrate (IRS) and phsophatidyl-ionstiol-3-OH kinase (PI3-kinase) (Singh *et al.* 2001). Following AGE degradation, the fragments are excreted via the kidneys and therefore proper kidney functioning is essential for the removal of AGEs. Impaired kidney function leads to AGE accumulation and vascular diseases can develop (Singh *et al.* 2001).

Apart from diabetes, AGEs have also been associated with other diseases, such as disorders associated with connective tissue, for example rheumatoid arthritis (Verzijl *et al.* 2002), nervous tissue such as Alzheimer's disease (Smith *et al.* 1994; Münch *et al.* 1997; Sasaki *et al.* 1998) as well as end-stage renal disease (Tanji *et al.* 2000). AGE related cross-linking as well as AGE-modified proteins accumulate in tissues such as coronary atheromas and cardiac muscle, the amyloid plaques in Alzheimer's disease, the cartilage in rheumatoid arthritis, the renal cortex, mesangium, glomerular basement membrane as well as the liver

and lungs resulting in stiffness of the tissue or alteration and impairment of function (Münch *et al.* 1997; Sasaki *et al.* 1998; Tanji *et al.* 2000; Verzijl *et al.* 2002). AGEs have also found to be a component of reactions associated with oxidative stress which may further contribute to the pathology (Singh *et al.* 2001). Whether these AGEs are the cause or merely a result of these pathologies is however still not clear (Singh *et al.* 2001). Currently there are no specific markers for AGEs or standard methodologies to quantify AGEs in tissue. Methodologies that are currently being used are HPLC, ELISA and immunohistochemistry (Singh *et al.* 2001). Research has shown that diabetic patients have been found to have higher than normal MGO levels in their blood, however levels vary between studies.

2.4.4 Clinical effects of methylglyoxal

2.4.4.1 Wound healing and other benefits of MGO

The process of wound healing occurs in a complex series of events. If any of these stages are disrupted complications may arise in the healing of a wound. The process can be summarised in 4 stages: Coagulation and haemostasis is the first step which occurs directly after injury. Its function is to protect the vascular system and keep it intact as well as to provide a matrix for new cells to migrate towards. Next is the inflammatory phase with the purpose of providing protection against invading microorganisms. Short-lived neutrophils arrive first and start to phagocytose microorganisms. These cells are followed by the monocytes that differentiate into macrophages and continue with phagocytosis. Monocytes have longer life span and also secrete growth factors that activate keratinocytes, fibroblasts and endothelial cells. Absence of monocytes/macrophages may seriously impede the healing process. The third phase is the proliferative phase and occurs when fibroblast migrate from the surrounding tissue to the injured area and deposit new matrix. Fibroblasts proliferate and produce the extra cellular matrix and differentiate into myofibroblasts. The myofibroblasts extend pseudopodia to attach to fibronectin and actin in the matrix. The last phase is the remodelling stage and may last up to several years. During this stage new epithelium is developed and scar tissue is formed (Velnar *et al.* 2009).

Several studies have been done on the effectiveness of Manuka and other types of honey as a wound healing product. Manuka has been shown to shorten the inflammatory phase in full thickness acute-phase burn wounds thereby reducing progression by decreasing the burn area, number of necrotic and inflammatory cells as well as inflammatory cytokine levels (Nakajima *et al.* 2013). Ranzato *et al.* (2012) demonstrated that treatment of scratch wounds with honey resulted in an increase in cell proliferation and locomotion leading to a decrease in time taken for re-epithelialization of keratinocytes. Rossiter *et al.* (2010) also reported in their study that honey can promote angiogenesis. Ranzato *et al.* (2012) did however report

that these results varied considerably between different types of honey from different floral origins and the authors suggest that combining different honeys many help to maximise the effect.

2.4.4.2 Methylglyoxal concerning diabetes and hyperglycaemia

The dicarbonyl compounds GO and MGO are elevated in patients with hyperglycemia and diabetes (Thornalley 1996). Both GO and MGO are formed through enzymatic and non-enzymatic degradation of glucose (Han *et al.* 2007). Also, Thornalley (1996) reported that if the flux of MGO precursors was increased so was the formation of MGO. Therefore, in hyperglycemic patients the formation of MGO is increased due to elevated levels of glucose and other precursors of MGO such as fructose, and D-glyceraldehyde (Kim *et al.* 2004; Han *et al.* 2007). Jagt and Hunsaker (2003) also reported that certain enzymes involved in MGO metabolism are elevated in diabetic patients. The serum concentration of MGO is 5-6 times higher in patients with insulin-dependent diabetes mellitus and 2-3 times higher in those with non-insulin-dependent diabetes mellitus (Thornalley 1996). Accumulation of MGO and the formation of AGEs also occur at an increased rate in patients with diabetes or hyperglycemia (Lo *et al.* 1994; Jensen *et al.* 2015). As AGE formation interferes with cell function it can lead to complications. Even though blood sugar levels are controlled in diabetic patients, these patients still have increased MGO levels that form per unit glucose (Jensen *et al.* 2015).

Several studies have been done on the involvement of MGO and AGE formation in diabetic complications. Loss of pericytes and potential blindness is one of the symptoms of diabetes. The reason for this is however not yet fully understood. One of the theories is that the formation of AGEs causes apoptosis. MGO levels are elevated in the lenses of diabetic patients and these MGO levels are believed to contribute to the formation of cataracts via MGO-mediated formation of AGEs. In a study done by Kim *et al.* (2004) the effect of elevated MGO levels on bovine retinal pericytes was evaluated. After 6 hours of exposure to MGO signs of apoptosis were observed in bovine retinal pericytes. However, the levels of MGO used in this study (200 – 800 µM) was however much higher than the plasma levels found in diabetic patients.

Another complication associated with long term diabetes is diabetic cardiomyopathy which is defined as ventricular dysfunction. Heart muscle cells become impaired due to the proliferation of cardiac fibroblasts and excessive formation of ECM components such as collagen and fibronectin. The reason as to why this happens is however not known. It has been suggested that the formation and accumulation of AGEs contributes to the stiffness of the heart muscle due to cross-linking, increased collagen formation or reduced production of NO. In a study by Oguri *et al.* (2014) it was found that MGO caused Ca^{2+} influx into human

adult ventricular cardiac fibroblast cells in a dose dependant manner. MGO was also found to promote progression in the cell cycle of these cells from the G_1/G_0 phase to the S phase as well as well as promote progression and differentiation of cardiac cells. It is thought that MGO causes the activation of transient receptor potential (TRP) channels, specifically TRPA1, which promotes cell cycle progression and differentiation via the increased influx of Ca^{2+}.

MGO exposure causes apoptosis in RINm5F insulin-secreting cells as well as in rat pancreatic β-cells after 4 – 6 hours to MGO concentrations of 0.1 – 10 mM (Sheader *et al.* 2001). This poses a risk to insulin secreting cells in patients with hyperglycemia as glucose levels are elevated in these patients. Fewer insulin secreting cells may lead to a reduced capacity to remove glucose from the blood (Sheader *et al.* 2001). Carbohydrates, such as glucose are precursors for the formation of MGO (Jia *et al.* 2012) Therefore further complications may also arise due to a reduced capacity to remove excess glucose from the blood resulting in increased MGO production.

Chang *et al.* (2011) discovered that MGO modifies and activates Atk1. When Atk1 becomes phosphorylated it becomes active and promotes cell proliferation and inhibits apoptosis. Atk1 normally forms a disulfide bond within its structure between Cys_{77} and Cys_{60}. This prevents phosphorylation and activation. MGO has the ability to break this thiol group causing phosphorylation. This then leads to increased vascular smooth muscle proliferation mediated by active Atk1. This activation and increased growth may be a contributing factor in diseases such as hypertension and diabetes. In agreement with this study Jia *et al.* (2012) discovered that increased MGO levels promoted the proliferation of 3T3-LI adipocyte-like cells. This was due activation and modification of Akt1 via phosphorylation. It caused the cells to progress faster through the phases of the cell cycle to the S phase. This study suggested that MGO exposure may lead to an increase in lipid accumulation and the number of adipocytes.

In addition to binding to and modifying certain proteins, MGO also modifies certain mitochondrial membrane proteins. This results in changes in the mitochondrial metabolism and a resultant increase in production of ROS. In diabetes these dysfunctions are caused in particular in tissues such as the heart, brain and skeletal muscle that rely heavily on aerobic metabolism (Rosca *et al.* 2005).

Aldehyde reductase protected cells against MGO toxicity. However, in diabetic patients, this enzyme is inactivated and consequently the detoxification of MGO will be less efficient (Suzuki *et al.* 1997). The GSH dependant glyoxylase I-II system is another method of MGO detoxification. Both GO and MGO in the blood binds GSH (Suzuki *et al.* 1997; Nomi *et al.* 2009). However since sugar, GO and MGO levels are higher than normal in diabetic and

hyperglycemic patients GSH can become depleted as there may be enough GSH available to keep up with the increased production of these compounds. This leads to subsequent inhibition of GSH dependent enzymes (Nomi *et al.* 2009).

MGO has been identified as the major antibacterial component of Manuka honey. This type of honey has been clinically shown to promote wound healing. Concern has been raised that the concentrations found in Manuka and other honey such as the MGO positive honeys from South Africa inhibits cellular growth.

2.5 Aim and objectives

2.5.1 Aim

The aim of this study is to determine if MGO levels as found in southern Africa honey samples effectively kills bacteria without causing cytotoxic cellular effects.

2.5.2 Objectives

1. To develop a rapid method to quantify MGO and determine the MGO content of South African honey samples.
2. To determine the antibacterial activity of a MGO concentration range on Gram positive and negative bacteria.
3. To determine the effect of MGO on the morphology of Gram positive and negative bacteria.
4. Based on the findings of objective 1 and 2, to determine whether the concentrations, as found in southern Africa honey samples, effectively kills bacteria.
5. To determine the cytotoxicity of a MGO concentration range in the SC-1, Caco-2 and RAW 264.7 cell lines.
6. To determine the effect of MGO on the morphology and degree of cellular differentiation in each cell line.
7. Based on the findings of objective 1 and 5, to determine if the levels of MGO found in South African honey samples causes cellular death.
8. Based on the findings of objective 4 and 7, to determine if MGO concentrations that effectively kill bacteria are cytotoxic.

Chapter 3: Development of a colorimetric method for methylglyoxal quantification in honey samples

3.1 Introduction

From as early as 1600 BC, honey was used for treating wounds by soaking linen in a honey-oil solution and then applying it to the wound. It was also used as an antimicrobial treatment and is still used today due to the fact that it is effective even against antibiotic-resistant bacteria (Stewart *et al.* 2014).

As previously mentioned the antibacterial and wound healing abilities of honey is attributed to several physical properties and molecules contained within the honey such as its high viscosity, hygroscopic and hyperosmotic nature as well as the honey's acidity. These properties are discussed in more detail in section 2.1.1 (Mavric *et al.* 2008; Stewart *et al.* 2014).

There is also the possibility that honey can be used to aid in the healing of nosocomial infections and chronic wounds as discussed in section 2.3.2 (Sassi-Gaha *et al.* 2010).

The use of Manuka honey to treat infections is a well characterised form of treatment that has been found to be effective against a wide range of wounds as well as wound- associated pathogens (Mavric *et al.* 2008; Pieper 2009). The antibacterial properties of Manuka are due to the presence of H_2O_2 and/or bee defensin, an antimicrobial peptide, as well as MGO (Mavric *et al.* 2008; Kwakman *et al.* 2010; Stewart *et al.* 2014).

Manuka honey, derived from *Leptospermum scoparium* indigenous to New Zealand, is specifically high in its MGO content (Stewart *et al.* 2014). It is prepared using gamma irradiation so as not to destroy some of the important components of the honey and in order to retain the highest possible concentration of MGO in the honey (Pieper 2009; Stewart *et al.* 2014). The UMF (unique Manuka factor) of the honey is directly related to its MGO content and the concentration of various types of Manuka honey ranges from 38.4 – 761 mg/kg (Mavric *et al.* 2008).

MGO has been identified as the main antibacterial component of Manuka honey since the honey retained its antibacterial activity after the removal of H_2O_2 using catalase (Kwakman *et al.* 2010).

Although Manuka honey is well characterised and an effective method of treating wounds it is expensive to import since the tree from which the bees feed on is indigenous only to New

Zealand. Southern Africa has a well described floral biodiversity with the possibility of an indigenous honey type being discovered with similar or greater wound healing properties than Manuka honey. The purpose of this part of the study is to collect honey samples within this region and to determine the MGO content of a selection of these samples using a newly developed colorimetric assay. If these samples are found to be comparable to Manuka honey with regards to MGO content it may be possible to investigate the possibility of making some of these honey into medical grade honey for the use of wound treatment in South Africa.

3.2 Aims and objectives

3.2.1 Aims

The aim of this study is to evaluate different methods of quantifying MGO and to develop a new rapid method determine the MGO content of 12 South African honey samples. The content of these samples was also compared to that of a UMF 15 Manuka honey.

3.2.2 Objectives

1. To develop a rapid method to quantify MGO and determine the MGO content of South African honey samples.

3.3 Materials and methods

3.3.1 Materials

3.3.1.1 Honey samples

Twelve honey samples from southern Africa were collected from 2014 – 2015 from previous studies (Majtan 2011). These included fynbos (FB) samples (FB4, FB6, FB15, Overberg FB, Malagas FB and Fynbos from Woolworths), gum tree samples (Blue gum and Rivergum), Malaga honey, raw Acacia and samples from Mozambique (MozmSemb and W6CH) as well as Manuka UMF 15 honey that served as control.

3.3.1.2 Reagents, equipment and disposable plastic ware

Methylglyoxal (MGO) ($C_3H_4O_2$), glyoxal (GO) ($C_2H_2O_2$), N-acetylcysteine (NAC) ($C_5H_9NO_2S$), Gluthathione (GSH) ($C_{10}H_{17}N_3O_6S$) and 5,5-Dithiobis-2-nitrobenzoic acid (DTNB) ($C_{14}H_8N_2O_8S_2$) was obtained from Sigma Aldrich, Johannesburg, South Africa (SA). Sodium hydroxide (NaOH), sodium chloride (NaCl), disodium phosphate (Na_2HPO_4), sodium phosphate monobasic dihydrate ($Na_2HPO_4 \cdot H_2O$) and ethanol (EtOH) was of analytical

quality and was obtained from Merck Chemicals, Modderfontein South Africa (SA). Water was double distilled (ddH_2O) and de-ionised ($dddH_2O$) with a Continental Water System.

Equipment used included an Omega plate reader (BMG Labtech, Johannesburg, SA), a Lambda LS5OB spectrophotometer (Separations Scientific, Honeydew, SA). A Crison GLP 21 pH Meter and Eppendorf pipettes from Eppendorf AG Hamburg, Germany supplied by the Scientific Laboratory Equipment Company (LASEC), Cape Town, S.A. was used.

Disposable plasticware includes: 24 well plates, 96 well plates, 50 ml, 15 ml tubes and pipette tips (10, 25, 100, 200, and 1000 µl) and was obtained from Greiner Bio-one also supplied by LASEC.

3.3.2 Methods

3.3.2.1 Stock and working solutions

3.3.2.1.1 MGO, GO, GSH, NAC and DTNB stock and working solutions

For all experiments the stock and working solutions were prepared in the same way.

A stock solution of MGO was prepared by diluting a 40% solution of MGO with ddH_2O to a ratio of 1:1. From this stock solution a working solution was prepared by diluting the working solution a further 40x using ddH_2O to give a final concentration of 81.18 mM.

A working solution of GO was prepared by diluting a 40% solution of GO with ddH_2O to a ratio of 1:1. This yielded a final concentration of 437.63 mM.

A 0.2 M PBS solution was prepared by dissolving 12.78 g Na_2HPO_4 in 450 ml dH_2O and, 2.76 g $NaH_2PO_4.H_2O$ in 100 ml dH_2O. Next 405 ml of the Na_2HPO_4 solution and 95 ml of the $NaH_2PO_4.H_2O$ solution was combined and 8.766 g NaCl was added to this solution. The pH was adjusted to 7.4 using NaOH/HCl.

A stock solution of 109.6mM GSH was prepared by dissolving 67.4 mg GSH in 2 ml PBS and a 109.6 mM NAC stock solution was prepared by dissolving 35.8 mg NAC in 2 ml PBS. Both solutions were diluted a further 50x using PBS to make working solutions of 2.19 mM.

A DTNB solution was prepared by dissolving 8 mg of DTNB powder in 1 ml 98% EtOH and then diluting the solution by adding 7 ml 0.2 M PBS, pH 7.4. This solution has a final concentration of 2.52 mM.

3.3.2.1.2 Honey working solutions

For all experiments a 25% (v/v) honey solution was used.

3.3.2.2 Quantification of methylglyoxal using existing methods

To achieve objective 1, it was first necessary to evaluate existing methods for MGO quantification and then develop a method for the rapid quantification of MGO in honey. MGO content can be determined by means of two commonly used methods. The first method measures the reaction that takes place between NAC and MGO (Figure 3.1 A). This reaction forms a product called N-α-acetyl-S-(1-hydroxy-2-oxo-prop-1-yl) cysteine that absorbs at 288 nm (Wild *et al.* 2012). The second method involves the reaction of MGO with GSH (Figure 3.1 B) to form a hemithioacetyl product which is enzymatically converted by glyoxalase 1 to S-D-lactoyl-glutathione that absorbs at 240 nm (Wild *et al.* 2012). The key to both reactions is the binding of MGO to a thiol- containing molecule. Due to the non-specificity of both methods (i.e. interference of other molecules such as protein at 240 nm and 288 nm) and the expense of the enzymatic method a new method based on the principles of the above methods that allows the quantification of MGO in the visible region if the light spectrum, was developed.

A

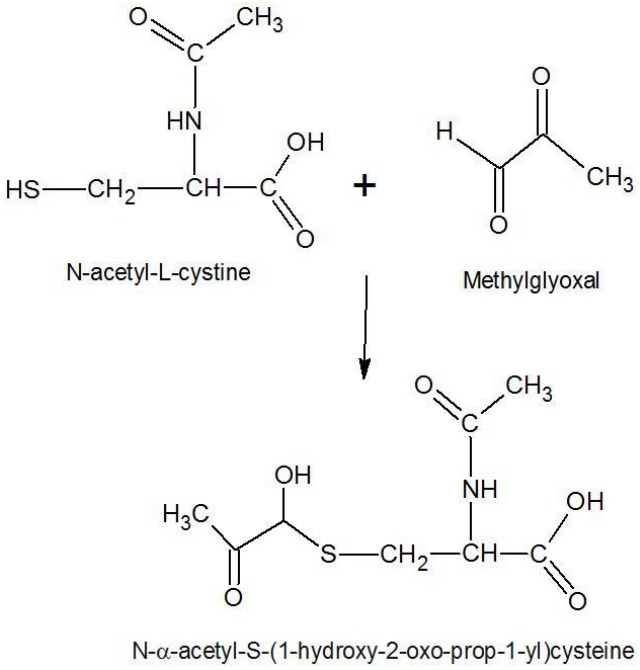

B

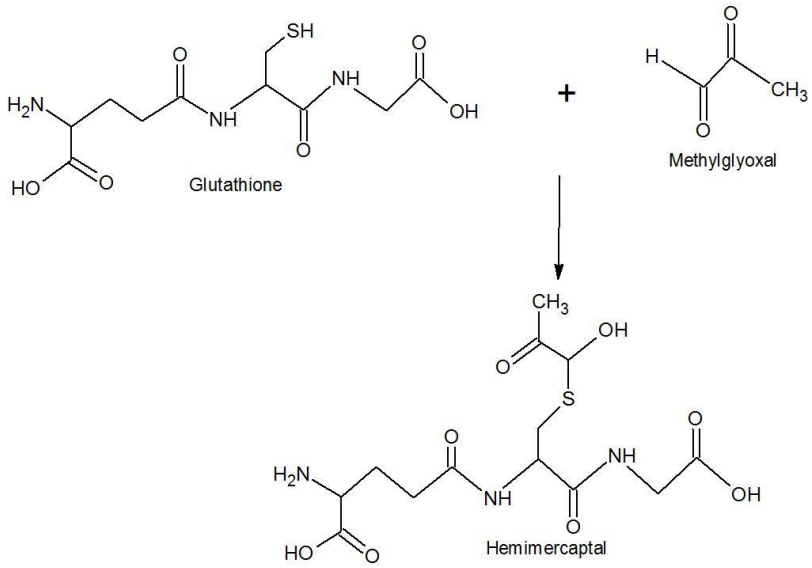

Figure 3.1: Chemical reactions of A): NAC and MGO and B) GSH and MGO

3.3.2.2.1 Quantification of methylglyoxal by means of the NAC assay

This method is based on the rapid reaction that takes place between NAC and MGO. The absorbance of the product, N-α-acetyl-S-(1-hydroxy-2-oxo-prop-1-yl) cysteine, can be read at 288 nm (Wild *et al.* 2012).

To prepare a standard curve, increasing concentrations of the MGO working solution as prepared in Section 3.1.2.1 was added to a 96-well plate in triplicate and made up to a final

volume of 180 µl with ddH_2O. A volume of 20 µl of NAC or GSH working solution was then added to each well. The final concentration of MGO in the wells ranged from 0 – 16.24 mM. The absorbance was measured at 288 nm.

The absorbance of MGO (0 – 12.177 mM) prepared to a final volume of 200 µl using ddH_2O and also measured at 288 nm.

3.3.2.2.2 Honey spectrum

At 288 nm, several molecules such as protein and polyphenols absorb strongly at 288 nm making the quantification of MGO in this region of the absorption spectrum difficult. In order to evaluate the extent of interference the absorption spectrum of 10 southern Africa honey samples as well as UMF 15 Manuka honey was determined from 220 – 500 nm. The samples were prepared by adding 50 µl of each honey working solution (as prepared in section 3.3.2.1.2) to 150 µl ddH_2O in the wells of a 96-well plate to make up a final volume of 200 µl. The final concentration of each sample was 6.25% (v/v).

3.3.2.3 Development of a new colourimetric method for the quantification of methylglyoxal

NAC and GSH both react rapidly with MGO (Wild *et al.* 2012). Both NAC and GSH can also react with DTNB due to the presence of a single thiol to form a yellow product that absorbs at 412 nm (Masip *et al.* 2006). These two reactions were used to develop a new method to quantify MGO.

3.3.2.3.1 Standard curve with NAC/GSH at 412 nm

The Ellman's method for quantifying thiol groups is based on the reaction of thiols with DTNB to form a yellow dianion of 5-thio-2-nitrobenzoic acid (Figure 3.2).

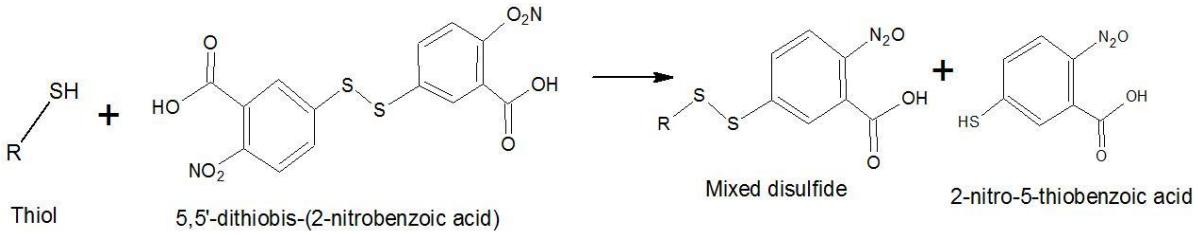

Figure 3.2: DTNB reaction with thiol group

A standard curve for NAC with MGO and GSH was prepared with a final concentration range of 0 – 0.218 mM. To increasing volumes (0 – 10 µl) of the working NAC and GSH solution were added in triplicate to the wells of a 96 well plate. Final volumes were 100 µl, prepared

with ddH_2O. Samples were mixed well and then 100 µl DTNB was added. Samples were mixed well before the absorbance was measured at 412 nm.

3.3.2.3.2 Standard curve with NAC/GSH and increasing MGO at 412 nm

As shown in Figure 3.1 MGO binds rapidly to NAC and GSH. If MGO is added to a solution that contains an excess GSH, MGO will bind GSH. With increasing concentrations of MGO there will be a concentration dependent decrease in the amount of GSH that can be quantified. Theoretically this amount of unreacted GSH can be quantified with DTNB.

To 0.138 mM NAC and 0.4023 mM GSH increasing concentrations of MGO was added. For NAC and GSH this was 0 – 16.44 mM and 0- 21.92 mM respectively. All samples were made to a final volume of 100µl. These were the MGO concentrations that resulted in a significant reduction in GSH levels. A volume of 100 µl DTNB was added, then the samples were mixed well and the absorbance was measured at 412 nm.

3.3.2.3.3 Absorbance spectrum of all reagent combinations at 412 nm

a) The absorbance of each reagent as used in the determination of MGO content of honey was evaluated. These were in triplicate the following mixtures were prepared in the wells of a 96 well plate.
    a. **H:** A volume of 50 µl of a honey working solution made to a final volume of 200 µl with ddH_2O.
    b. **GSH:** A 50 µl volume of the of GSH working solution B, and 100 µl DTNB was added together mixed well and then was made to a final volume 200 µl.
    c. **H + GSH (OBS):**A volume of 50 µl of a honey working solution and 50 µl volume of the of GSH working solution B were added together mixed well before 100 µl DTNB was added to a final volume 200 µl.
b) **CALC:** $Abs_H + Abs_{GSH}$

3.3.2.4 Other dicarbonyls

Other dicarbonyls found in honey are 3-DG and GO. GO and MGO have a similar structure which means that GO might also react with GSH or NAC giving and over estimation of the amount of MGO present in a sample.

3-DG was not commercially available and therefore the reactivity of 3-DG with NAC or GSH is unknown. An extensive search of the literature provided no information on a possible interaction between NAC or GSH and 3-DG.

To determine if GO also reacts with NAC or GSH the assay described in Section 3.3.2.3.2 was repeated using GO instead of MGO. All the solutions used in this experiment were prepared as described in Section 3.3.2.1.1.

Increasing concentrations of GO was added to the wells of a 96-well plate in triplicate for each concentration. All the wells were made up to an equal volume of 80 µl using ddH_2O. A volume of 20 µl (0.219 mM final concentration) NAC working solution was then added to each well. Next a volume of 100 µl DTNB was added to each well. This yielded a final concentration range for GO of 0 – 875.26 mM. Absorbance was measured at 412 nm. The data was compiled in a graph of concentration GO vs. Absorbance. The same procedure was then carried out using GSH instead of NAC.

3.3.2.5 Quantification of MGO in honey samples from southern Africa

In order to achieve objective 1 the MGO content of 12 South African honey samples was determined using a newly developed colorimetric method. All the solutions used in this experiment was prepared as described in Section 3.3.2.1.1 and the honey samples were prepared as described in Section 3.3.2.1.2.

3.3.2.6 Summary of methodology

The assay was done as follows:

a) A standard GSH curve was prepared.
b) A MGO and GSH standard curve was also prepared which is used for the calculation of the conversion factor.
c) A GSH concentration was selected that gave an absorbance reading of approximately 0.9. For most of the standard curves it was found that a concentration of 0.1097 mM (10 µl) of GSH. From this data a working solution (1 GSH: 4 PBS), solution B was prepared.
d) For each honey sample a 25% solution was prepared.
e) In triplicate the following mixtures were prepared in the wells of a 96 well plate.
    a. **H:** A volume of 50 µl of a honey working solution made to a final volume of 200µl with ddH_2O.
    b. **GSH:** A 50 µl volume of the of GSH working solution B, and 100 µl DTNB was added together mixed well and then was made to a final volume 200 µl.
    c. **H + GSH (OBS):** A volume of 50 µl of a honey working solution and 50 µl volume of the of GSH working solution B were added together mixed well before 100 µl DTNB was added to a final volume 200 µl.

f) **CALC:** $Abs_H + Abs_{GSH}$
g) **CALC – OBS**, absorbance of bound GSH. Using the standard curve in a) the concentration of GSH can be calculated.
h) mM GSH can be converted to mM MGO using the conversion factor = 50.
i) mM, mmol/l can be converted to mg/kg (molecular mass of MGO is 72.063 g/mol,, density 1ml = 1.3 mg).
j) Controls must include UMF honey with a known MGO content.

3.4 Results and discussion

MGO has been identified as the major antibacterial component of honey (Mavric *et al.* 2008). The MGO detoxification pathway serves as the basis of methodologies used for the quantification of MGO due to its ability to bind thiol groups. To quantify the MGO content there are several methods that can be used. The gold standard method is an enzyme catalysed method that makes use of glyoxylase I to isomerise the hemithioacetal product of GSH and MGO to S-D-lactoylglutathione (Wild *et al.* 2012). A disadvantage to this method is that recombinant or purified glyoxylase I is expensive. Also, the absorbance of the product is measured at 240 nm, a wavelength where other proteins and polyphenols interfere (Serem and Bester 2012).

The formation of methylglyoxal-bis-2,3-DNP-hydrazone via the reaction of MGO with 2,4-dinitrophenylhydrazine (2,4-DNPH) can also be used for the quantification of MGO. Although methylglyoxal-bis-2,3-DNP-hydrazone absorbs at 432 nm (Wild *et al.* 2012), DNPH is sensitive to friction and can therefore be dangerous as the reagent can explode. Another drawback is that the product, MG-bis-2,3-DNP-hydrazone, sometimes precipitates out of the solution resulting in an underestimation of MGO content (Wild *et al.* 2012).

Another method developed by Wild *et al.* (2012) is based on the rapid reaction between MGO with NAC forming N-α-acetyl-S-(1-hydroxy-2-oxo-prop-1-yl) cysteine which absorbs strongly at 288nm (Wild *et al.* 2012), a wavelength where protein and polyphenols cause interference.

The HPLC method is an accurate analytical method that is often used for the quantification of MGO. A limitation is that this technique is expensive and requires the use of specialised equipment (Schalkwijk 2015).

Therefore an objective of this study was to evaluate the method of Wild *et al.* (2012) and then based on this method develop a colorimetric method for the quantification of MGO.

3.4.1 Quantification of methylglyoxal by means of the NAC assay

Briefly, as described in Section 3.2.2.1, to a standard NAC increasing concentrations of MGO was added and the absorbance of the product that forms was measured at 288 nm (Figure 3.3 A). GSH also reacts with MGO in a manner similar to NAC and for this reason the absorbance of the product that forms between GSH and MGO were also evaluated (Figure 3.3 B). The absorbance of MGO in the absence of NAC and GSH was also evaluated (MGO only, Figure 3.1).

A

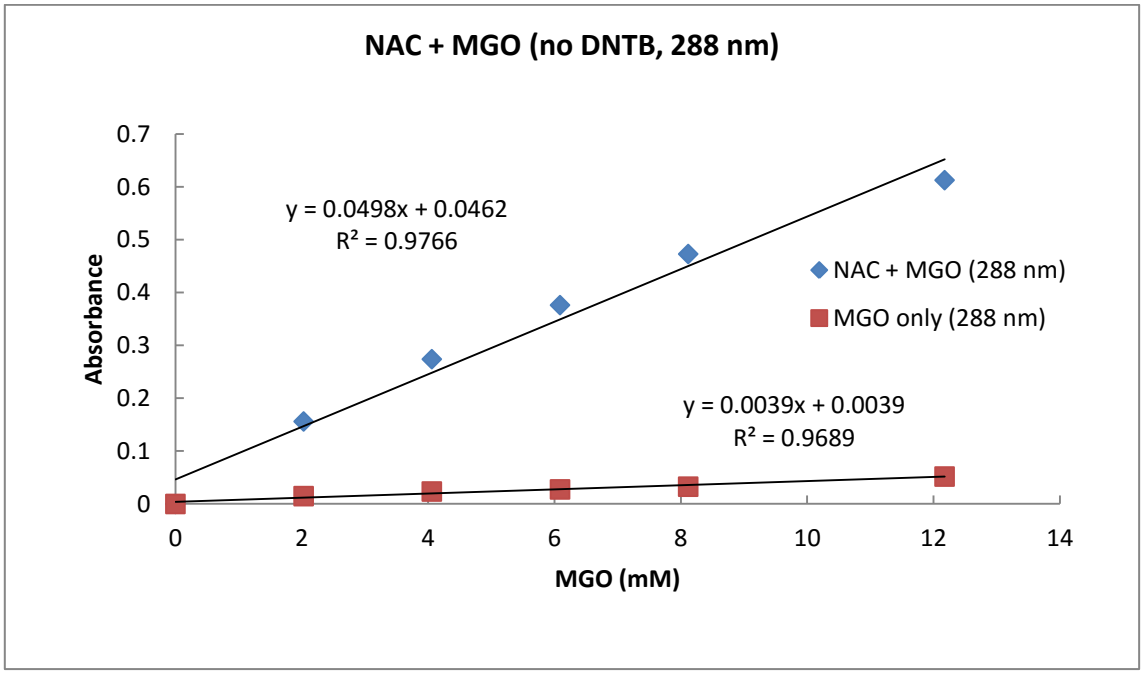

B

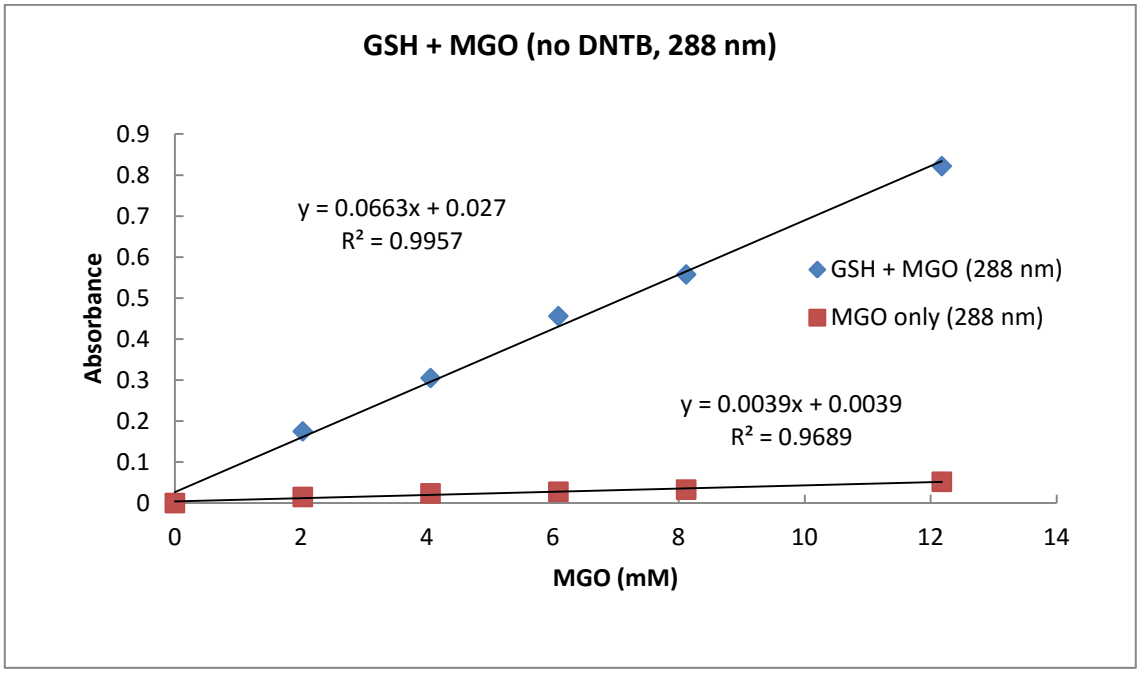

Figure 3.3: Increasing concentrations of MGO added to (A) NAC and (B) GSH and absorbance was measured at 288 nm. Data is an average of three experiments ± SEM.

A good linear correlation was obtained when NAC or GSH is added to increasing MGO concentrations and measured at 288 nm with an r^2 value of 0.957 and 0.974 for NAC and GSH respectively. Both the NAC and the GSH graph have a similar slope (0.0498 vs. 0.0663, 1.33 fold difference) meaning that either NAC or GSH can be used as both reagents rapidly form products that absorb at 288 nm. The absorbance of MGO is low and is 12.76 and 17 fold less than that of MGO + NAC and MGO + GSH. Wild *et al.* (2012) reported an

extinction coefficient of 249 $M^{-1}cm^{-1}$ for the reaction between MGO and NAC. Other studies have reported a value of 98±6 $M^{-1}cm^{-1}$. Using the value reported by Wild *et al.* (2012) the concentration of MGO in the working solution can be determined to be 0.66 mM. This lower MGO level may be due to differences in format used for quantification (cuvette vs. microplate), temperature and/or the occurrence MGO as the free monomer, monohydrate, dehydrate and other oligomerisation products in solution.

3.4.2 Honey spectrums

To confirm that honey contains molecules that cause interferences at 288 nm, the absorbance spectrums each of 10 southern Africa honey samples as well as UMF 15 Manuka honey were compiled (Figure 3.4). All honey samples showed strong absorbance at 288 nm (indicated as red line) whereas absorbance at 412nm was reduced (Table 3.1). Honey contains proteins such as enzymes and peptides. Proteins have absorption maxima from 275 – 280 nm due to the absorbance of the two aromatic amino acids tryptophan (Trp) and tyrosine (Tyr) and to a lesser extent the absorbance of cysteine disulphide linkages (Schmid 2001). Polyphenols also have a typical aromatic structure and also absorb strongly in this region of the spectrum.

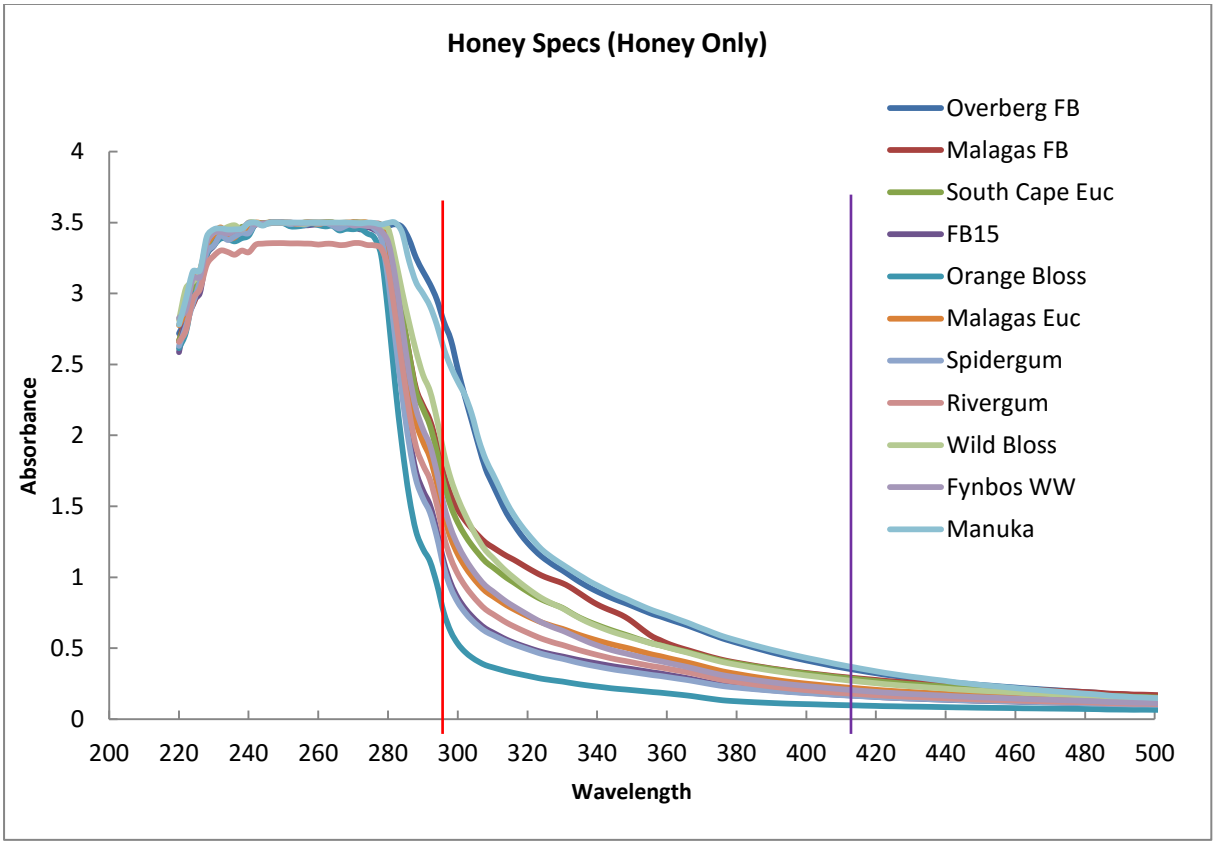

Figure 3.4: Absorbance of honey samples from 220 – 500nm. Data is an average of five experiments. Red and purple line indicates absorbance at 288 and 412 nm respectively.

Table 3.1: Average absorbance readings at 288 and 412 nm		
Wavelength	**Absorbance range**	**Average absorbance reading**
288 nm	1.324 – 3.253	2.2345
412 nm	0.097 – 0.327	0.2384

3.4.3 Development of a new colorimetric method for the quantification of methylglyoxal

As mentioned before NAC and GSH react with both MGO and DTNB (Masip *et al.* 2006; Wild *et al.* 2012). In an excess of NAC and GSH the unreacted NAC and GSH theoretically can be quantified based on the ability of NAC and GSH to react with DTNB to form a yellow product (Nekrassova *et al.* 2002) which absorbs at 412 nm. At this wavelength the interference by proteins and polyphenols is reduced (Figure 3.4 and Table 3.1).

3.4.3.1 Standard curve with NAC/GSH at 412 nm

A standard curve using NAC or GSH (0 – 0.218 mM) was prepared (Figure 3.5). The gradient was 3.344 and 3.666 for NAC and GSH respectively. The r^2 was 0.9997 for both standard curves. From the molar extinction co-efficient for DTNB, 14.15 x 10^3 $M^{-1}cm^{-1}$ at 25°C, (Eyer *et al.* 2003) an absorbance of 0.5 is equivalent to 0.118 mM NAC or GSH. Using the line equations, an absorbance of 0.5 is equivalent to 0.151 and 0.138 mM respectively which is 127.9% and 116.9% from the calculated value. This data shows that DTNB effectively binds the single thiol group of NAC and GSH.

A

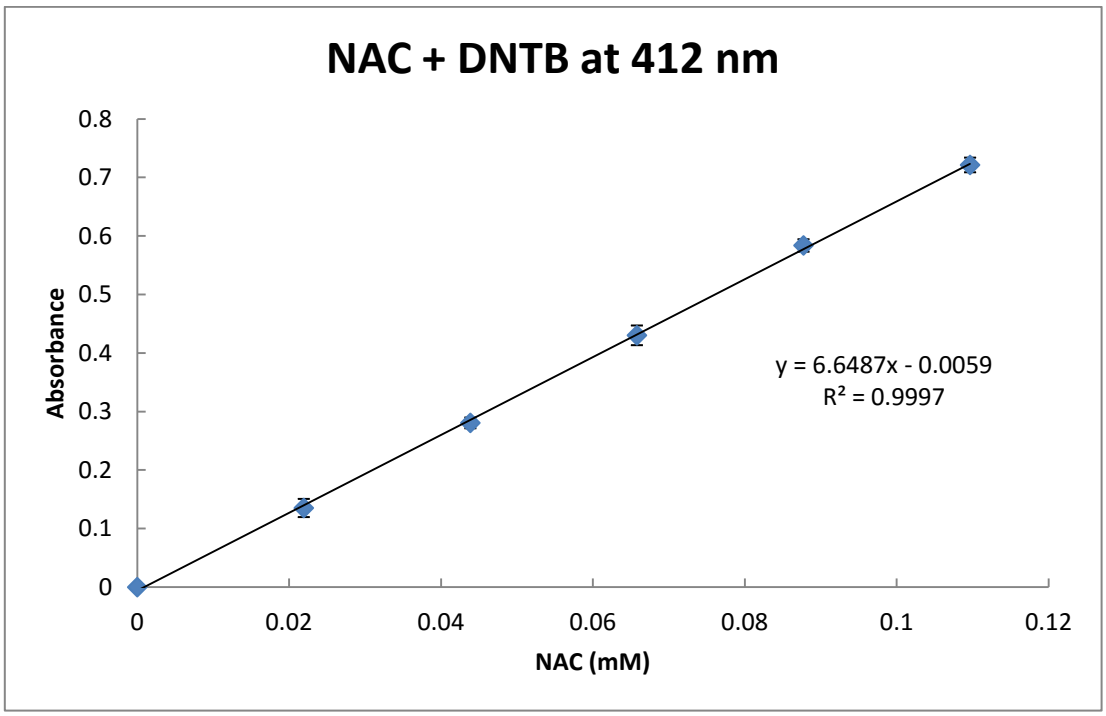

B

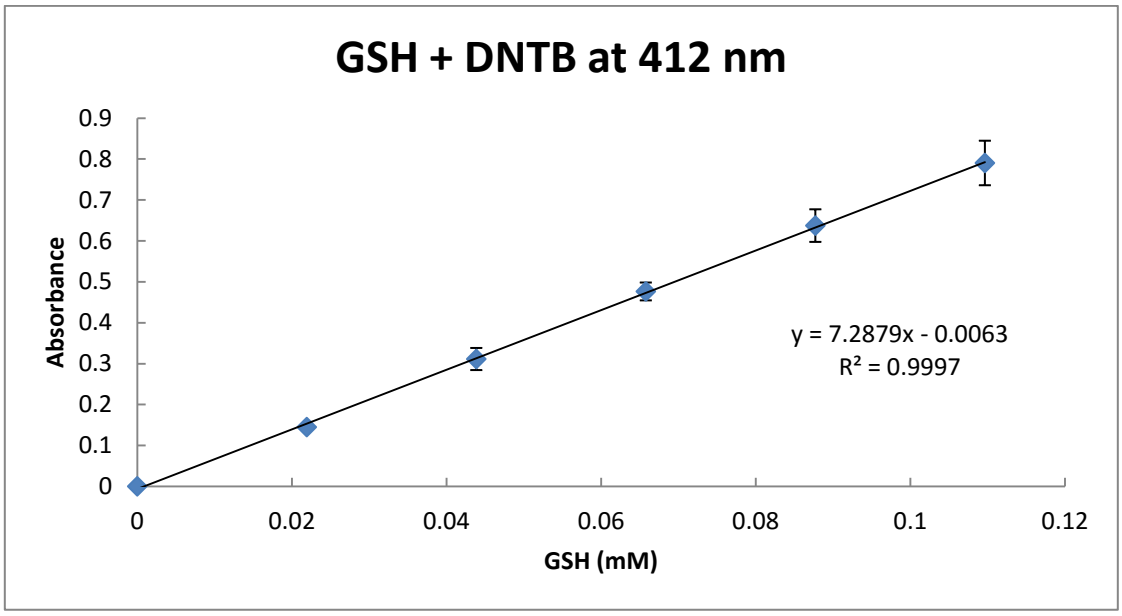

Figure 3.5: Standard curve for NAC and GSH determined with DTNB. Data is an average of four independent experiments ± SEM for A and five independent experiments for B.

3.4.3.2 Standard curve with NAC/GSH and increasing MGO at 412 nm

To a standard concentration of 0.151 mM NAC and 0.367 mM GSH increasing concentrations of MGO was added. The concentration of MGO required to cause a significant decrease in the measured absorbance of GSH is several fold higher than expected (Figure 3.6). Decrease in measured absorbance was -0.0106 and -0.035 for NAC

and GSH respectively. R^2 was 0.968 for NAC and 0.970 for GSH. From this data the percentage decrease in absorbance relative to the control, no MGO can be calculated. This data for both NAC and GSH is presented in Figure 3.7.

A

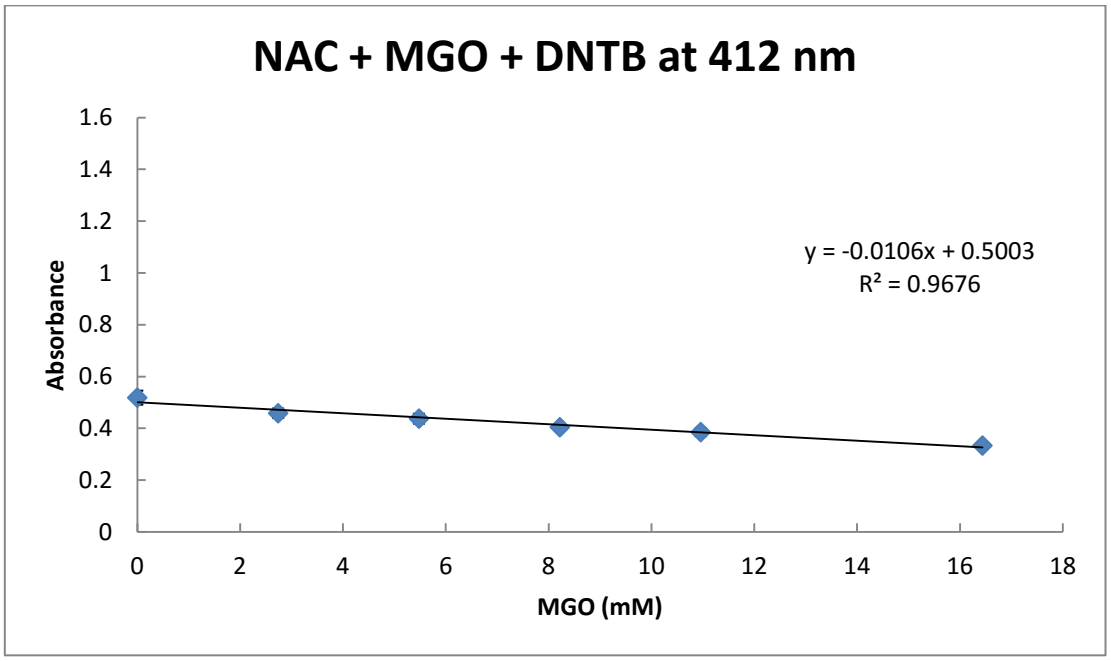

B

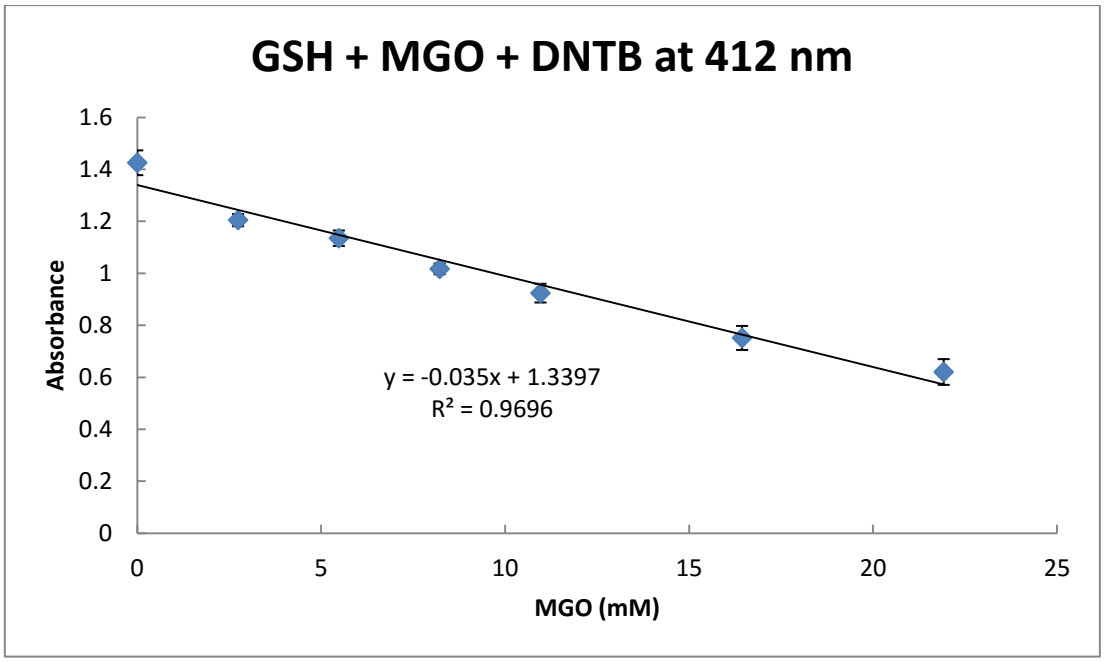

Figure 3.6: Effect of increasing MGO added to (A) 0.151 mM NAC and (B) 0.367 mM GSH. Unreacted NAC and MGO were quantified with DTNB. Data is an average of three experiments ± SEM.

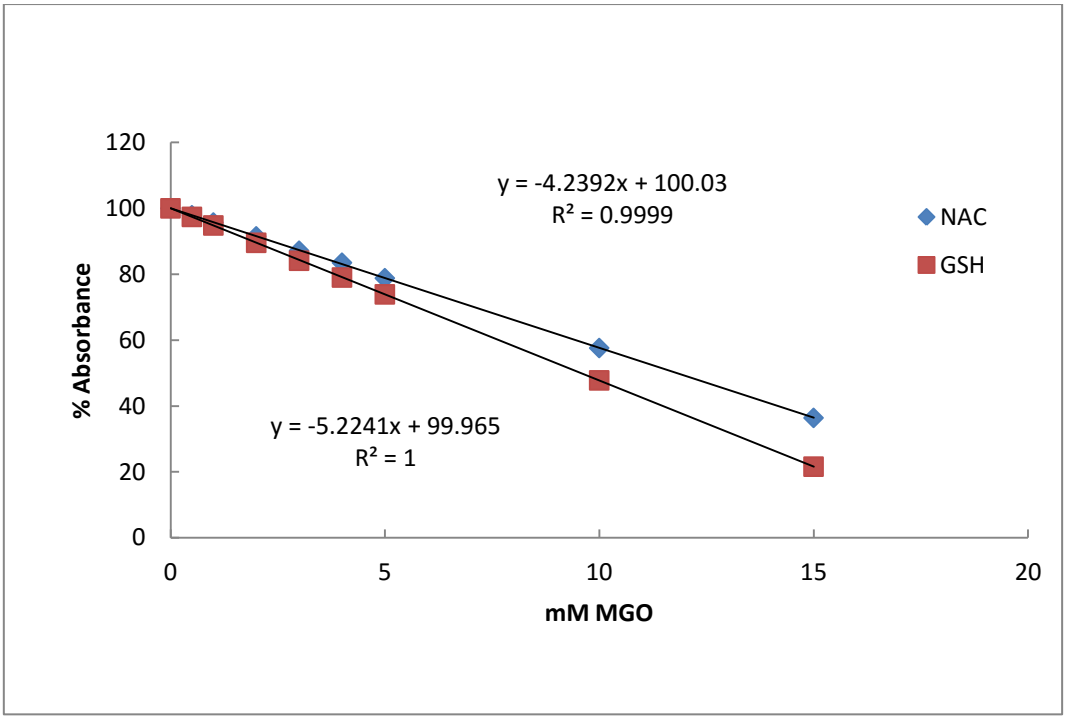

Figure 3.7: Calculated percentage change in absorbance with the addition of increasing concentrations of MGO (0 – 15.12 mM) to a constant concentration of 0.151 mM NAC and 0.367 mM GSH respectively.

With increasing MGO concentrations there is a linear decrease in absorbance due to a decrease in the amount of free GSH. The gradient for NAC and GSH is -4.239 and -5.224 respectively.

From this data the decrease that represents the mM NAC or GSH that has bound can be plotted against the mM MGO. Inverse of the gradient provides information on the amount of mM MGO that binds 1 mM NAC or GSH. This data is presented in Figure 3.8. This value can be used to convert the mM NAC or GSH to mM MGO. For NAC and GSH this value is 50.00 and 156.25 respectively. As the ratio for NAC is large, further analysis of MGO in honey samples was undertaken with GSH.

The obtained ratios indicate that for every mM GSH or NAC several fold more MGO is required to cause a decrease in absorbance. In the reaction it was expected that equimolar reactions would occur between NAC or GSH and MGO. Likewise the unreacted NAC or GSH would react in an equimolar manner with DTNB. Therefore if 5 mM of NAC or GSH is in solution and 1 mM of MGO is added, then 4 mM NAC or GSH would be remaining to react with DTNB. In the DTNB reaction, the concentration of DTNB is in excess of the thiol containing molecule which in this study is NAC and GSH. Under these conditions DTNB is partially consumed and TNB is formed together with a stoichiometric amount of mixed disulfide (Smitha *et al.* 1988).

In Figure 3.2, TNB^{2-} also contains a free thiol group to which MGO can also bind. The ability of MGO to bind NAC or GSH as well as TNB^{2-} results in more MGO being required before a significant decrease in the levels of GSH or NAC is observed. This effect is very much dependent on the concentration of each reagent and this may account for the larger conversion factor required for NAC (0.151 mM) compared to GSH (0.367 mM). MGO does not only bind thiol groups but also Arg, Lys and terminal amines. GSH is a tripeptide of a Glu, Cys and Gly. MGO can therefore also bind the amine group of Glu.

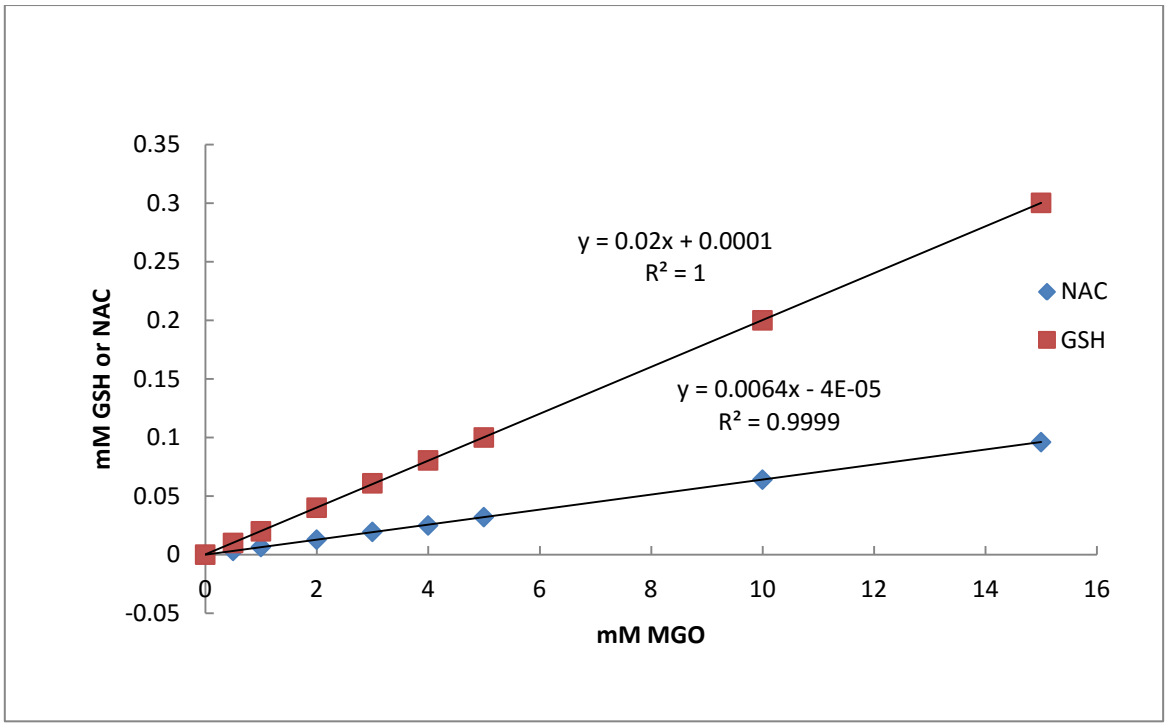

Figure 3.8: The ratio between concentration MGO added to the solution and concentration NAC or GSH reacted with MGO.

3.4.3.3 Calculation of the MGO content of honey

To quantify the MGO content of a selection of southern Africa honey samples a plate was prepared containing the following samples, a) honey alone (made to the same final volume as b and c), b) no honey GSH + DTNB (final absorbance 0.9 – 1.00) and c) honey + GSH + DTNB.

To calculate the MGO content, the calculated GSH content (CALC) was determined (a + b). As MGO present in the honey binds GSH, the amount of free GSH is reduced and this is measured at c), labelled as OBS (Figure 3.9). Therefore CALC – OBS will be a measurement of GSH bound to MGO. Using the conversion factor determined in section 4.2.2, the amount of MGO in each honey sample can be calculated.

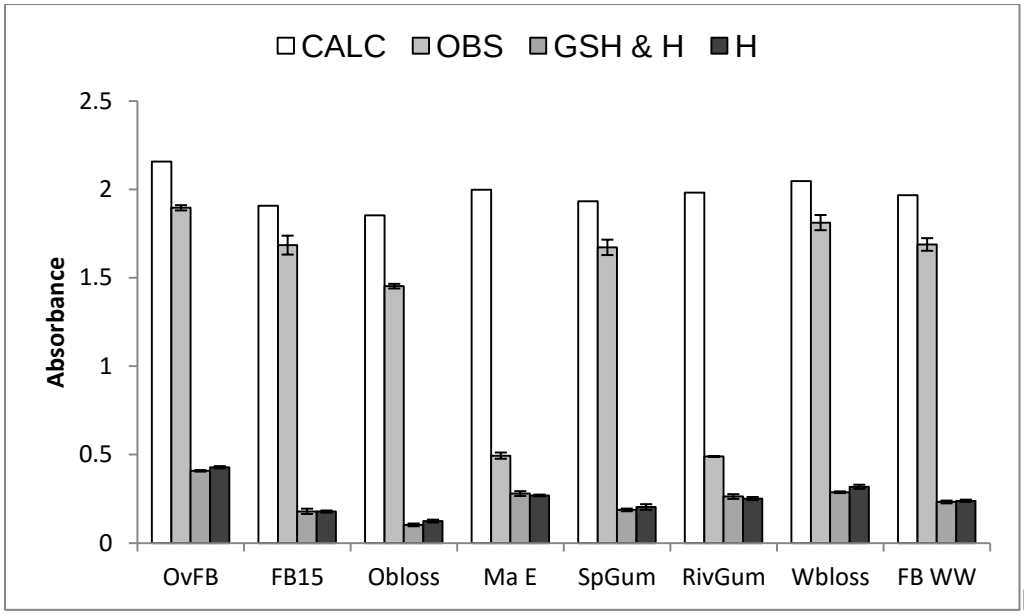

B

Figure 3.9: CALC is (GSH + DTNB) + H, OBS is GSH added to honey + DTNB, GSH + H (no DTNB added) and H only for a selection of 8 honey samples.

3.4.4 Other Dicarbonyls

Other dicarbonyls present in honey are GO and 3-DG. The structure of GO and MGO (Figure 2.1) are similar in structure and therefore it is possible that GO may also react with NAC or GSH resulting in an overestimation of MGO levels. According to Mavric *et al.* (2008) the GO concentration is 1.2, 4.2 and 7.0 mg/kg for UMF 10, 20 and 25 respectively. That is, 0.288%, 0.566% and 0.9% of the MGO for UMF 10, 20 and 25 respectively. Therefore the effect of GO is minimal. Using the same strategy as for MGO, only high GO concentrations (109.41 – 875.26 mM or 6350.16 – 50800 mg/kg) caused a decrease in absorbance (Figure 3.10). In addition the colour of the product that formed between NAC or GSH and DTNB faded rapidly.

Therefore as honey only contains low amounts of MGO and only levels that are 100 fold greater than MGO causes a decrease in the amount of NAC or GSH measured, it can be concluded the effect of GO is negligible. The levels of 3-DG in commercial honey is high, 119 – 1451 mg/kg (Table 2.3). It was not possible to evaluate the effect of 3-DG on this reaction as 3-DG is not commercially available. Due to the structure of 3-DG (Figure 2.1) steric effects may limit the binding of 3-DG to NAC or GSH.

A

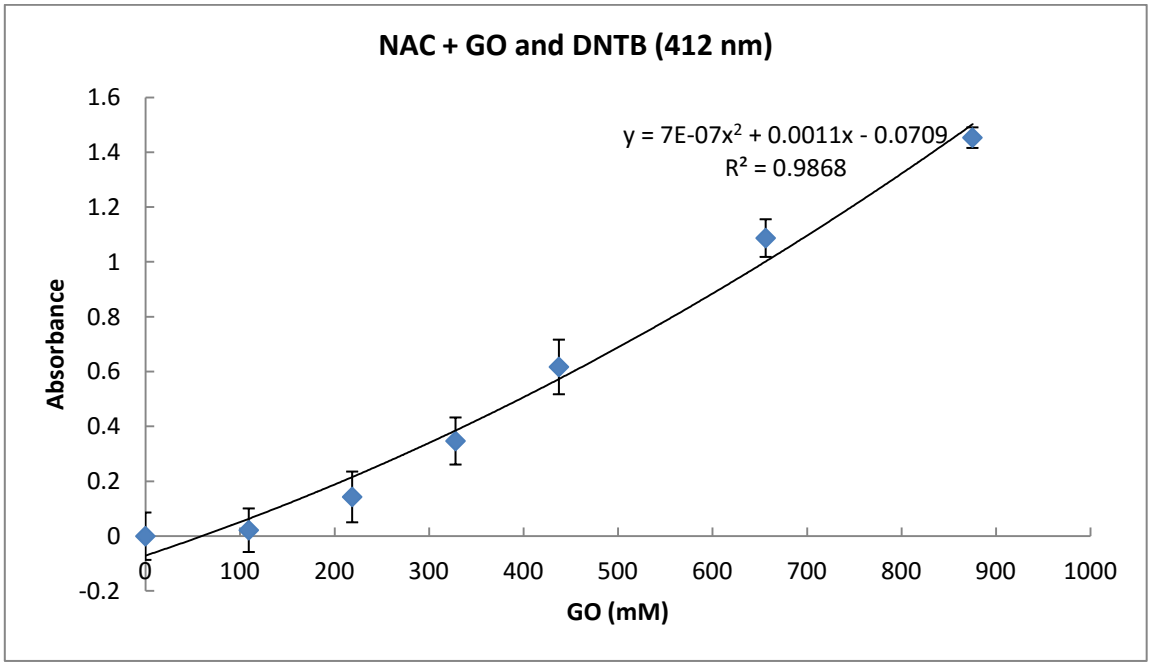

B

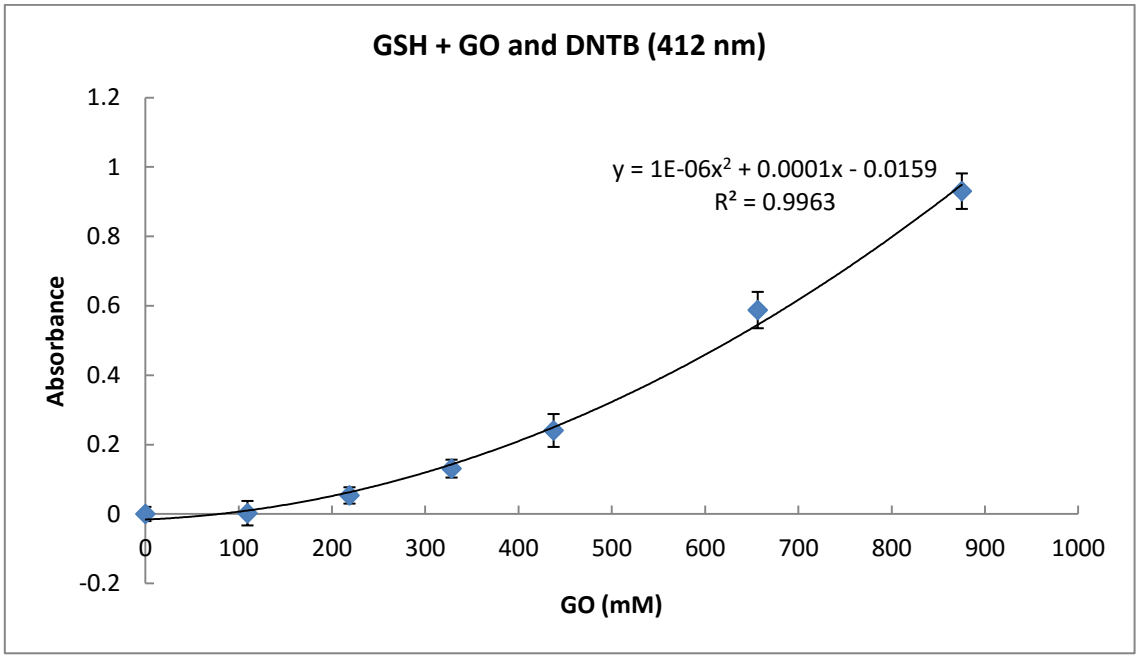

Figure 3.10: The binding between increasing concentrations of GO and NAC and GSH. Unbound NAC or GSH was quantified with DTNB measured at 412 nm. Data is an average of three experiments ± SEM.

3.4.5 Quantification of MGO in honey samples from South Africa

In order to achieve objective 1 the MGO content of 12 South African honey samples was determined using a newly developed colorimetric method as described in Section 3.3.2.5 (Figure 3.11).

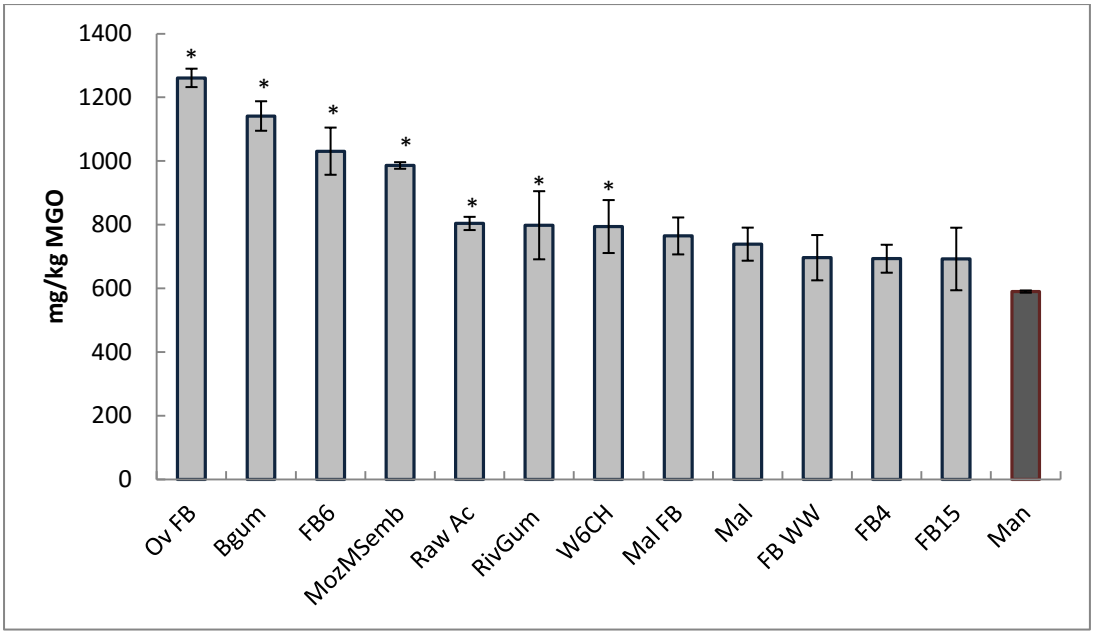

Figure 3.11: The MGO concentrations of 12 honey samples from South Africa as well as a Manuka honey sample using the GSH and NAC method with DTNB at 412 nm. Data is an average of three experiments ± SEM.

MGO content of UMF 15 Manuka as found in this study was an average of 590.28 mg/kg. This compares well to the reported MGO content as stated by the Unique Manuka Factor Honey Association which states that UMF 15 Manuka honey contains no less than 514 mg/kg. The reason it is slightly higher may be because it has been stored for an extended period of time and MGO content increases with storage time. The MGO of the southern Africa honey was 692.587 – 1216.23 mg/kg. According to a one-way-ANOVA analysis the MGO levels in FB15, FB4, Fynbos WW, Malagal and Malagas FB are similar to Manuka UMF 15. The rest of the samples all had levels of MGO that are significantly higher.

3.5 Conclusion

Protein and polyphenols in honey interfere at the wavelengths that are usually used for the quantification of MGO. Based on the ability of MGO to bind NAC and GSH a colorimetric method was developed whereby excess NAC or GSH was quantified using DTNB. In this preliminary study MGO levels in a small selection of southern Africa honey was found to be similar or higher than that present in UMF15 Manuka honey.

Chapter 4: The antibacterial effects of methylglyoxal

4.1 Introduction

As discussed in section 2.1.1 honey contains several molecules as well as physical properties that contribute towards its antibacterial properties. In addition to this the presence of molecules such as MGO, H_2O_2, the peptide bee defensin as well as flavonoids and phenolic acids such as catechin, apigenin, myricetin, caffeic acid and ferrulic acid also contributes to the antibacterial activity of honey (Wahdan 1998; Emsen 2006; Henriques *et al.* 2010; Irish *et al.* 2011).

High levels of MGO and bee defensin accounts for specific antibacterial properties of therapeutic Manuka and Revamil™ source (RS) honey (Mavric *et al.* 2008; Kwakman *et al.* 2010; Sherlock *et al.* 2010; Stewart *et al.* 2014) respectively. Due to these unique antibacterial properties, these honeys are used for therapeutic treatment of many type of wounds including skin grafts, abscesses, pressure ulcers, burns and surgical wounds (Pieper 2009).

Manuka honey is graded according to a Unique Manuka Factor (UMF) which indicates the presence of dihydroxyacetone, leptosperin and variable amounts of MGO (Adams *et al.* 2008; UMFHA 2015). Manuka honey with a UMF > 10 is used for therapeutic purposes and has an MGO content of ≥ 263 mg/kg. Therapeutic honey is sterilized using gamma radiation (Pieper 2009; Stewart *et al.* 2014).

Manuka has been reported to have antibacterial activity against a wide range of bacteria including bacteria resistant to other treatments (Pieper 2009; Stewart *et al.* 2014). MGO effectively kills *E. coli* and *S. aureus* (Talukdar *et al.* 2009) as well as methicillin and oxacillin resistant *S. aureus* (Stewart *et al.* 2014). Kilty *et al.* (2011) reported that MGO was also effective against biofilms of *P. aeruginosa* and *S. aureus* as well as methicillin resistant *S. aureus* although effective concentrations were several times greater than required for plantonic bacteria.

A recent study by Roberts *et al.* (2014) found that Manuka honey reduced the swarming and swimming motility of *P. aeruginosa* due to de-flagellation. The expression of the major structural protein, flagellin was reduced as well as flagellin-associated genes, fliA, FliC, flhF, fleN, fleQ and fleR. De-flagellation of bacteria by Manuka honey would limit bacteria mobility, reduce bacteria adhesion and prevent biofilm prevention. Due to the complexity of honey it is unknown if this de-flagellation effect is directly due to MGO, the major antibacterial component of Manuka honey.

4.2 Aims and Objectives

4.2.1 Aims

The aims of this part of the study was to evaluate the antibacterial activity of MGO using two Gram positive (*S. aureus* and *B. subtilis*) and two Gram negative bacteria (*E. coli* and *P. aeruginosa*) bacteria. The effects of MGO on the morphology of *B. substilis* and *E. coli* and specifically the structure of fimbriae and flagella were then investigated. Finally, it was determined whether the MGO content of southern Africa honey would effectively kill the Gram positive and negative bacteria used in this study.

4.2.2 Objectives

1. To determine the antibacterial activity of a MGO concentration range on Gram positive and negative bacteria.
2. To determine the effect of MGO on the morphology of Gram positive and negative bacteria.
3. Based on the findings of objective 1, chapter 1 and objective 1, chapter 2, to determine whether the concentrations, as found in southern Africa honey samples, effectively kills bacteria.

4.3 Materials and methods

4.3.1 Materials

4.3.1.1 Bacteria lines and reagents

Bacteria were obtained from the Department of Biochemistry, Faculty of Natural and Agricultural Sciences, University of Pretoria. *Escherichia coli* (700928), *Pseudomonas aeruginosa* (10145), *Bacillus subtilis* (13933) that was supplied to them by the American Type Culture Collection and *Staphylococcus aureus* (U3300) supplied to them by the University of Kwazulu Natal.

4.3.1.2 Reagents, equipment and plastic ware

Methylglyoxal ($C_3H_4O_2$) was obtained from Sigma Aldrich, Johannesburg, South Africa (SA). Sodium hydroxide (NaOH), sodium phosphate dibasic dehydrate ($Na_2HPO_4 \bullet 2H_2O$), sodium phosphate (NaH_2PO_4), sodium chloride (NaCl), was of analytical quality and will be obtained from Merck Chemicals, Modderfontein South Africa (SA).

Shimadzu UV-160A, UV-visible recording spectrometer (Kyoto, Japan), a multiscan Ascent V1.24 96-well micro-titre plate reader and a Zeiss Ultra plus FEG SEM was used. Eppendorf pipettes from Eppendorf AG (Hamburg, Germany) supplied by the Scientific Laboratory Equipment Company (LASEC), Cape Town, SA was used.

Disposable plasticware included: 24 well plates, 96 well plates, 50 ml, 15 ml tubes and pipette tips (10, 25, 100, 200, and 1000 µl) and was obtained from Greiner Bio-one also supplied by LASEC.

4.3.1.3 Media, supplements and reagents

Fixatives, polypeptides, salts and organic solvents such as glutaraldehyde, Poly-L-lysine, ethanol (EtOH), sodium hydroxide (NaOH), sodium chloride (NaCl), Hexamethyldisilazane (HDMS), Luria Bertani (LB) Agar plates and LB broth were of analytic grade and purchased from Sigma Aldrich, SA were used.

Water was double distilled and de-ionised (ddH_2O) with a continental water system and all medium, enzyme solutions and buffers was sterilized by filtration through a Millex 0.2 µm filter. Glassware was sterilised at 121°C for 20 min in a Prestige Medical Autoclave (series 2100).

4.3.2 Methods

4.3.2.1 MGO working solution

For all experiments the same stock and working solutions were used. Firstly a stock solution of MGO was prepared by diluting a 40% solution of MGO with ddH_2O to a ratio of 1:1. From this stock solution a working solution of 8.8 mM was prepared using ddH_2O.

4.3.2.2 Antibacterial effects of MGO on Gram positive and Gram negative bacteria

To achieve objective 1 the minimum inhibitory concentration (MIC) of MGO was determined using two Gram positive (*S. aureus* and *B. subtilis*) and two Gram negative (*E. coli* and *P. aeruginosa*) bacteria. Bacteria were grown aerobically in Luria-Bertani (LB) broth at 37°C.

4.3.2.2.1 Culturing of bacteria

The bacteria stock solutions were removed from the -70°C freezer. The bacteria were streaked on separate LB agar plates [1% tryptone, 0.5% yeast extract, 1% sodium chloride, pH 7.5, 2% (w/v) bacteriological agar] using a sterile streaker and grown overnight at 37°C in order to establish single colonies of bacteria. Once single colonies were established, one colony of each bacterium was selected and placed in a flask containing 10 ml LB broth (1%

tryptone, 0.5 % yeast extract, 1% sodium chloride, pH 7.4). The flasks were placed in a shaking incubator at 37°C at 150 rpm and left to grow overnight (14 – 16 h). After the incubation period the bacteria were then diluted 100x using 10 ml of LB broth and left to grow for another 3 hours in the incubator at 37°C on a shaker set at 150 rpm to reach the exponential growth phase. At this point the optical density of the bacteria was read at 600 nm using a 1 cm quartz cuvette. To obtain bacteria in the mid-logarithmic phase, bacteria were grown overnight, diluted 100 times in LB broth and proliferated until an OD_{600} of 0.5 was reached.

4.3.2.2.2 Turbidity assay

The antibacterial activity of MGO, objective 1, was measured as described by Sherlock *et al.* (2010). A MGO working solution was prepared from a 40% MGO solution (Sigma Aldrich, South Africa) with sterile ddH_2O. Midlog phase bacteria were diluted to an OD600 of 0.01 and were exposed to a serial dilution of 0.4 – 4.4 mM MGO. Absorbance of the plate was measured immediately (T0) using a Multiscan Ascent V1.24 96 well micro-titre plate reader at 620 nm. The plate was then placed in an incubator for 24 h at 37°C on a shaker set at 150 rpm. After this incubation period the absorbance was measured again (T24). The absorbance at T0 was subtracted from the absorbance at T24 in order to determine bacterial growth after exposure to MGO. The percent growth inhibition from T0 to T24, compared to the control was calculated.

4.3.2.3 Morphological effects of MGO on Gram positive and negative bacteria

In order to achieve objective 2 the ultrastructure of one Gram positive (*B. subtilis*) and one Gram negative (*E. coli*) bacteria was selected and examined using a scanning electron microscope after having been exposed to MGO.

4.3.2.3.1 Preparation for SEM

Before the bacteria were cultured for SEM, cover slips were coated with poly-L-lysine in order to ensure bacterial attachment to this surface. The cover slips were prepared a minimum of three days prior to the cultivation of the bacteria, to ensure optimal coating. Coating was done as follows: The glass cover slips were washed in an ethanol and NaOH solution in a petri-dish. A 60% ethanol solution and a 10% NaOH solution was prepared separately and then combined in a 1:1 ratio before adding to the cover slips. The perti-dish containing the cover slips was placed on the shaker for 2 hours at room temperature. After incubation the ethanol:NaOH solution was removed and the glass cover slips were then washed 5x in ddH_2O. Following this washing step all further procedures were undertaken

under sterile conditions in a flow hood. The glass cover slips were washed again with ddH_2O and then finally with 100% ethanol for 30 mins. The glass cover slips were then removed from the ethanol and placed on their side in a clean petri-dish in order to dry. Once dry the glass cover slips were placed in a solution of poly-L-lysine for 2 h. The glass cover slips were then removed from the poly-L-lysine solution and washed 7x in ddH_2O. The glass cover slips were then dried for 3 days or longer in order to ensure that the poly-L-lysine has dried properly before placing them in a well plate for cell culturing.

The effect of MGO on the ultrastructure of Gram negative, *E. coli* and Gram positive *B. subtilis*, (objective 2), was determined. The bacteria were exposed to a low (0.5 mM), medium (1 mM) and high (2 mM) concentration of MGO. For SEM a 100 µl volume of the bacteria were transferred to the wells of a 24-well plate containing poly-L-lysine coated cover glass slides. After 90 min incubation at 30°C, samples were fixed for 1 h using a solution of 2.5% formaldehyde and gluteraldehyde in 0.075 M sodium potassium phosphate (NaP) buffer pH 7.4. The slides were then rinsed 3 times for 15 min each time with the NaP buffer before undergoing secondary fixation in 1% osmium tetraoxide for 30 min. The cover glass slides were then rinsed again 3 times for 10 min each in buffer. Next the samples were dehydrated using an increasing concentration series of ethanol (30%, 50%, 70% and 90%) with a final rinse of 3 times in 100% ethanol. The cover glass slides were dried using critical point drying and were then mounted with carbon tape on aluminium stubs and coated with carbon before viewing with a Zeiss Ultra plus FEG SEM.

4.3.2.4 MGO content of southern African honeys and suspected effect based on antibacterial effect of MGO concentrations

To achieve objective 3 the MIC and morphological effects of the three chosen MGO concentrations was compared to that found in the South African honey samples that were evaluated in order to determine if the concentration MGO found in these samples was high enough to exhibit antibacterial activity. Concentrations use were identical to those used int he morphological study.

4.4 Results and discussion

When bacteria are exposed to high levels of endogenous MGO, MGO has been found to have both bacteriostatic and bactericidal effects across a broad spectrum of wound bacteria (Pieper 2009) (Table 2.1). Although there is no clear distinction between bacteriostatic and bactericidal, a bacteriostatic agent is generally defined as a compound that kills of 90 – 99% of bacteria within 18 – 24 hours whereas a bacteriocidal agent kills more than 99.9% of bacteria within 18 – 24 hours. Whether an agent has bacteriostatic or bactericidal activity is

determined by several factors such as growth conditions and bacterial density. However, a compound can be bacteriostatic in one situation but bactericidal in another (Pankey and Sabath 2003).

The aim of objective 1 of this part of the study was to investigate the antibacterial as well as morphological effects of MGO on four different strains of bacteria: Gram positive *B. subtilis* and *S. aureus* and the Gram negative *E. coli* and *P. aeruginosa.* Both Gram positive and negative bacteria are used when evaluating antibacterial effects due to the fact that there are structural differences between that two that may result in different reactions. The main structural difference between Gram positive and Gram negative is in the cell wall surrounding the cell membrane. The cell walls of Gram positive bacteria are thicker but less complex than that of Gram negative bacteria. Gram positive cell walls consists of several layers of the polysaccharide known as peptidoglycan, whereas the cell walls of Gram negative bacteria consists of only two layers; an outer cell membrane and a periplasm layer between the outer and inner membranes. The outer membrane contains polysaccharides that form a complex with the lipids of the outer membrane making up a lipopolysaccharide (LPS) layer. It is this layer in Gram negative bacteria that play an important role in the bacteria's toxicity. (Masip *et al.* 2006) (Figure 4.1).

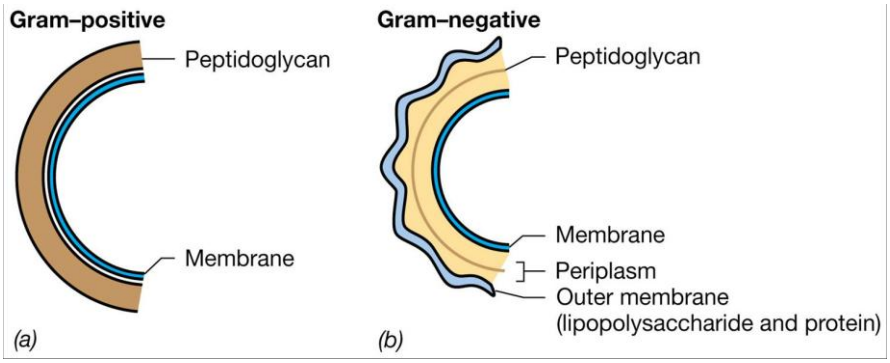

Figure 4.1: Structure of the cell wall of a gram positive and negative bacterium (Jensen *et al.* 2015)

The bacteria used in this study are commonly occurring bacteria. *B. subtilis* is an abundant rod shaped spore forming Gram positive bacteria (deBoer and Diderichsen 1991; Abdullah *et al.* 2015) found mainly in water, soil and decaying plant matter (deBoer and Diderichsen 1991; Tam *et al.* 2006) and occasionally in bread moulds. Although *B. subtilis* does occasionally get ingested it is considered harmless. In rare cases spores germinate and cause food poisoning (Tam *et al.* 2006), however, this is most common in patients receiving immune suppressing medication or with a compromised immune system (deBoer and Diderichsen 1991).

S. aureus is a Gram positive non-motile bacterium that grows in grape-like clusters (Mandal 2012). It is a major cause of nosocomial post-surgical infections and can be found in superficial lesions, deep-seated infections such as osteomyelitis and endocarditis, and may cause food poisoning. It can also cause toxic shock syndrome as well as urinary tract infections (Foster 1996). About 30% of healthy individuals carry *S. aureus* in their nasal passages, the back of their throat, on their skin or intestinal tract (Foster 1996; Mandal 2012). This does however not normally lead to infection as the bacterium is considered to be an opportunist pathogen. *B. subtilis* causes secondary infections in an infected area rather than being the primary cause of the infection. It has the ability to affect a wide range of species and can be transmitted between human and animals. It is transmitted via aerosol or direct contact (Mandal 2012).

E. coli is a commonly occurring Gram negative bacterium that colonises the human intestines as part of the normal intestinal flora and is usually harmless (CDC 2014). However it is very easily transmitted via water or food contaminated with human faecal matter as well as food that has been stored too long or poorly prepared, causing intestinal infection (Klemm 1985; Pietrangelo 2012; CDC 2014).

P. aeruginosa is ubiquitous, rod shaped, Gram negative bacteria (Todar 2008) found in many plant, animal and human sources as well as soil and water (Todar 2008; Lister *et al.* 2009). It has also been found in swimming pools that have not been properly chlorinated as well as contact lenses (CDC 2013). It is however, part of the normal human flora and seldom causes infections unless the patient has a compromised immunity (Lister *et al.* 2009). *P. aeruginosa* is an opportunistic pathogen and mostly infects areas that have already been compromised (Todar 2008). Patients at risk of being infected are those with catheters or on breathing apparatuses (CDC 2013). Most frequently occurring infections of *P. aeruginosa* are nosocomial. In a survey done in 1986 – 1998 it was found to be the fifth most common nosocomial pathogen. It was also the second most common cause of nosocomial pneumonia and third most common cause of urinary tract infections (Lister *et al.* 2009).

4.4.1 Antibacterial activity of MGO on Gram positive and negative bacteria

The exact mechanism by which MGO kills bacteria is still unknown but it is thought to react with nucleic acids within the DNA thereby interfering with protein synthesis and cell division (Ferguson *et al.* 1998). MGO is also thought to interfere with the structural proteins in the flagella causing reduced motility and adherence (Tam *et al.* 2006). This reduction in motility as well as ability to replicate due to impaired cell division will limit a bacteria's ability to spread, adhere and form biofilms (Ferguson *et al.* 1998; Tam *et al.* 2006; Kilty *et al.* 2011).

The effect of increasing concentrations of MGO on Gram positive and negative bacterial growth was determined using a turbidity assay.

MGO inhibited the growth of Gram-positive (*S. aureus* and *B. subtilis*) and Gram-negative (*E. coli* and *P. aeruginosa*) bacteria (Figure 4.2 A and B). The MIC for Gram-positive bacteria was 1.2 mM and 0.8 mM and for *S. aureus* and *B. subtilis* respectively, while for Gram-negative bacteria *P. aeruginosa* and *E. coli* the MIC was 1.2 mM and 1.0 mM respectively (Table 4.1).

A

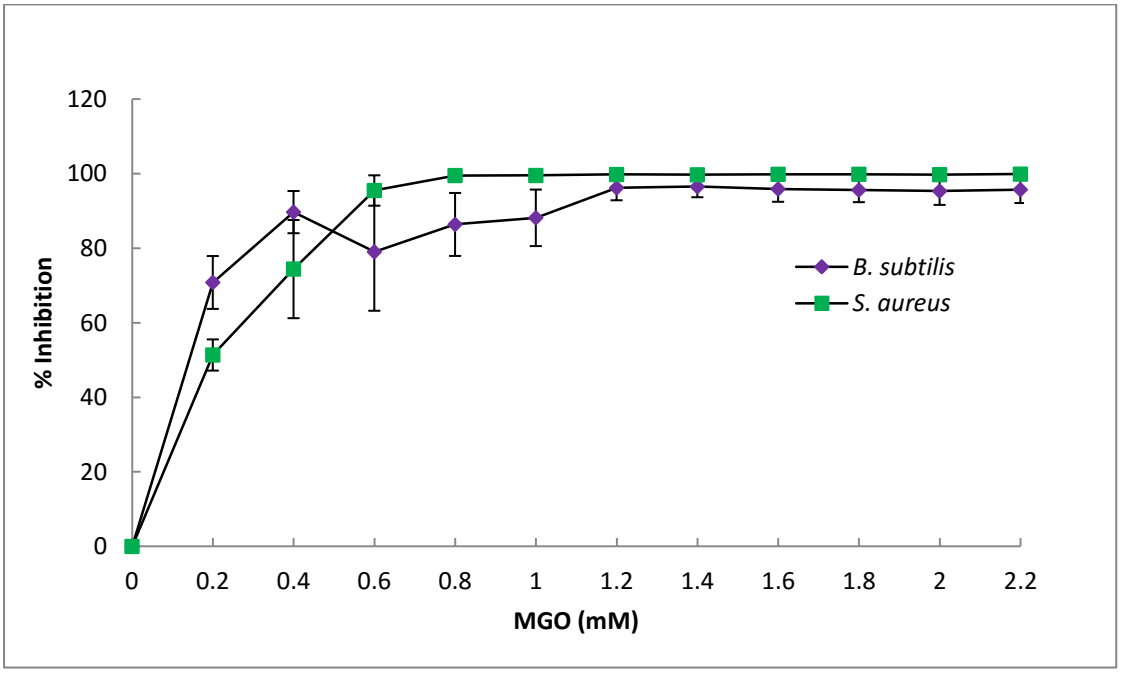

B

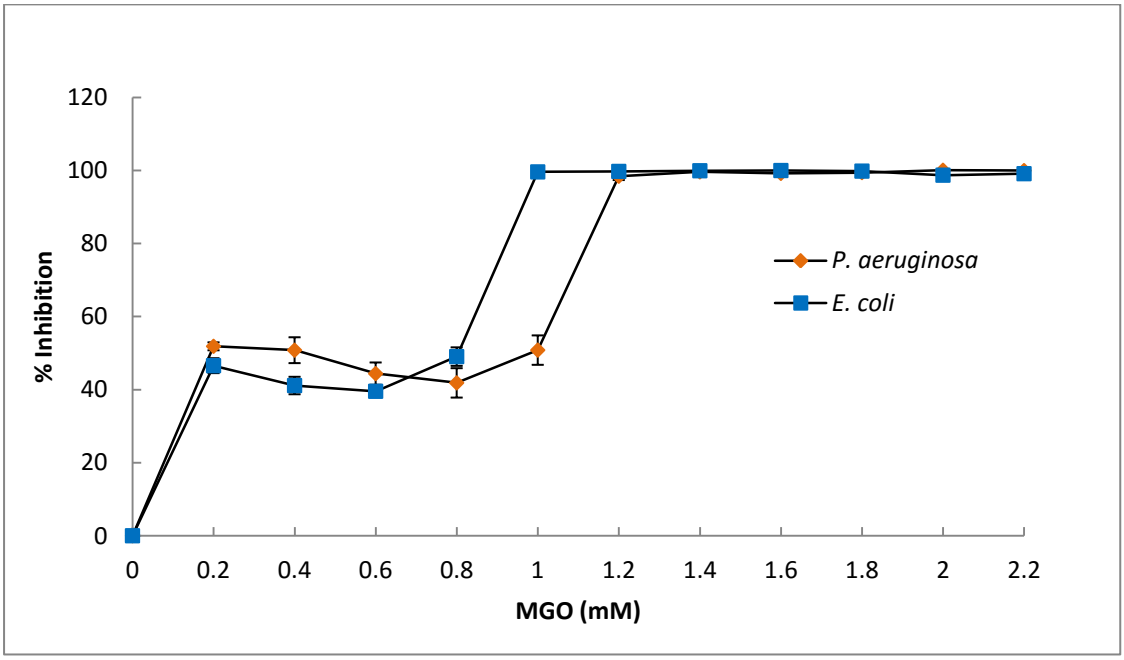

Figure 4.2: Percentage inhibition of bacterial growth by increasing concentrations of MGO. (A): Gram positive: *S. aureus* and *B. subtilis* and (B) Gram negative: *E. coli and P. aeruginosa*. Data is expressed as a mean of 3 independent experiments ± SEM.

Table 4.1: The MIC of MGO (mM) for Gram positive and negative bacteria

Gram Positive		Gram Negative	
S .aureus	0.6 – 0.8	***E. coli***	0.8 – 1.0
B .subtilis	1.0 – 1.2	***P. aeruginosa***	1.0 – 1.2

4.4.2 The morphological effects of MGO on gram positive and negative bacteria using scanning electron microscopy

An example of Gram positive and negative bacteria was selected and the effect of three MGO concentrations on the ultrastructure of *B. subtllis* and *E. coli* was evaluated. These concentrations were low; 0.5 mM, medium; 1.0 mM and high: 2.0 mM.

Both *B. subtilis* and *E. coli* were exposed for 24 hours and images were taken using scanning electron microscopy. A concentration of 0.5 mM is less than the MIC for both bacteria, 1.0 mM is within the MIC range and 2.0 mM is above the MIC range (Figure 4.3 A – D).

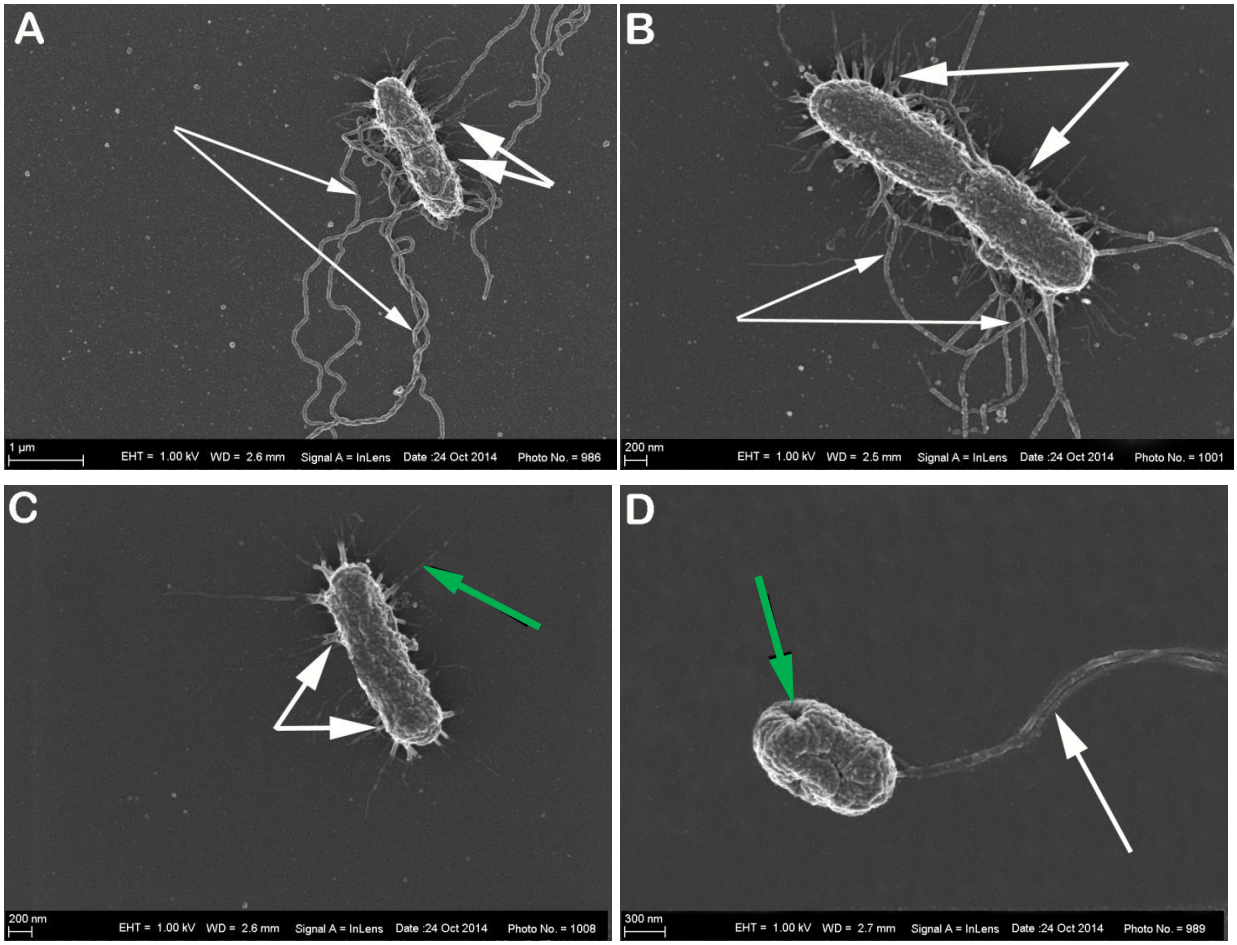

Figure 4.3: SEM micrographs of *B. subtilis* exposed to increasing concentrations of MGO. (**A**) Control; (**B**) 0.5 mM MGO; (**C**)1.0 mM MGO; (**D**) 2.0 mM MGO. Thin white arrows indicate the flagella; thick white arrows indicate the fimbriae and the green arrow in D indicates a hole in the cell; green arrow in C shows a pilus.

Typical morphology can be seen in Figure 4.3 A with arrows showing the fimbriae and peritrichous flagellae extending from the bacteria. Figure 4.3 B indicates that 0.5 mM of MGO had no real effect on the morphology of these bacteria as they have a similar appearance to that of the control related to shape, surface morphology and number and arrangement of flagella. At 1 mM the fimbria and flagella appear reduced in size (indicated by white and green arrows) or missing suggesting that the bacterium cell has lost its ability to move. In addition, the presence of fewer flagella also suggests a loss of ability to attach to surfaces (Figure 4.3 C). At a concentration of 2 mM MGO no flagellae or fimbriae are visible which suggests total loss of motility. Some bacteria also have the appearance of having holes in the membrane (green arrow) as well as loss of cell contents (white arrow) (Figure 4.3 D) indicating cell lysis. These images confirm that MGO has antibacterial activity and results in morphological changes associated with bacterial death.

Scanning electron microscopy images were taken and these images were then compared to images of a control group that contained no MGO (Figure 4.4 A - D).

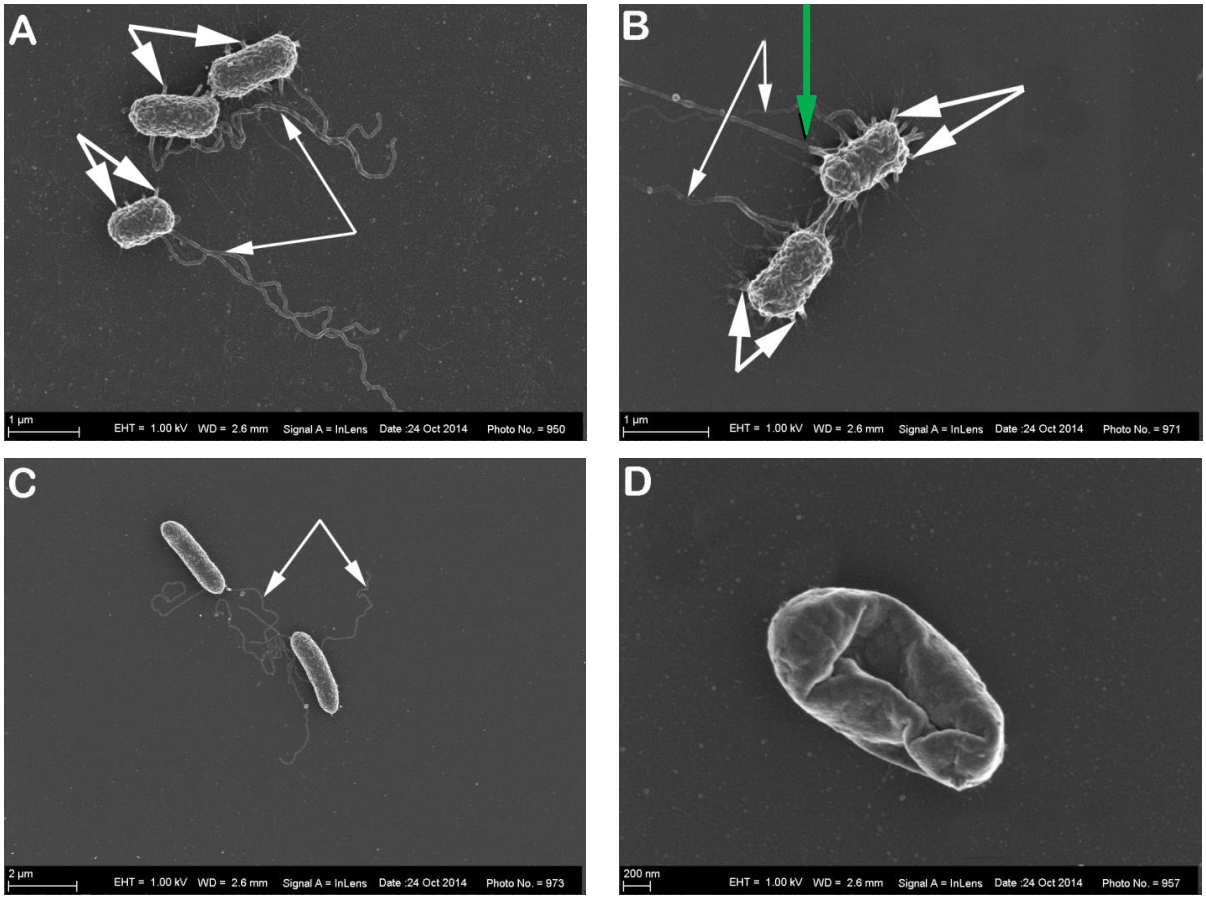

Figure 4.4: SEM micrographs of *E. coli* exposed to increasing concentrations of MGO. (**A**) Control; (**B**) 0.5 mM MGO; (**C**) 1.0 mM MGO; (**D**) 2.0 mM MGO. Thin white arrows indicate the flagella; thick white arrows indicate the fimbriae; green arrow in B shows a pilus.

The typical rod shaped morphology has been shown in Figure 4.4 A with arrows indicating the fimbriae and peritrichous flagellae extending from the bacteria.

As with *B. subtilis*, at 0.5 mM MGO had no real effect on the morphology of E. *coli.* The low concentration group also had a similar appearance to that of the controls related to the presence of fimbriae (white arrow) and flagellae (green arrow) extending from the cell's surface (Figure 4.4 A & B). At 1.0 mM the effect of MGO is visible. Although still present, the number of fimbriae and flagellae extending from the bacterium's surface is greatly reduced (white arrows). This suggests that the bacteria are losing their motility. The surface also has a smoother appearance (Figure 4.4 C). At a MGO concentration of 2.0 mM, which is above the MIC for *E. coli*, no fimbriae or flagella are visible. This implies the bacteria have lost their ability to move and attach. The membranes of some cells have collapsed and they have a dehydrated appearance (Figure 4.4 D) indicating lysis.

In order for bacteria to have a pathogenic effect it is important for them to be able to grow fimbrae and flagellae. These are complex surface organelles that enable bacteria to migrate towards, attach to the surface and invade host cells or organisms (Sherlock *et al.* 2010;

Guttenplan and Kearns 2013). The fimbriae are shorter than the flagellae and enable the bacteria to stick to the surface (Masip *et al.* 2006). Flagellae are longer and enable the bacteria to move (Masip *et al.* 2006). The flagellae are also the structure from which virulent factors are secreted (Ramos *et al.* 2004; Sherlock *et al.* 2010). Afimbriate aflagellate bacteria are less virulent as they are less capable of attaching to and invading hosts cells (Ragione *et al.* 2000; Ramos *et al.* 2004).

As can be seen from the ultratuctural morphology of the bacteria exposed to MGO in this study, the bacteria that have been exposed to a MGO concentration of 1.0 mM and above have a smooth aflagellate surface (Figure 4.3 & 4.4). This would suggest that the bacteria are unable to migrate, unable to adhere to a surface and unable to secrete virulent factors as all of these functions require flagella. This would suggest that exposure to high enough concentrations of MGO would inhibit or decrease a bacteria's virulence preventing its pathogenic effects.

A study by Burt *et al.* (2007) exposure of bacteria to cavacrol, present in essential oils, resulted in the bacteria having a smoother surface morphology and fewer flagella. These authors suggested that this was due to changes in the composition of peptides and peptidoglycans in the cell wall.

A concern related to bacterial infection is the occurrence of chronic wounds and the formation of biofilms. Chronic infections normally occur in patients with diabetes, especially in the lower extremities and often results in amputation of the infected limb. As previously mentioned the healing of chronic wounds is especially complicated due to the nature of the wound. It has been suggested that chronic infections occur as a result of biofilm formation instead of just normal bacterial infection (James *et al.* 2008). A biofilm is a heterogenous bacterial colony with a complex three dimensional structure that require multistep processes for their formation (James *et al.* 2008). In order for a biofilm to form the formation of flagella needs to cease. This requires two main events to occur: The first is a shorter event that involves the functional inhibition of flagella rotation. The second involves the long term inhibition of gene transcription of flagella proteins, thus halting flagella assembly and enabling the bacteria to stop moving so that it can adhere to the surface to from the biofilm structure (Guttenplan and Kearns 2013).

Manuka honey is known to be effective against several strains of bacteria including resistant bacteria (Pieper 2009; Kilty *et al.* 2011). The MGO in Manuka has been found to be effective in eradicating biofilms formed by some bacteria (Jervis-Bardy and Tan 2011; Kilty *et al.* 2011).

As already mentioned this study showed that exposure to MGO decreases the number of fimbriae and flagellae visible on the bacteria's surface. This suggests that MGO will decrease the virulence of these bacteria as well as decrease their ability to colonise and persist in areas that MGO positive honey has been applied. The application of honey containing MGO may also help prevent the formation of biofilms in the wound as the formation of fimbria and flagella are required in order for biofilms to form (James *et al.* 2008; Jervis-Bardy and Tan 2011).

4.5 Summary of results

MGO levels of southern Africa honey was compared to the MIC of each bacterium (Table 4.2).

Table 4.2: MGO concentrations found in SA samples in comparison to MICs for tested bacteria

	GSH	NAC
	Range	**Range**
MGO in SA samples (mM)	13.27 - 36.79	23.28 - 73.66
Bacterial MIC (mM)		
S. aureus	0.8	
E. coli	1.0	
B. subtilis	1.2	
P. aeruginosa	1.2	

MGO levels as found in a selection of southern Africa honey would effectively kill bacteria possibly via the inhibition of fimbriae and flagella formation as described for Manuka honey as well as lysis.

4.6 Conclusion

Roberts *et al*. (2014) showed that Manuka honey inhibited flagella associated genes; the present study clearly shows that MGO, the major antibacterial constituent of Manuka honey either directly damages or inhibits the formation of fimbriae and flagella. At concentrations > MIC, MGO causes bacteria lysis. Likewise MGO, as found in southern Africa honey is greater than the MIC required to kill bacteria. How MGO affects fibrillin gene expression and protein structure is an important aspect that needs to be further investigated.

Chapter 5: The *in vitro* cellular effects of methylglyoxal

5.1 Introduction

MGO is not only present in honey but also in certain beverages and food stuffs and is also formed during cellular metabolism (Thornalley 1996; Yuen *et al.* 2010). High levels of MGO are toxic, causing the disruption of normal cellular pathways leading to cellular death (Thornalley 1996). The main pathway by which the accumulation of MGO and its consequent toxic effect is prevented is via the glutathione-dependent glyoxalase I-II system (Ferguson *et al.* 1998). This pathway converts MGO into D-lactate via glyoxalase I and II (Ferguson *et al.* 1998; Tötemeyer *et al.* 1998; Yadav *et al.* 2005; Wild *et al.* 2012). MGO accumulation is of special concern in patients with diabetes or hyperglycemia since these patients already have elevated levels of MGO (Suzuki *et al.* 1997; Mangram *et al.* 1999; Nomi *et al.* 2009).

The reason for this is that MGO is a highly reactive electrophilic molecule that readily reacts with nucleic acids and proteins (Thornalley 1996; Ferguson *et al.* 1998). It has an especially high affinity for Arg, Lys and Cys and alters the structure and activity of several cellular proteins (Thornalley 1996; Ferguson *et al.* 1998). When MGO accumulates to high levels within a cell it results in cross-linking of proteins and enzymes (Lo *et al.* 1994; Singh *et al.* 2001) which leads to the formation of advanced glycation end-products (AGEs) (Thornalley 1996). This interferes with normal protein functioning (Yadav *et al.* 2005). MGO also has a high affinity for the nucleotide guanine causing altered nucleotide structure which leads to DNA mutations and incorrect transcription (Thornalley 1996; Ferguson *et al.* 1998; Yadav *et al.* 2005).

Despite the negative effects of MGO it also has several potentially beneficial effects such as the fact that it effectively kills a number of pathogens including malaria, certain bacteria including some resistant strains, mycobacteria and viruses (Kim *et al.* 2004; Pieper 2009). It also has the ability inhibit the growth of certain tumours such as neuroblastomas and leukaemia and cause apoptosis in MCF7 breast cancer and RKO colon cancer cell lines (Kim *et al.* 2004). Of concern is that although MGO and MGO containing honey effectively kills bacteria in wounds, very little is known about the effect on cells in the wound site, especially in diabetic patients.

The aim of this study was to evaluate the effect of MGO on cell number and vitality using spectrophotometery and light microscopy. Also to examine changes in morphology after exposure to MGO using scanning electron microscopy in order to determine if the

concentrations of MGO, as found in South African honeys, is cytotoxic. Finally also to determine if the MGO concentrations that kill bacteria are cytotoxic.

5.2 Aims and Objectives

5.2.1 Aims

In Chapter 4, MGO was shown to effectively kill Gram positive and negative bacteria with a MIC of between 0.6 – 1.2 mM. The aim of this study was to determine the cellular effects of MGO across a concentration range that includes the MIC of each bacterium as well as the MGO concentrations found in the southern Africa honey samples.

5.2.2 Objectives

1. To determine the cytotoxicity of a MGO concentration range in the SC-1, Caco-2 and RAW 264.7 cell lines.
2. To determine the effect of MGO on the morphology and degree of cellular differentiation in each cell line.
3. To determine if the levels of MGO found in South African honey samples cause cellular death.
4. Based on the findings of objective 1, chapter 1 and objective 1, chapter 5, to determine if the levels of MGO found in South African honey samples causes cellular death.
5. Based on the findings of objective 3, chapter 4 and objective 4, chapter 5 to determine if MGO concentrations that effectively kill bacteria are cytotoxic.

5.3 Materials and methods

5.3.1 Materials

5.3.1.1 Cell lines

The human colorectal adenocarcinoma cells Caco-2 (ATCC® HTB37™) were obtained from Sigma-Aldrich Company, Atlasville, SA. Mouse macrophages RAW 264.7 (ATCC® TIB71™) were obtained from the European Collection of Cell Culture (ECACC) and mouse fibroblasts SC-1 (SC-1 ATCC® CRL-8756™) were obtained from Highveld Biological Company, (Johannesburg, SA).

5.3.1.2 Media and supplements

Eagle's Minimum Essential Medium (EMEM) powder, Dulbecco's Modified Essential Medium (DMEM), fetal calf serum (FCS) and antibiotic solution containing, streptomycin, penicillin and fungicide was obtained from Highveld Biological Company (Johannesburg, SA).

5.3.1.3 Reagents, equipment and disposable plastic ware

Cystal Violet (CV), 3-(4,5-Dimethylthiazol-2-yl)-2,5-diphenyltetrazolium bromide (MTT) and 4,5,6,7-Tetrachloro-2′,4′,5′,7′-tetraiodofluorescein disodium salt (Rose Benagal Sodium salt) were obtained from Sigma-Aldrich, Atlasville, SA. Fixatives, acids, salts and organic solvents such as: formaldehyde, gluteraldehyde, ethanol (EtOH), acetic acid, formic acid, isopropanol, ethylene diamine tetra acetate (EDTA), dimethyl sulphoxide (DMSO), sodium hydroxide (NaOH), sodium chloride (NaCl), disodium phosphate (Na_2HPO_4), sodium phosphate monobasic dihydrate ($NaH_2PO_4.H_2O$), poly-L-lysine, osmium tetroxide (OsO_4) and Hexamethyldisilazane (HMDS) were of analytic grade and purchased from Merck (SA). Trypsin was obtained from Life Technologies Laboratories and was supplied by Gibco BRL products, Johannesburg, SA. Water was double distilled (ddH_2O) and de-ionised ($dddH_2O$) with a Continental Water System and all medium, enzyme solutions and buffers were sterilised by filtration through a Millex 0.2 µm filter.

Equipment used included an Omega plate reader (BMG Labtech Johannesburg, S.A). and a Zeiss Ultra plus FEG SEM. A Hermle Z300 centrifuge, a Crison GLP 21 pH Meter and Eppendorf pipettes from Eppendorf AG (Hamburg, Germany) was also used.

Disposable plastic ware include: 24 well plates, 96 well plates, 50 ml, 15 ml tubes and pipette tips (10, 25, 100, 200, and 1000 µl). These were obtained from Greiner Bio-one also supplied by LASEC. Sartorius cellulose acetate membrane filters 0.22 µm were obtained from National Separations (Johannesburg, SA). Glassware was sterilised at 121°C for 20 min in a Prestige Medical Autoclave (series 2100).

5.3.2 Methods

5.3.2.1 MGO, CV, MTT, Rose Bengal and PBS stock and working solutions

For all experiments the same stock and working solutions were used.

PBS was prepared as described in chapter 3.

A working solution of MGO was prepared by diluting a 40% solution of MGO with ddH_2O to a ratio of 1:1. This was done under sterile conditions using a laminar flow hood. A 0.1% (w/v)

CV solution was prepared by adding 1 mg CV powder to 1 ml ddH_2O and diluting a further 10 times using dH_2O. A 1mg/ml MTT solution was prepared by dissolving 1 mg MTT per ml PBS. A 1 mg/ml Rose Bengal (RB) solution was prepared by dissolving 1 mg RB salt per 1 ml ddH_2O.

5.3.2.2 The cellular effects of methylglyoxal

Fibroblasts are very abundant in the skin and their formation and growth is essential in order for a wound to be able to heal. Both epithelial cells and fibroblasts are present in wounds and with inflammation macrophages are also present (ATCC 2014).

To achieve objective 1 the cellular effects of MGO was determined in three cell lines including mouse macrophages (RAW 264.7), human colorectal adenocarcinoma cells (Caco-2) and mouse fibroblasts (SC-1). These three cell lines were chosen to represent morphologically and physiologically different cell types. RAW 264.7 cells are mouse macrophage cells that are semi-adherent cell lines (ATCC 2014). Caco-2 cells are human colorectal adenocarcinoma cells that have a typical epithelial phenotype (ATCC 2014). SC-1 cells are mouse fibroblast cells.

5.3.2.2.1 Cultivation, maintenance and preservation of the RAW 264.7, SC-1 and Caco-2 cell lines

The SC-1 cells were maintained in EMEM and the Caco-2 and RAW 264.7 in DMEM. Both media were supplemented with 10% FCS (EMEM/FCS and DMEM/FCS) and a 1% antibiotic solution containing streptomycin, penicillin and fungizone. A volume of 10 ml of the antibiotic stock solution was added to 1 litre of the prepared medium. The antibiotic solution was kept at -10ºC and thawed when needed and mixed with the serum supplemented media and sterile filtered through a 0.22 µm membrane filter under aseptic conditions in a laminar flow hood cabinet. Media was aliquoted (250 ml) and stored at 4°C and warmed to 37°C before use.

All three cell lines were plated at a concentration of $4x10^4$ cells per ml in 25 cm^2 and 75 cm^2 cell culture flasks and maintained until confluent at 37°C at 5% CO_2. Once confluent, the cells were passaged with a 5% trypsin solution prepared in 100 ml of a PBS solution.

For the SC-1 cells, the cells were passaged by removing the medium from the confluent monolayer then adding 1 ml of a 5% trypsin solution before placing the flask at 37°C for 1 - 2 min. Once the cells had detached a volume of 5 ml medium was then added to the flask, the solution was mixed well before transferring it to a 15 ml centrifuge tube. The cells were then collected by centrifugation at 2250 x g for 2 min. The medium was removed and the pelleted

cells were re-suspended in 5 ml EMEM/FCS. Cell number was determined by counting a 10 µl aliquot of cells using a haemocytometer.

For the Caco-2 cells, the cells were passaged by removing the medium from the confluent monolayer. The monolayer was rinsed rapidly with 5 ml of a 0.53 mM EDTA solution, which was prepared using PBS. A 1 ml volume of a 5% trypsin solution was then added and the flask was incubated at 37°C for 1 - 2 min. The cells were collected and counted as described for the SC-1 cells.

The RAW 264.7 cells were passaged by removing the medium from the flask and scraping the cells off the surface using a cell scraper and then collecting the cells by centrifugation. The cells were counted as described for SC-1 cells. For subculturing into flasks, cells were split in the following ratio, 1:2 in the case of T25 flasks or 1:1 in the case of T75 flasks. For all experiments $5x10^4$ RAW 264.7 cells and $4x10^4$ SC-1 and Caco-2 cells in a volume of 200 µl were plated in each well of a 48-well flat bottom plate. The cells were incubated for 24 h at 37°C and 5% CO_2 to allow the cells to attach to the tissue culture surface before exposure to MGO.

5.3.2.2.2 Exposure to methylglyoxal

The sterile MGO working solution was prepared as described in Section 5.3.2.1. All three cell lines were exposed for 48 h to a 10x serial dilution of MGO, yielding final concentrations of 0 – 324.7294 mM. The plates were then incubated for 24 h at 37°C and 5% CO_2 prior to the evaluation of the effect of increasing MGO concentrations on each cell line using the CV and MTT assays.

5.3.2.2.3 Cell number: Crystal Violet assay

CV is a positively charged dye that binds negatively charged cellular components such as DNA and negatively charged proteins. The CV assay therefore provides a measure of the number of cells *in vitro.* Cellular toxicity can cause cell detachment or inhibition of cellular proliferation and consequently a decrease in CV staining, therefore indicating a reduction in cell number. Cell number was quantified as follows:

After exposure to MGO, 20 µl of a 20% formaldehyde solution was added to the medium in each well. The plates were then incubated at 37˚C for 20 min. The fixative containing medium was then removed and dried well before adding100 µl of the 0.1% (w/v) CV solution prepared as described in Section 5.3.2.1. For staining of the plates were left to stand at room temperature for 30 min. The CV dye was then removed and the plates were washed well to remove excess dye and dried. The CV dye was then extracted with 200 µl of a 10% acetic

acid solution on a shaker for 10 mins. A volume of 150 µl from each well was transferred to a separate 96-well plate and the absorbance was read at 570 nm with a Biotek plate reader.

5.3.2.2.4 Cell viability: MTT Assay

The MTT assay makes use of a tetrazolium dye and measures the metabolic activity of a cell after being exposed to a toxic compound such as MGO. In a viable cell the enzyme succinate dehydrogenase reduces the tetrazolium dye to an insoluble purple formazan product (Frei 2015). The amount of dye extracted is proportional to cellular viability. The MTT assay was done as follows:

After exposure to MGO, 20 µl of the MTT solution prepared as described in Section 5.3.2.1 was added to the medium in each well. The plates were placed back into the incubator for 3 h, after which the medium was removed and the plates thoroughly blotted dry on tissue paper. The dye was extracted for 10 min on a shaker with 200 µl of a 1:1 DMSO:ethanol solution. A 150 µl volume of this extract was transferred to a separate 96-well plate and the absorbance was read at 570 nm on a Biotek plate reader.

5.3.2.2.5 Changes in charge using the Rose Bengal assay

As a result of MGO binding to amino acids such as positively charged Lys and the formation of cross-links there may be a change in the amount of positive and negative charges within the cells. RB is negatively charged and will bind positively charged proteins. If there is a change in charge as a result of MGO modification the results from the RB assay will differ to that of the CV assay in that the absorbance readings from the RB assay will be lower than that of the CV assay.

As RB is an ionic dye, the method used is similar to that used for the CV assay. Following the fixing of the cells, the fixative containing medium was removed and dried well before adding 100 µl of a 0.1% (w/v) RB solution prepared as described in Section 5.3.2.1. The plates were placed on the shaker for 30 min. The RB dye was then removed and the plates were washed well and dried. The RB dye was extracted with 200 µl of a 125 mM NaOH solution. A volume of 150 µl from each well was transferred to a separate 96-well plate and the absorbance was read at 570 nm with a Biotek plate reader.

5.3.2.3 Evaluation of cellular morphology with scanning electron microscopy

To achieve objective 2 the effect of MGO on the morphology of Caco-2, RAW 264.7 and SC-1 cells was evaluated using scanning electron microscopy. Poly-L-lysine glass cover slips were prepared as described in Chapter 4, section 4.3.2.3.1 and each cell line was grown at

the same density as in Section 5.3.2.2.1. The cells were exposed to three different concentrations of MGO representing low (0.000325 mM), medium (0.324729 mM) and high (324.7294 mM) concentrations. Samples for SEM were prepared as described in Chapter 4, Section 4.3.2.3.1.

5.3.2.4 Evaluation of the effect of honey and antibacterial MGO concentrations on cell number and viability

To achieve objective 3 and 4 the effect of MGO as observed in this study was compared to the findings in other studies. In addition the concentrations of MGO as found in the SA honeys samples (9.61 – 17.5 mM MGO) as well as the concentrations of MGO that was observed to be bactericidal (0.4 – 1.2 mM MGO) was evaluated in comparison to the effects of corresponding MGO concentrations on cell number and viability. A summary was tabulated in Table 5.2.

5.3.2.5 Data management and statistical analysis

All data is expressed as mean ± SEM and is a minimum of three independent experiments. MTT and CV data was expressed as percent control no MGO added. Cell viability and number was also expressed as a ratio. This ratio was defined as: a greater increase in viability than in cell number (> 1.1) representing hormesis, no change in viability or cell number or an equal change in both viability and cell number (0.9 – 1.1) representing normal growth and percent viability that is lower than percent cell number to control (< 0.9) representing toxicity.

5.4 Results and discussion

The aim of this study was to evaluate in a cell culture the toxicity of MGO. Classical toxicity is generally a dosage dependent decrease in cell functioning or number with increasing concentration of the toxic compound. In contrast, a hormetic response is a biphasic response where a low concentration is beneficial or stimulating to a cell's growth and metabolism where as a higher concentration is toxic or inhibitory (Calabrese and Baldwin 2002; Mattson 2008; Cedergreen 2010). Cells that have previously been exposed to a low dose exhibit increased resilience when exposed to higher concentrations of the same substance in comparison to cells that have had no previous exposure (Mattson 2008). It has also been observed that exposure to one hormetic agent resulted in an increase in resistance to other stressors (Mattson 2008). However, this response does not only include toxic substances, but also potentially harmful environmental conditions (Kouda and Iki 2010).

Recent findings have shown that dietary restriction (specifically a reduction in glucose metabolism) resulted in an extended life span in some model organisms (Hipkiss 2007; Kouda and Iki 2010). This is thought to be due to an increase in the production of ROS in the mitochondria that leads to an adaptive response known as mitochondrial hormesis or mitohormesis (Kouda and Iki 2010). Too much ROS can be damaging however, too little can also lead to a decrease in cellular proliferation and host defensive response. It is therefore important that there be a balance (Ji *et al.* 2006). Evidence also suggests that in addition to an increased life-span, dietary restrictions help to lessen the severity of spontaneously occurring neoplasias, aids in the reduction of damage to the brain from ischemia, delays onset and severity of allergic dermatitis and increases the resistance to toxins in models related to Parkinson's and Alzheimer's disease (Kouda and Iki 2010).

Other examples where the hormetic response has been found to have a beneficial effect are increased resistance to a full-blown heart attack or stroke after exposure to mild ischemia. It is also believed that the beneficial effects seen from consuming certain fruits or vegetables are due to the activation of stress response pathways in cells and nerves. The same has been said about certain medications (Mattson 2008). The benefit is thought to be gained due to an over-compensation after homeostasis has been disrupted by a low dose of the hormetic agent (Kouda and Iki 2010).

Hormesis can result in a change in cellular metabolism without a change in cell number or can increase both metabolism and cell number. Toxicity will cause a decrease in cell viability and/or cell number. To determine the effect of MGO on cell number and viability three cell lines were exposed to increasing MGO concentrations. Cellular effects were determined using two different assays that measure two different aspects of cellular function namely the number of cells (CV) and cell viability (MTT).

5.4.1 The cellular effects of MGO on RAW 246.7 macrophages

The effect of increasing concentrations of MGO was tested on RAW 264.7 cells, which are mouse macrophage cells (ATCC 2014). The effect of 48 hours of exposure was evaluated using the CV assay to evaluate cell number (Figure 5.1 A) and MTT to evaluate cell viability (Figure 5.1 B). Data was expressed relative to the control group expressed as 100% with no MGO added.

5.4.1.1 CV and MTT assay

For the CV assay at 0.0003 and 0.0032 mM MGO a slight but not statistically significant increase in cell number was observed with a cell number percentage of 107.07 and 110.42%

respectively. At concentrations of 0.033 and 0.32 mM MGO a small but insignificant decrease in cell number was observed in comparison to control with a percentage growth of 89.51 and 89.18% for 0.0325 and 0.3247 mM MGO respectively. At 3.2473 mM MGO no significant change in cell growth was observed with a growth of 106.51%. At high concentrations of MGO (32.4729 mM and 324.7294 mM) cell number increased significantly again with a growth percentage of 126.66 and 154.44% respectively (Figure 5.1 A).

For the MTT assay which measures cell viability a large and statistically significant increase in cell viability was observed from 0.0003 – 0.0325 mM of MGO with a viability of 643.732, 629.69 and 503.52% for 0.0003, 0.0032 and 0.0325 mM of MGO respectively. From a concentration of 0.3247 – 324.7294 mM MGO a small and statistically insignificant increase in viability was observed with a viability of 251.12, 199.42, 134.9 and 133.23% for 0.0325, 0.3247, 3.2473 and 324.7294 mM MGO respectively (Figure 5.1 B).

A

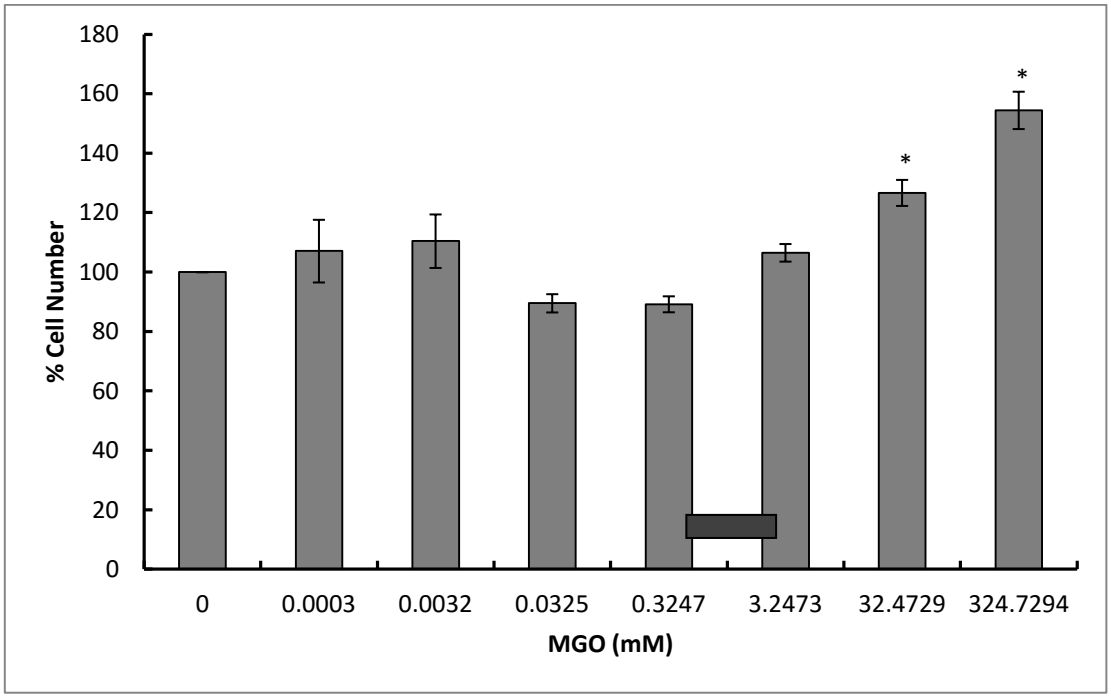

B

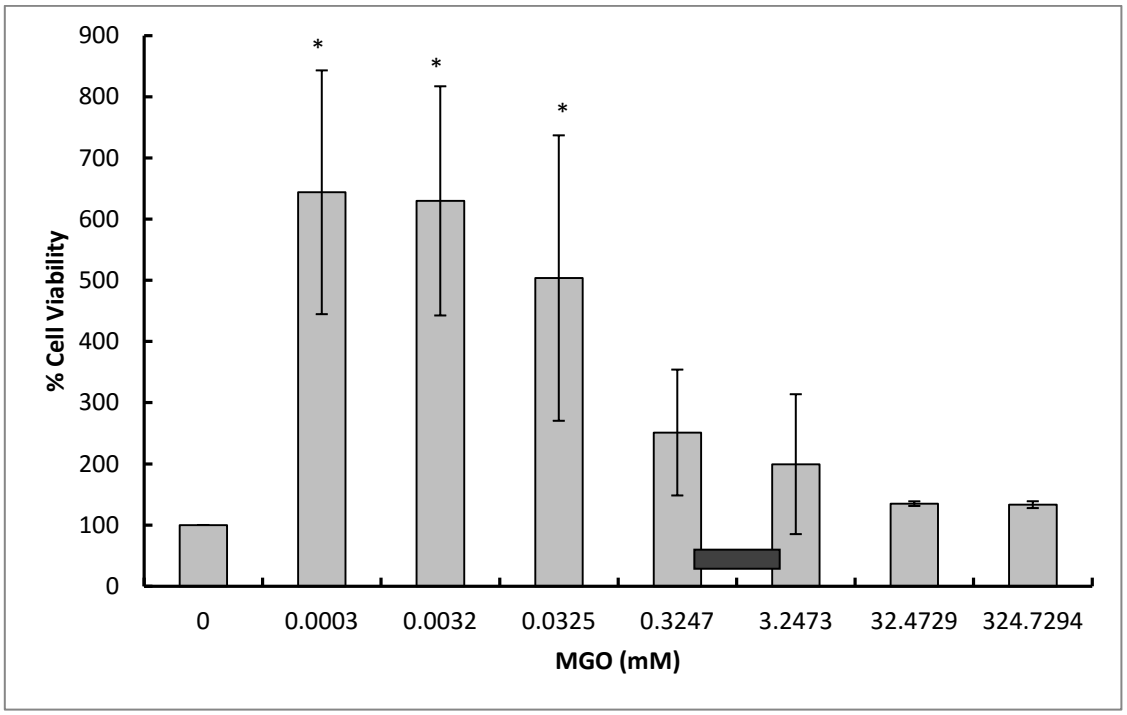

Figure 5.1: RAW 264.7 cells exposed to increasing concentrations of MGO showing (A) CV assay indicating percent growth and (B) MTT indicating percent viability after 48 h exposure measuered as a percentage of a control with no MGO added. Data is an average of four (MTT assay) and five (CV assay) experiments ± SEM. Means with stars are significantly different, p≤0.005. Bar indicates the MIC range for all bacteria in chapter 4, section 4.4.1.

Although the effect of MGO on RAW 264.7 cells was determined in four independent experiments, a large standard error of mean was obtained for MGO concentrations of 0.0003

– 3.2473 mM. This is due to the fact that RAW 264.7 cells are a semi-adherent cell line and attach poorly to the surface. The formation of formazan crystals causes the cells to detach easily which means they are discarded along with the medium after the MTT has been absorbed but before the dye can be extracted from them. This lowers the reproducibility of data. In order to overcome this Alamar Blue ® can be used for this cell line instead as this assay does not require removing of the medium and cells in order to dissolve the dye as with MTT. Therefore the semi-adherent cells will not be discarded before their viability can be taken into account. In contrast the SEM is reduced for Caco-2 and SC-1 cell lines which are adherent cell lines (Figure 5.6 and Figure 5.10).

In contrast to the classical toxicity response which shows a decrease in viability with increasing concentrations, the MTT assay showed a significant increase in the amount of dye extracted from 0.0003 – 0.0325 mM MGO. In addition, at 32.4729 and 324.7294 mM MGO there was also a significant increase in the amount of CV that was extracted from the cells compared to the control. This suggests an increase in cell number instead of a decrease as expected for classical toxicity. To determine whether this is due to increased amount of dye binding or an increase in cell number the cells were exposed to 0.0003 - 324.7294 mM MGO, stained using CV and the density was evaluated with light microscopy. The images are presented bellow (Figure 5.2 A – H). Normal RAW 264.7 cells do not spread evenly over the surface in cell culture but grow in clumps or clusters as indicated in Figure 5.2 A by the arrow (Lee *et al.* 2008).

A: Control

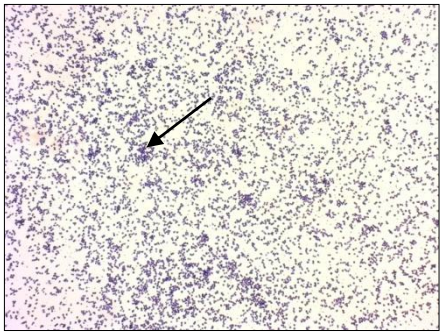

B: 0.0003 mM

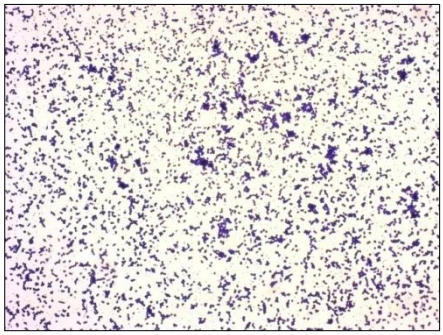

C: 0.0032 mM

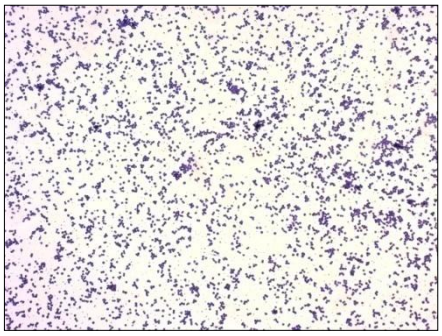

D: 0.0325 mM

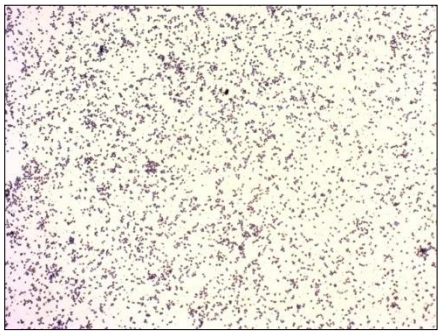

E: 0.3247 mM

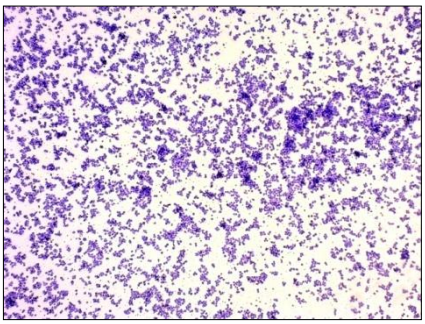

F: 3.2473 mM

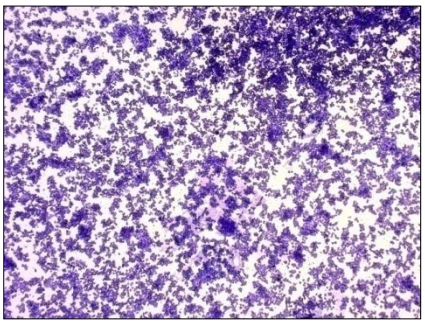

G: 32.429 mM

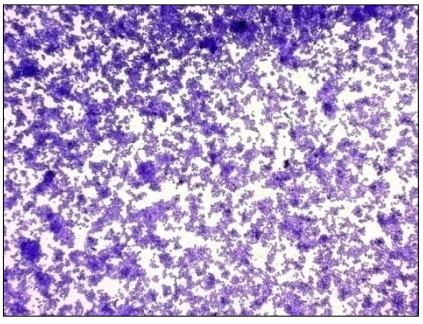

H: 324.7294 mM

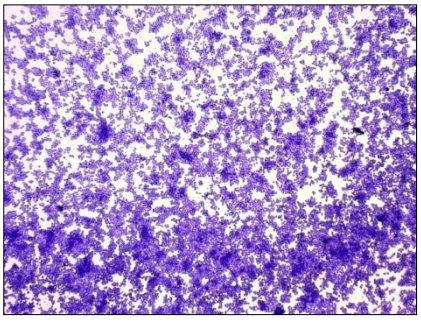

Figure 5.2: Light microscope images at x4 magnification of RAW 264.7 cells showing differences in cell number using CV staining. (A): Control. (B – H): cells exposed to increasing concentrations of MGO.

As seen from the images, in comparison to the control (Figure 5.2 A) there is a slight increase in staining from 32.429 – 324.7294 mM MGO. This reflects the data represented in Figure 5.1 A.

It was suspected that hormesis was observed following exposure to low concentrations of MGO since an increase in cellular metabolism is observed using the MTT without a corresponding increase in cell number (CV assay) instead of the classical toxicity response where an increase in concentration corresponds to a decrease in cellular metabolism and cell number. In order to evaluate this more clearly the data from the CV and MTT assays was then expressed as a ratio of cell viability:cell number. A ratio > 1.1 implies hormesis, 1± 0.1 is normal growth and <0.9 is toxicity. The data was represented in Figure 5.3. From this image it can be seen that at MGO concentrations of 0.0003 - 3.2473 mM MGO hormesis occurs. At a concentration of 32.4729 mM MGO cell growth and vitality is normal and at 324.7294 mM MGO minor toxicity with a ratio of 0.862 occurs.

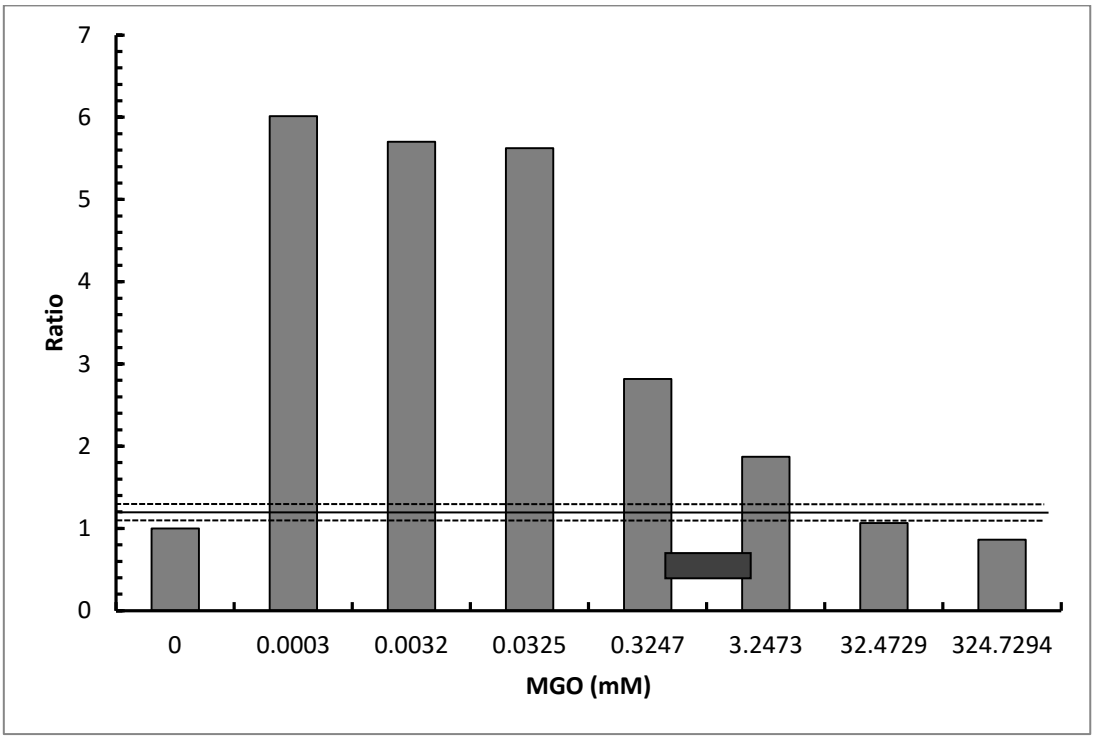

Figure 5.3: Summary showing the ratio between cell viability :cell number for RAW 246.7 cells exposed to increasing concentrations of MGO where 1±0.1 indicates normal growth, > 1.1 indicates hormesis and < 0.9 indicates toxicity. Bar indicates the MIC range for all bacteria in chapter 4.

These results suggest that, although low concentrations MGO are not toxic, it is stimulating the RAW 264.7 cells to increase their metabolism in order to protect against potential toxicity at higher concentrations. In order to further evaluate and confirm these effects RAW 264.7 cells were evaluated using scanning electron microscopy and two additional cell lines were evaluated in the same way.

5.4.1.2 Scanning electron microscopy

The three concentrations from the CV and MTT assays were chosen that represent increased cell number and viability (0.0003 mM MGO) (Figure 5.4B), no change in cell number with a slight decrease in viability (0.324 mM MGO) (Figure 5.4 C) and a large increase in cell number with a small increase in cell viability (324.729 mM MGO) (Figure 5.4 D) compared to control (Figure 5.4 A). RAW 264.7 cells were exposed to these three concentrations for 48 hours under identical conditions as for the CV and MTT assays and then prepared for and photographed using a scanning electron microscope. The images are presented in Figure 5.4 (A – D).

The RAW 264.7 cells in the control group (Figure 5.4 A), not exposed to MGO, were spherical in shape with no signs of activation (Figure. 5.4 A) The cells that were exposed to low and medium concentrations of MGO (Figure 5.4 B – C) show similar morphology to that of the control group. The cells that were exposed to high MGO concentrations (Figure 5.4 D) show signs of macrophage activation with ruffles on the cell's surface and pseudopodia extending from the cells (Adams *et al.* 2008; Pieper 2009).The cell surfaces of all the groups showed absence of apoptotic blebbing (Pieper 2009). However the cell membranes in Figure 5.4 D have small holes indicating possible toxicity.

A: Control

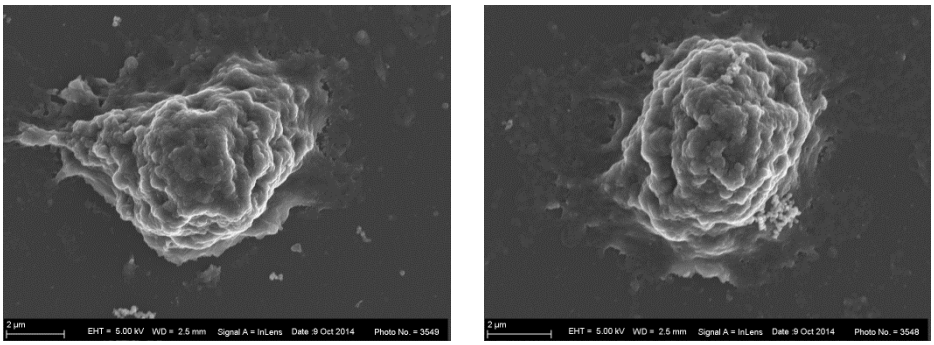

B: 0.000325 mM (Low)

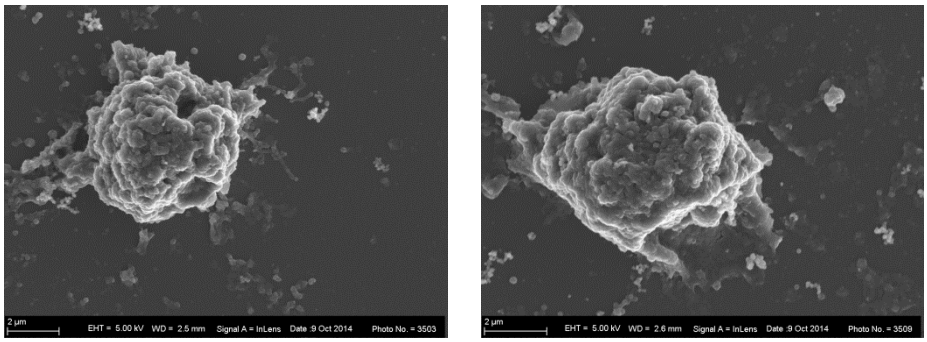

C: 0.324729 mM (Medium)

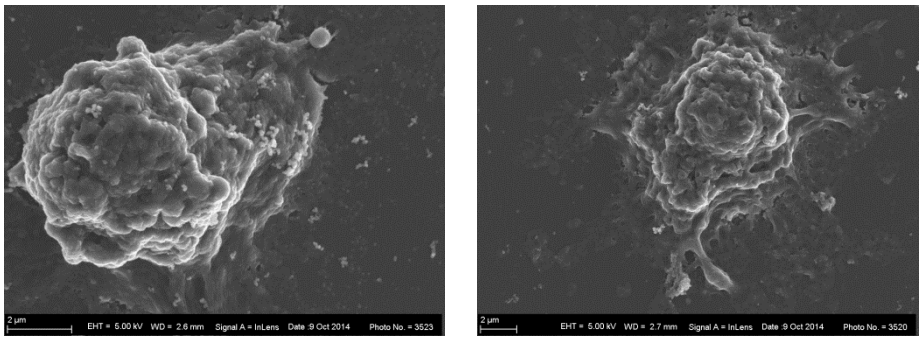

D: 324.7294 mM (High)

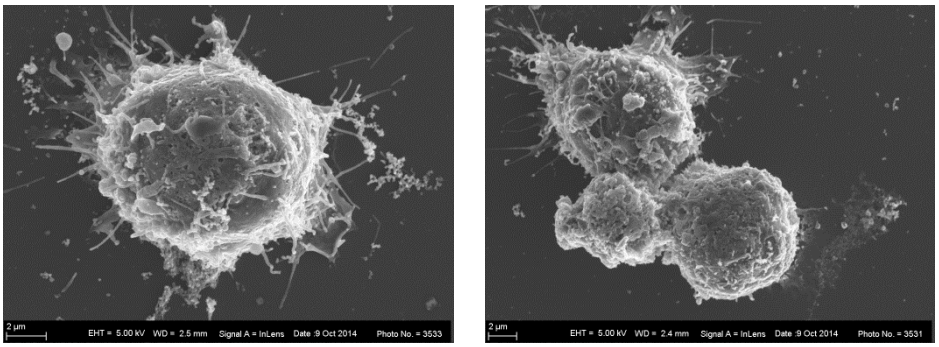

Figure 5.4: SEM images of RAW 264.7 cells exposed to 3 different MGO concentrations. A: Control group with no MGO added. B: Low MGO concentration (0.000325 mM) showing similar surface formation to that of the control (A). C: Medium MGO concentration (0.324729 mM) showing similar surface formation to that of the control (A). D: High MGO concentration (324.7294 mM) showing pseudopodia and surface ruffles.

The RAW 264.7 cells exposed to high concentrations of MGO (324.7294 mM) grew cytoplasmic extensions and became clustered in appearance when exposed to high concentrations of MGO (Figure 5.4 D). A similar morphological change was observed in the study done by Saxena *et al.* (2003) when RAW 264.7 cells were exposed to LPS. The cells developed cytoplasmic extensions when exposed to LPS and was suggested to a result of mature macrophage differentiating into dendritic cells (DCs) which are immune cells that present antigens to naive T cells during a primary immune response. These authors suggest that this is a possible mechanism by which macrophages are recruited and activated to become DCs in order to fight off localised bacterial infections. Activated RAW 264.7 cells normally have the appearance of DCs (Lee *et al.* 2008). A similar morphological change in RAW 264.7 cells morphology was observed following exposure to MGO. Although the cell membrane shows changes such as pores that are associated with cellular death (Figure 4.5 D).

LPS is also known to activate RAW 264.7 cells and stimulate the production of nitric oxide (NO) (Gao *et al.* 1999). There is normally a sharp increase in the production of NO in a wound (Shekhter *et al.* 2005). Correct and sufficient production of NO is essential for and has several beneficial effects during the wound healing process. These include vasodilation and an increase in the permeability of blood vessels which promotes blood flow to the area of injury, antibacterial activity, antiplatelet effects and an increase in angiogenisis. In addition it also stimulates the release of chemoattractant cytokines. This plays a role in matrix deposition and remodelling of tissue as well as cellular proliferation, differentiation and apoptosis. Deficient NO synthesis has been linked to impaired wound healing and it is therefore important that NO concentration in a wound sight is correctly balanced (Schwentker *et al.* 2001).

The morphological change observed in RAW 264.7 macrophages due to MGO exposure is of special interest as honey contains MGO. When used as a wound dressing tissue macrophages in the wound site would enhance wound healing if activated by MGO. Increased NO production by activated macrophages may be an additional beneficial effect promoting wound healing abilities. In relation to antibacterial activity, MGO has primary direct antibacterial activity and a secondary response related to the activation of macrophages.

5.4.2 The cellular effect of MGO on Caco-2 colon carcinoma cells

5.4.2.1 Crystal violet and MTT assay

The effect of MGO on Caco-2 cells, which are epithelial like human colon cancer cells (ATCC 2014) was evaluated using two different assays as for the RAW 264.7 cells. After 48

hrs exposure to increasing concentrations of MGO changes in cell number and cell viability was determined using the CV (Figure 5.5 A) and MTT (Figure 5.5 B) assays respectively. Data was expressed relative to the control group expressed as 100% with no MGO added.

Using the CV assay, from 0.0003 – 0.0325 mM, a statistically significant increase in cell number is observed from 100% to 193.2, 188.5 and 178.09% for 0.0003, 0.0032 and 0.0325 mM respectively. At concentration of 0.3247 mM no significant change in cell number compared to control was observed. At a concentration of 3.2473 mM a small but statistically insignificant decrease in cell number was observed with a growth percentage of 90.09%. At concentrations of 32.4729 – 324.729 mM MGO cell number increased significantly to 218.373 and 366.062% for 32.4729 and 324.7294 mM respectively (Figure 5.5 A).

For the MTT assay which measures cell viability a statistically significant increase in cell viability was observed from 0.0003 – 0.3247 mM of MGO with a viability of 385.089, 371.300, 347.246 and 244.656% for 0.0003, 0.0032, 0.0325 and 0.3247 mM of MGO respectively. Almost no change in viability was observed at 3.2473 mM MGO with a viability of 105.406% and a slight but significant increase in viability was again observed from 32.4729 – 324.7294 mM MGO with a viability of 144.595 and 152.092% respectively (Figure 5.5 B).

A

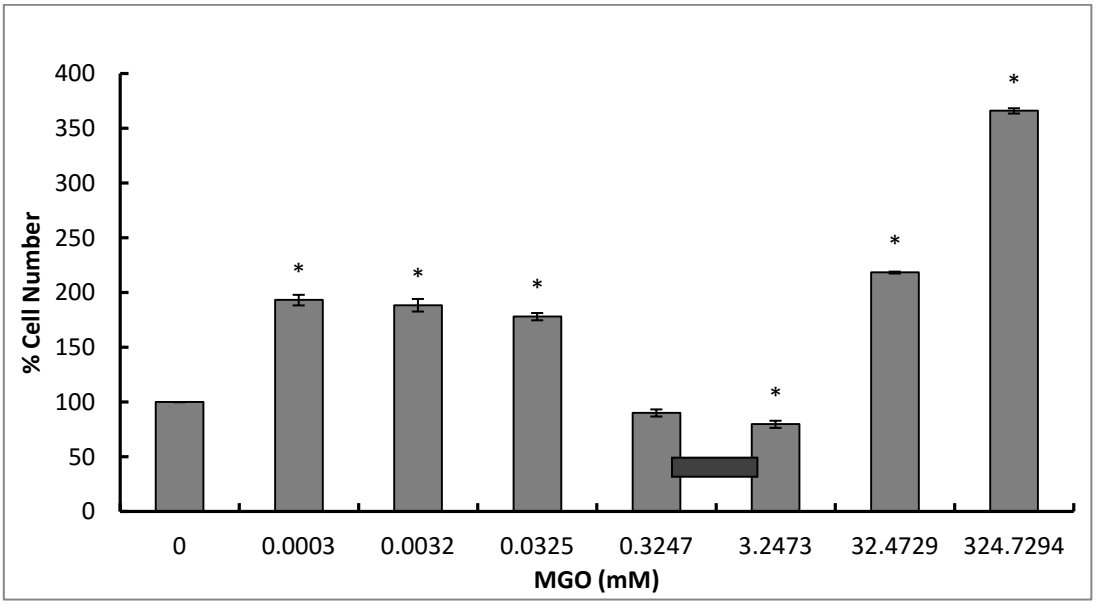

B

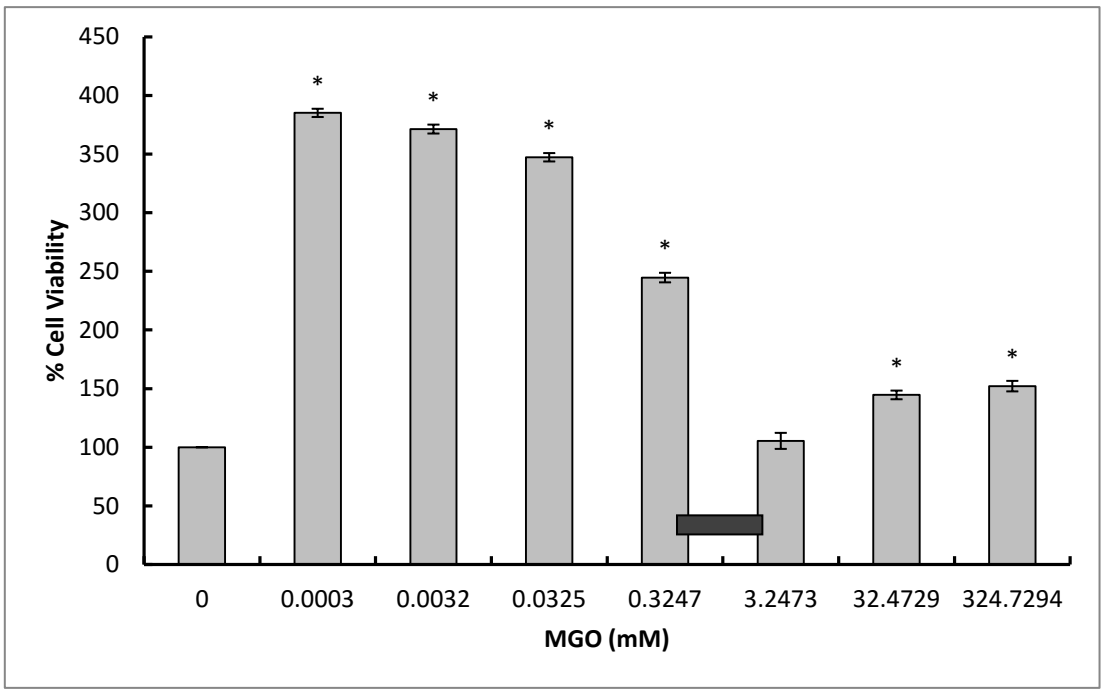

Figure 5.5: Caco-2 cells exposed to incresing concentrations of MGO showing (A) CV assay indicating percent growth and (B) MTT indicating percent viability after 48h exposure measuered as a percentage of a control with no MGO added.Data is an average of four (MTT assay) and four (CV assay) experiments ± SEM. Means with stars are significantly different, p≤0.005. Bar indicates the MIC range for all bacteria in chapter 4, section 4.4.1.

Similarly to what was seen with the RAW 264.7, the Caco-2 cells did not display classical toxicity. A significant increase in cell number was observed at concentrations of 0.0003 – 0.0325 mM MGO and again from 3.247 – 324.729 mM MGO for CV and from 0.0003 – 0.324 mM MGO and 32.473 – 324.729 mM MGO for MTT. Light microscopy with CV staining was used to confirm whether these changes are associated with an increase in cell density.

Images are presented below (Figure 5.6 A – H). Normal Caco-2 cells grow in clumps after 1 – 2 days of culturing (Black arrow) and develop a brush border after several days of growth (Briske-Anderson *et al.* 1997).

A: Control

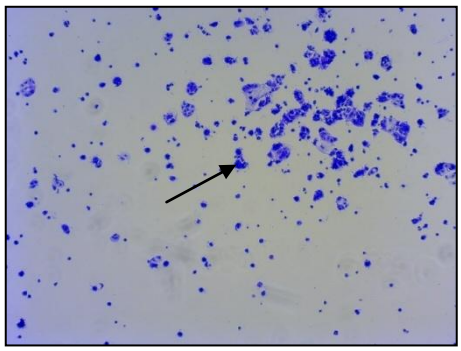

B: 0.0003mM

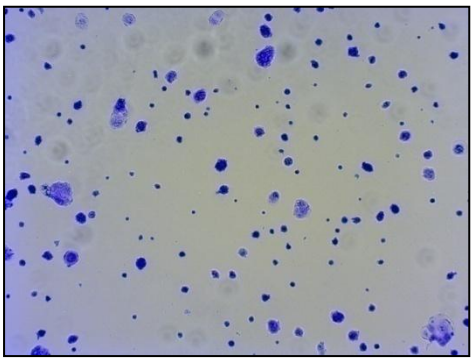

C:0.0032 mM

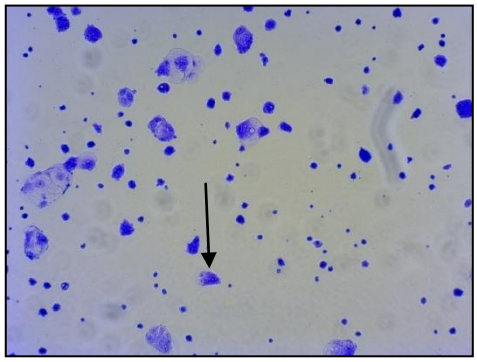

D:0.0325 mM

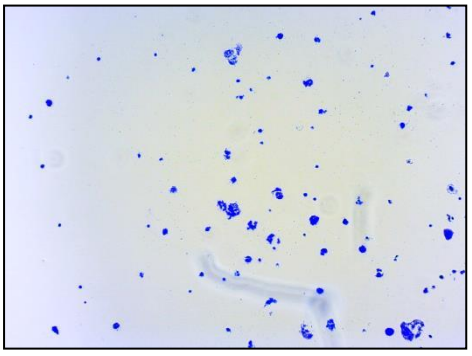

E: 0.3247 mM

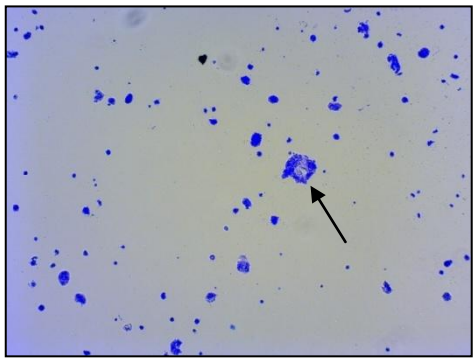

F: 3.2473 mM

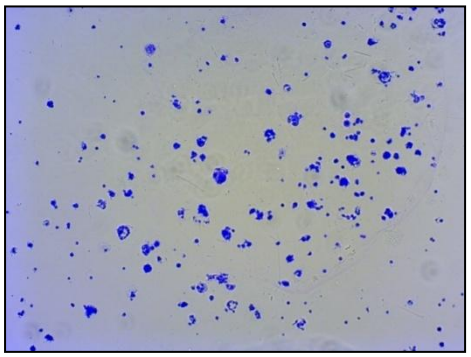

G: 32.4729 mM

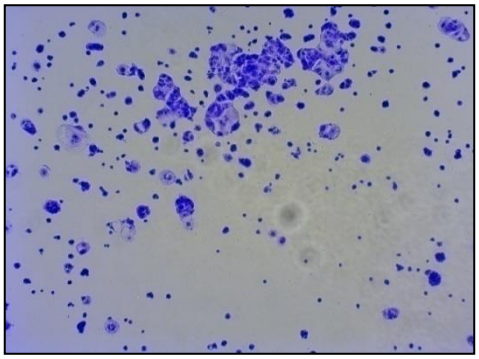

H: 324.7294 mM

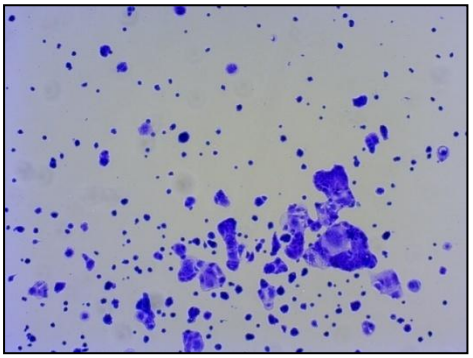

Figure 5.6: Light microscope images at x4 magnification showing differences in cell number and increase in colonies Caco-2 cells. (A): Control with no MGO and (B – H) exposed to increasing concentrations of MGO. Arrows indicate colonies.

In Figure 5.6 G – H an increase in staining and size of cell colonies can be observed.

As with the RAW 264.7 cells the data from the CV and MTT assays for Caco-2 was then expressed as a ratio of viability:cell number in order to determine if hormesis is occurring. The same ratios were used as for the RAW 264.7 cells (Figure 5.7).

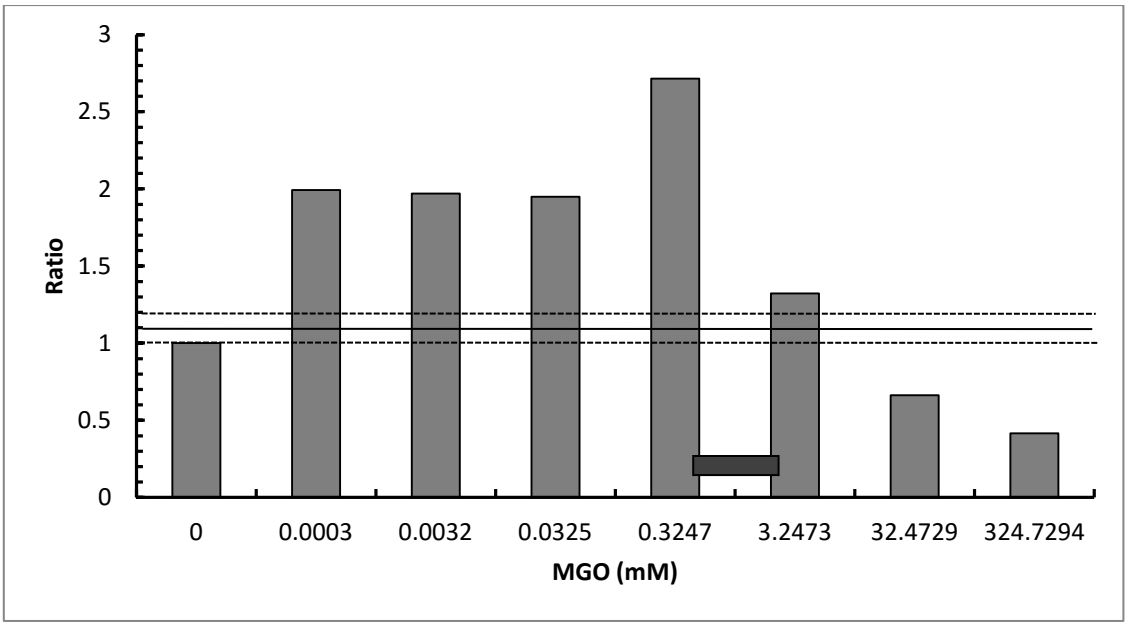

Figure 5.7: The ratio between cell viability and cell number for Caco-2 cells exposed to increasing concentrations of MGO where 1±0.1 indicates normal growth, > 1.1 indicates hormesis and < 0.9 indicates toxicity. Bar indicates the MIC range for all bacteria in chapter 4.

The values from Figure 5.7 indicate hormesis occurring from 0.0003 – 3.247 mM MGO and toxicity from 32.4729 – 324.7294 mM MGO.

5.4.2.2 Scanning electron microscopy

Caco-2 cells were exposed to the same three concentrations that were chosen of the RAW 264.7 cells and represent control (Figure 5.8 A), low (0.0003 mM) (Figure 5.8 B), medium (0.3247 mM) (Figure 5.8 C) and high (324.7294 mM) (Figure 5.8 D) concentrations of MGO. The cells were exposed in the same way as for the CV and MTT assays.

The Caco-2 cells in the control group (Figure 5.8 A), not exposed to MGO were ovoid and formed compact groups of colonies where each cell could be identified. At a low concentration (Figure 5.8 B) the cells were similar to the control. At a medium concentration (Figure 5.8 C), although the cells are still spherical it is more difficult to indentify individual cells. At high MGO concentration (Figure 5.8 D) the cells are spherical and tightly packed together with outgrowths extending from the cells' surface indicating differentiation.

A: Control

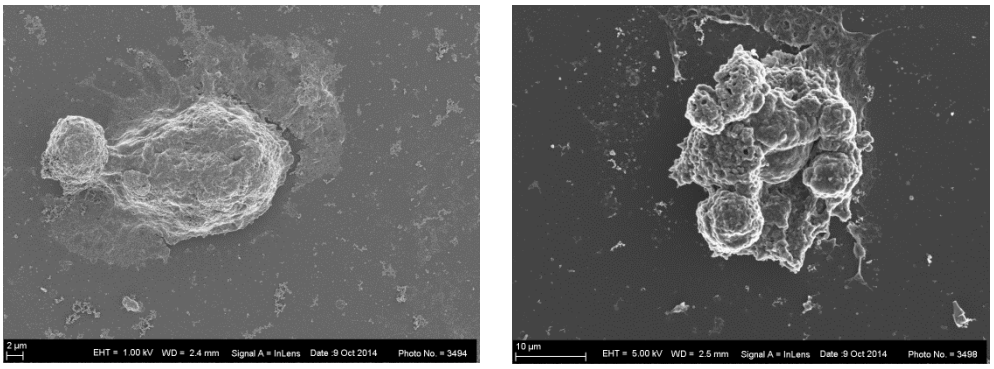

B: 0.0003 mM (Low)

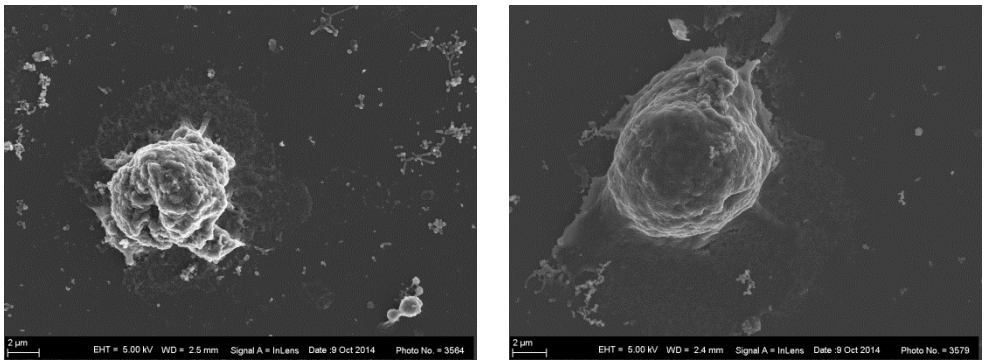

C: 0.3247mM (Medium)

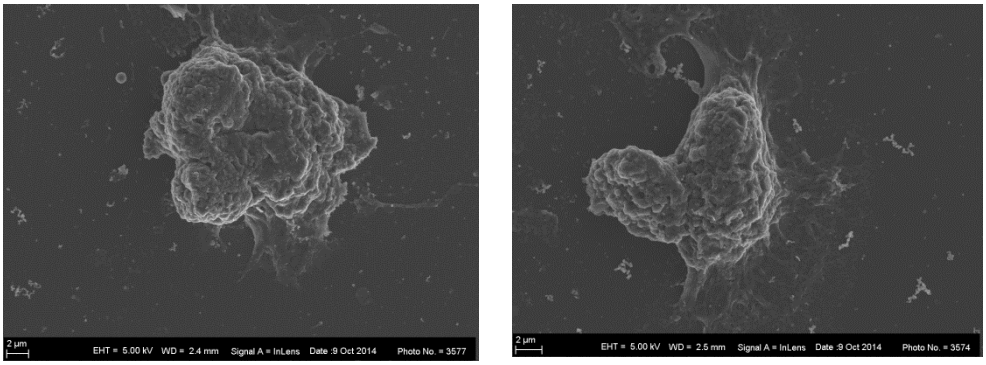

D: 324.7294 mM (High)

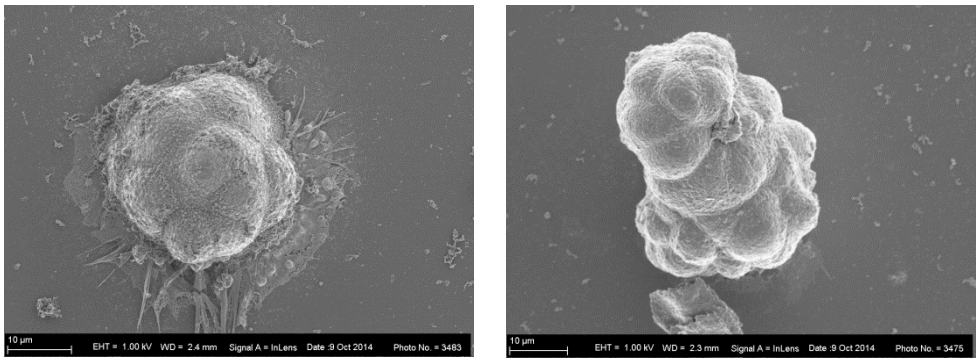

Figure 5.8: SEM images of Caco-2 cells exposed to 3 different MGO concentrations. A: Control group with no MGO added. B: Low MGO concentration (0.0003 mM) showing blebbing on the cell's surface C: Medium MGO concentration (0.3247 mM) showing multiple nuclei and some blebbing on the cell surface. D: High MGO concentration (324.7294 mM) showing multiple compact cells with extensions.

From the images in Figure 5.9 it can be seen that the morphology of the Caco-2 cells change from being adherent (Figure 5.9 A – C) to being less adherent and spheroid (Figure 5.9 D). The surface of the adherent cells had more protrusions and is less smooth in comparison to the spheroid cells that have a smoother surface. A scale of 2 µm in Figure 5.9 A – C in comparison to a scale of 10 µm in Figure 5.9 D is indicative of an increase in size of the spheroid cells at higher MGO concentrations. In a study done by Yan *et al.* (2013) these authors described similar morphological changes in human lung cancer cell lines A549 and H446. The cells that formed the spheroid like morphology were cultured in serum free conditioned medium (DMEM/F12 supplemented media) and B27 supplemented media. The use of B27 supplement eliminates the need to supplement the medium with serum since the exact composition of serum is undefined and varies from batch to batch (Gu *et al.* 2011). With B27 supplementation cells developed a more tumour like morphology (Yan *et al.* 2013) whereas cells grown in serum based medium had an adherent morphology. The spheroid cells were stem cell-like and highly expressed stem cell markers, Oct4 and Sox2. Sox2 is very strongly expressed in breast cancer tissue and it has been found to promote endothelial-mesenchymal transition in MCF-7 cells which is an important process during tumour metastasis (Li *et al.* 2013). Cancer stem cells (CSCs) contribute to tumour initiation, maintenance, metastasis as well as drug resistance (Yan *et al.* 2013). Caco-2 cells exposed to high MGO levels had a similar morphology however further studies will have to be done in order to determine whether MGO stimulates stem cell-like morphology and the expression of stem cell markers.

5.4.3 The cellular effect of MGO on SC-1 fibroblasts

5.4.3.1 Crystal Violet and MTT assays

The effect of exposure to increasing concentrations of MGO on SC-1 cells, which are mouse fibroblast cells (ATCC 2014) was evaluated in the same way as for the previous two cell lines. Following 48 hrs MGO exposure changes in cell number (Figure 5.9 A) and cell viability (Figure 5.9 B) was evaluated. Data was expressed relative to the control group expressed as 100% with no MGO added.

With the CV assay from 0.0003 – 0.0032 mM a small but significant increase in cell number is observed from 100% with a growth percentage of 115.51 and 119.36% for 0.0003 and 0.0032 mM MGO respectively. At concentration of 0.0325 mM no significant change in growth was observed with a growth percentage of 105.09. At 0.3247 mM MGO a small but significant decrease in growth was observed with 66.33% growth at this concentration. At 3.2473 mM MGO no significant change in cell growth was observed in comparison to the control. At higher concentrations of MGO (32.4729 mM and 324.7294 mM) cell number

increased significantly with a growth percentage of 137.92 and 197.52% respectively (Figure 5.9 A).

For the MTT assay which measures cell viability a statistically significant increase in cell viability was observed from 0.0003 – 0.0325 mM of MGO with a viability of 340.435, 353.721 and 333.146% for 0.0003, 0.0032 and 0.0325 mM of MGO respectively. A slight but significant decrease in viability was observed at 0.3247 mM MGO with viability of 64.281% and at 3.2473 mM MGO a slight but not statistically significant decrease in growth was observed with 81.696% viability. A significant increase in viability was again observed at 32.4729 mM MGO with a viability of 127.870%. No significant change in viability was observed at 324.7294 mM with a viability of 109.270% (Figure 5.9 B).

A

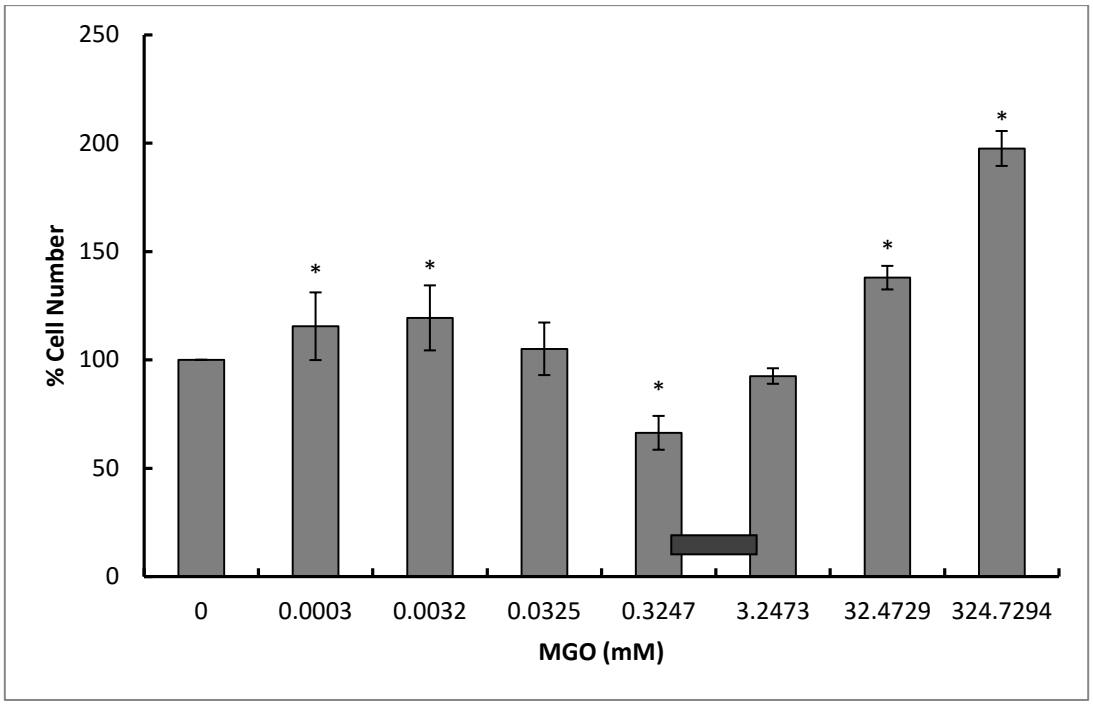

B

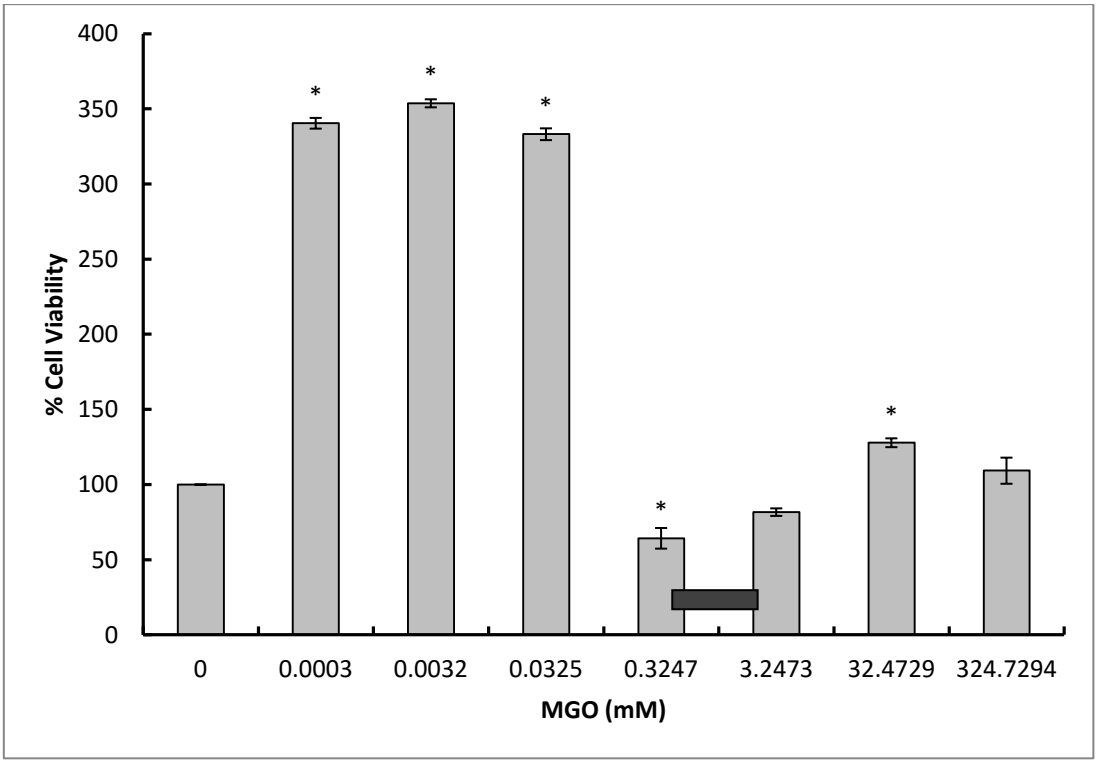

Figure 5.9: SC-1 cells exposed to increasing concenetrations of MGO showing (A) CV assay indicating percent growth and (B) MTT indicating percent viability after 48 h exposure measured as a percentage of a control with no MGO added. Data is an average of four (MTT assay) and four (CV assay) experiments ± SEM. Means with stars are significantly different, p≤ 0.005. Bar indicates the MIC range for all bacteria in chapter 4, Section 4.4.1.

As with the RAW 264.7 and Caco-2 cells a non-classical toxic response was observed. At the concentrations of 0.0003 – 0.0325 mM MGO and 32.473 – 324.7294 mM MGO an increase in cell number was observed. Likewise, at the concentrations of 0.0003 – 0.0325 mM MGO and again at 32.4729 mM an increase in cell viability was observed.

5.4.3.2 Rose Bengal assay

There is a lot of evidence suggesting that MGO exposure may result in AGE formation (Thornalley 1996; Bierhaus *et al.* 1998; Uchida 2000; Singh *et al.* 2001; Stitt 2001; Rachman *et al.* 2006; Nomi *et al.* 2009). The cross-linking that occurs due to this reaction may cause an increase in the amount of negative charge or a decrease in the amount of positive charge within a cell since the formation of AGEs involves positively charged amino acids such as Lys and Arg. This would result in an overestimation of cell number using the CV assay since the CV dye binds to negatively charged proteins and DNA. In order to evaluate the possibility of this effect the cells were stained using Rose Bengal. Rose Bengal dye binds to positively charged molecules and staining is therefore related to the number of positive charges. Less Rose Bengal dye will be absorbed by the cells in comparison to CV if positively charged molecules (lysine and argentine) are modified by AGES. The amount of Rose Bengal dye taken up into the cells was compared to the amount of CV dye absorbed (Figure 5.10).

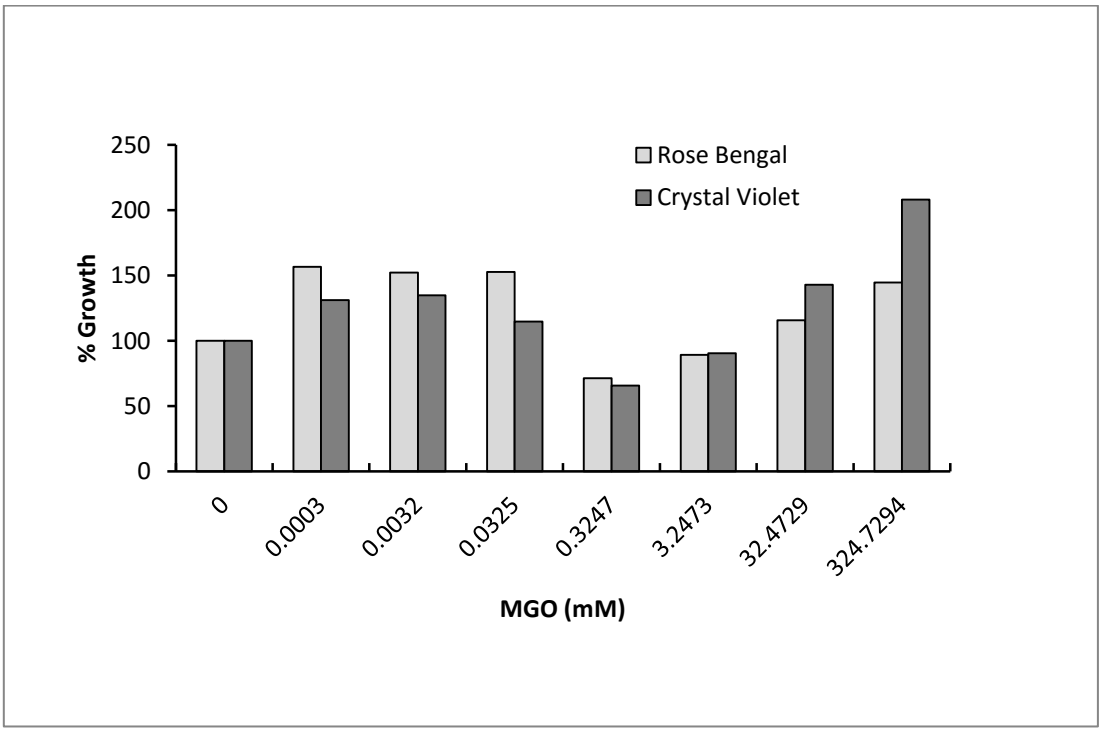

Figure 5.10: Comparison of percent growth according to Rose Bengal and CV assays showing a similar trend.

As shown in Figure 5.10 the results from the Rose Bengal assay show a similar trend to that of the CV assay was obtained (Figure 5.9 A).This indicates that CV staining does reflect cell number and increased staining is due to binding to cellular components and not for example the cell culture surface.

The effect of MGO exposure on cell density of SC-1 cells was also evaluated in the same way as for the previous two cell lines. The cells were exposed in the same manner as the RAW 264.7 and Caco-2 cells. The cell density of CV stained SC-1 cells was evaluated using light microscopy. Images are presented in Figure 5.11 A – H. SC-1 cells have typical spindle morphology (Figure 5.11 B, Black arrow). The density of the fibroblasts has increased at the highest concentrations (32.4729 – 324.7294 mM) and dispersed between the fibroblasts with a typical spindle morphology are larger cells, possibly myofibroblasts (Figure 5.11 H, Red arrow).

A: Control

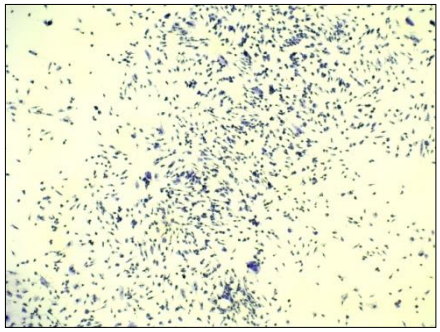

B: 0.0003 mM

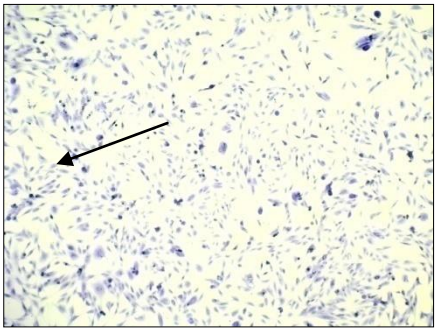

C:0.0032 mM

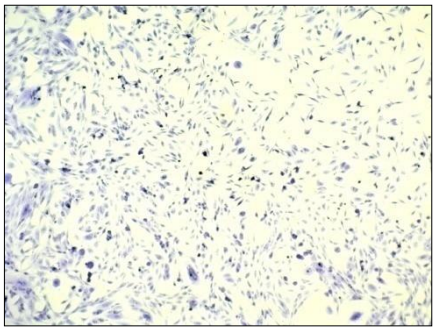

D:0.0325 mM

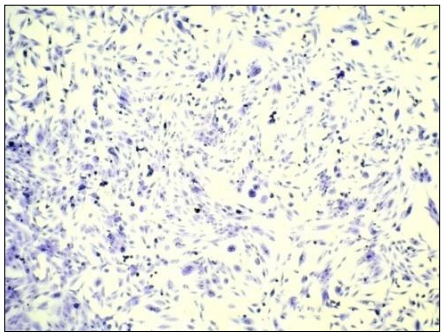

E: 0.3247 mM

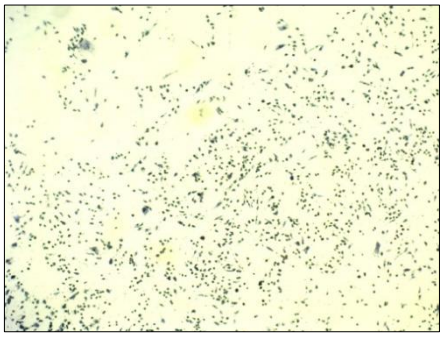

F: 3.2473 mM

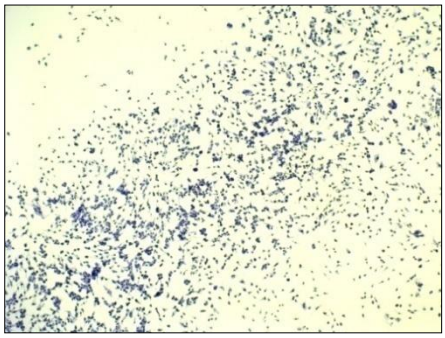

G: 32.4729 mM

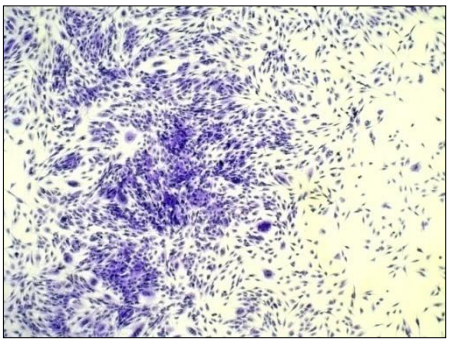

H: 324.7294 mM

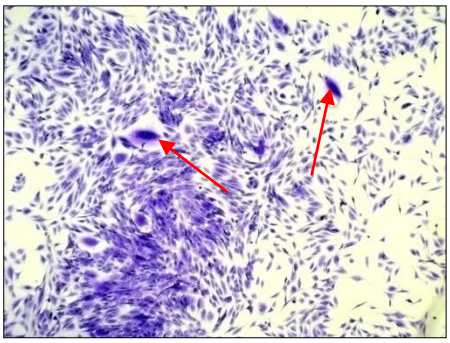

Figure 5.11: Light microscope images at x40 magnification of SC-1 cells exposed to increasing concentrations of MGO showing differences in cell number and size. (A): Control with no MGO and (B – H) exposed to increasing concentrations of MGO. Arrows indicate myofibroblasts.

A similar trend can be seen from the images above as with the RAW 264.7 and Caco-2 cells with an increase in cell number at higher concentrations of MGO (32.4729 – 324.7294 mM). The cells at this concentration also appeared to from whorls with larger cells (red arrows) amongst the smaller cells.

As with the previous two cell lines, a non-classical biphasic toxicity response was observed in the SC-1 cell line. The data from the CV and MTT assays for SC-1 was also expressed as a ratio of viability:cell number using the same ratios as for the previous two cell lines to indicate normal growth, hormesis or toxicity (Figure 5.12).

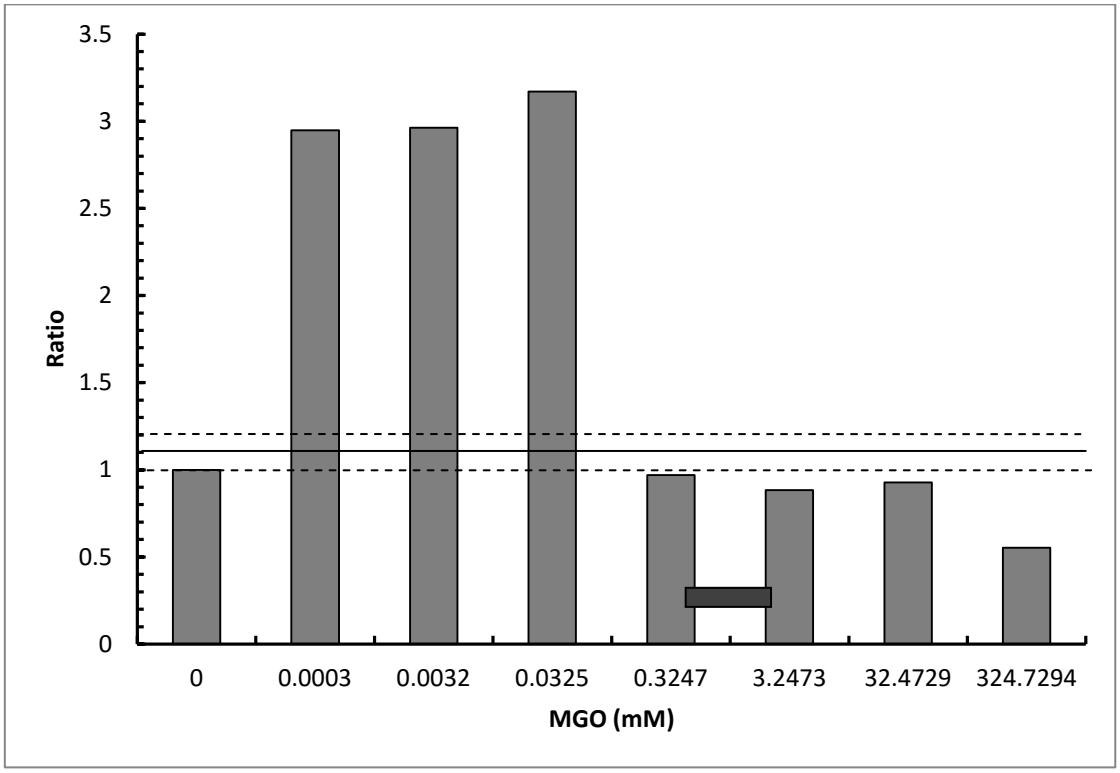

Figure 5.12: The ratio between cell viability and cell number for SC-1 cells exposed to increasing concentrations of MGO where 1±0.1 indicates normal growth, > 1.1 indicates hormesis and < 0.9 indicates toxicity. Bar indicates the MIC range for all bacteria in chapter 4, Section 4.4.1.

From Figure 5.12 it can be seen that from a MGO concentration of 0.0003 – 0.0325 mM hormesis occurs. From a concentration of 0.3247 – 32.4729 mM MGO cell growth and viability is normal and at 324.7294 mM MGO toxicity occurs (Figure 5.12).

5.4.3.3 Scanning electron microscopy

The same three concentrations that were chosen for the previous two cell lines were used for the SC-1 cells in order to evaluate the morphological changes that occur due to MGO exposure. Control (Figure 5.13 A), Low (0.0003 mM MGO) (Figure 5.13 B), medium (0.3247 mM MGO) (Figure 5.13 C) and high (324.7294 mM MGO) (Figure 5.13 D) concentration

groups were compared. The cells were exposed in the same way as the previous two cells lines and photographed using a scanning electron microscope. The images are shown in Figure 5.13 A – D.

The SC-1 cells in the control group (Figure 5.13 A), not exposed to MGO, were spindle shaped cells with no blebbing visible on the cells' surface. The fibroblasts that were exposed to low and medium MGO concentrations (Figure 5.13 B & C) show a similar appearance to that of the control group. The cells that were exposed to a high MGO concentration (Figure 5.13D) show that appearance of fillopodia extending from the surface of the cell (Yuen *et al.* 2010).

A: Control

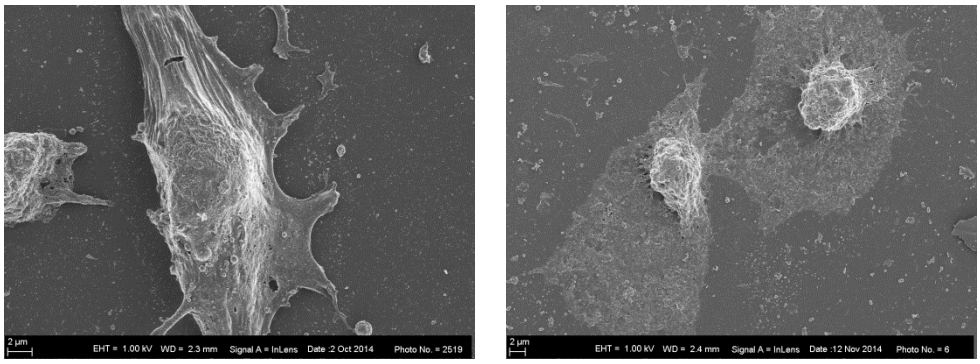

B: 0.0003 mM (Low)

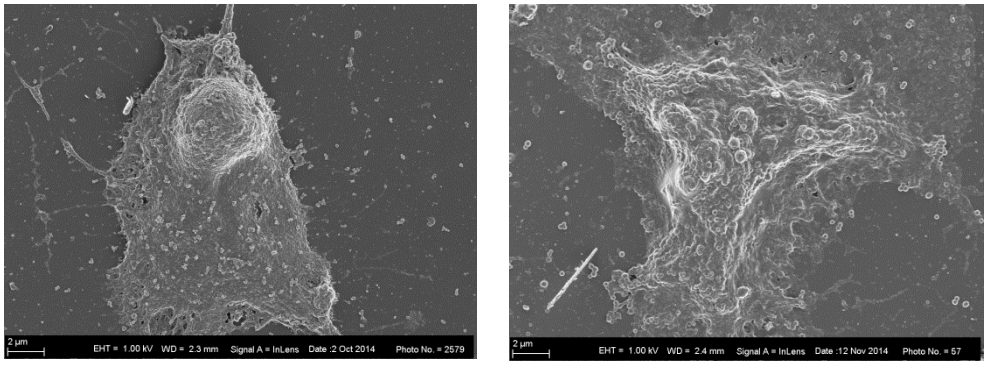

C: 0.3247 mM (Medium)

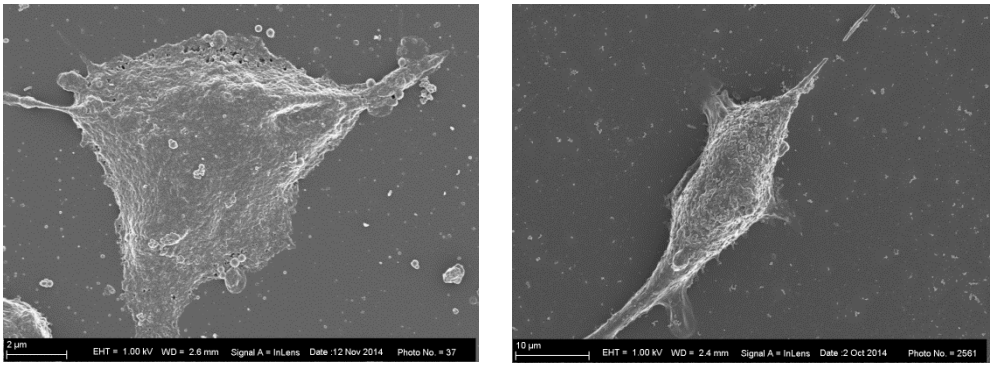

D: 324.7294 mM (High)

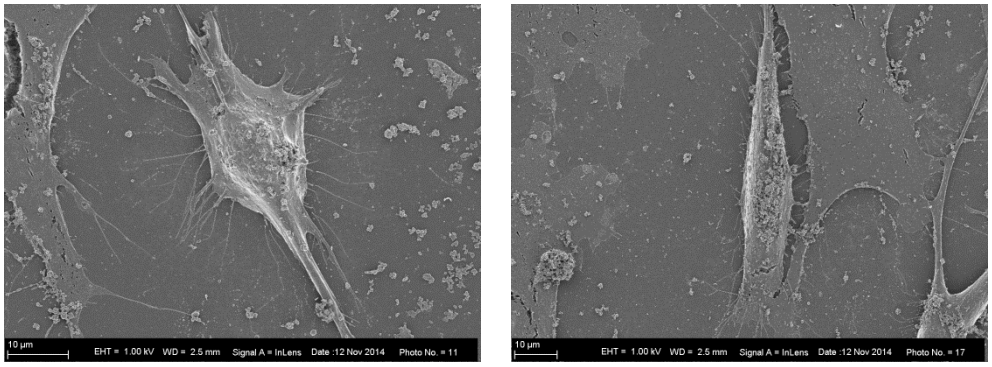

Figure 5.13: SEM images SC-1 cells exposed to 3 different MGO concentrations. A: Control group with no MGO added. B: Low MGO concentration (0.0003 mM) showing similar surface morphology to that of the control (A). C: Medium MGO concentration (0.3247 mM) showing similar surface formation to that of the control (A). D: High MGO concentration (324.7294 mM) showing *extensions/outgrowths* from the cell's surface.

The SC-1 cells in this study became more spindle shaped and grew extensions and filopodia at higher concentrations (324.7294 mM).The scale increase from 2 µm to 10 µm in Figure 5.13 D also indicates an increase in cell size. In a study done by Oguri *et al.* (2014) on human cardiac fibroblasts, these researchers found that increased concentrations of MGO activates the process by which the cells progress from the G1/G0 phase to the S and G2/M phase. These cells were stimulated to differentiate into myofibroblasts which are large spindle shaped stellate cells with numerous cytoplasmic processes. Yuen *et al.* (2010) discovered that fibroblasts cultured on MGO-treated collagen expressed more proteins associated with differentiation into myofibroblasts. When observed using SEM the fibroblasts had a similar appearance to the fibroblasts examined in the present study. In addition Oguri *et al.* (2014) also discovered that the fibroblasts cultured on MGO-treated collagen grew in clusters on the matrix instead of spreading out evenly. These cells were also found to be less adherent to the collagen matrix. The collagen matrix was more contracted and the fibres had increased in size. In the cardiac tissue of diabetic patients the differentiation of fibroblasts into myofibroblasts is associated with heart failure in these patients (Yuen *et al.* 2010). However, the rearrangement of actin-cytoskeletal components and the formation of these extensions or filopodia in fibroblasts are essential in order for the cells to be able to migrate towards one another in a wound so that it can close up and heal (Bartling *et al.* 2009; Velnar *et al.* 2009). If the use of MGO as a wound dressing could help to stimulate and activate fibroblasts in the skin this may aid the wound healing process. There is however some concern with regards to diabetic patients since they already have an elevated MGO level in their blood (Paul and Bailey 1999; Bartling *et al.* 2009). MGO and increased AGE formation has also been associated with the formation of myofibroblasts in the heart which is thought to contribute to ventricular dysfunction and diabetic cardiomyopathy due to stiffness in the heart (Sassi-Gaha *et al.* 2010; Oguri *et al.* 2014).

5.5 Summary of results

In general exposure to a low MGO concentration caused a significant increase in cellular metabolism for all cell lines and only a slight increase in cell number. A significant increase in cell number was observed at higher MGO concentrations (Figure 5.14). This was not due to change in charge as indicated by Rose Bengal staining used on SC-1 cells but rather due to increase in cell number.

A

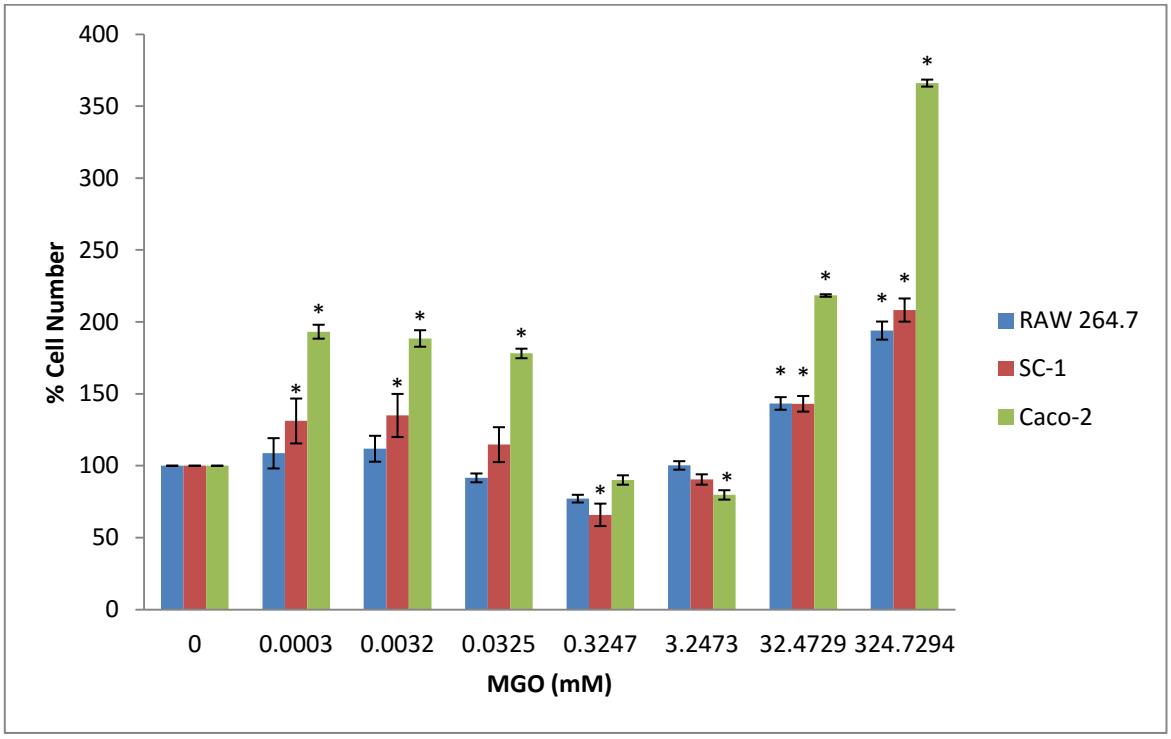

B

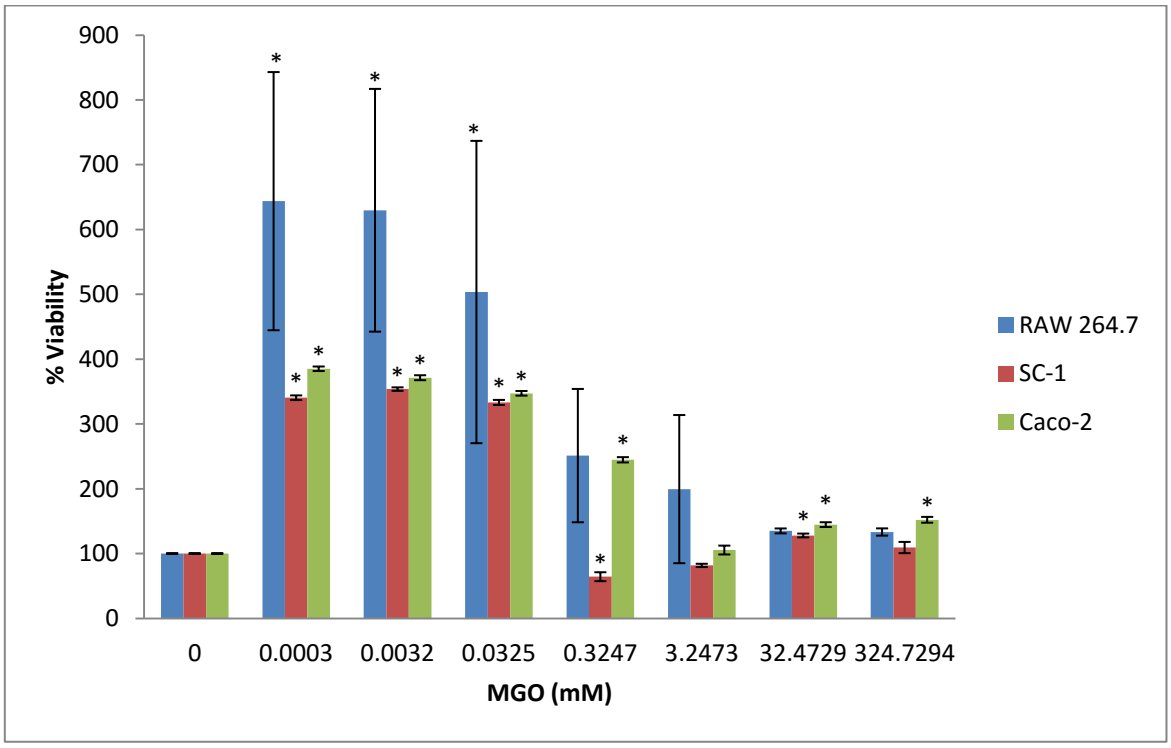

Figure 5.14: Comparison of the effect of a MGO concentration range on RAW 264.7, SC-1 and Caco-2 cell lines using (A) crystal violet and (B) MTT assays. Data is an average of four experiments ± SEM. Means with stars are significantly different, p≤0.005.

Hormesis occurs at low MGO concentrations and this can be seen from the large increase in cellular metabolism (MTT) but not in cell number (CV) with the ratio of MTT:CV being > 1.1. This suggests that MGO stimulates cellular metabolism at lower concentrations in order to prepare for higher, more toxic MGO concentrations. A ratio of < 0.9 at high MGO concentrations indicates that MGO is toxic. Clinically at low concentrations MGO will stimulate cellular metabolism but at high concentrations may be toxic.

Scanning electron microscopy revealed no morphological changes at low and medium concentrations of MGO (0.0 – 0.235 mM) for any of the three cell line evaluated. At the highest concentration evaluated (324.729 mM) changes in morphology was observed.

MGO appears to stimulate fibroblasts to become activated and differentiated and more spindle shaped with filopodia which are essential for the wound healing process to take place (Velnar *et al.* 2009). Larger fibroblasts that seem to have the morphology of myofibroblasts are also present and these cells play an important role in wound contraction.

Honey was also found to be non-toxic when tested on human HaCaT skin keratinocytes and it stimulates pathways of cellular proliferation and locomotion that lead to keratinocyte re-epithelialization (Ranzato *et al.* 2012).

In diabetic patients blood MGO levels are high and in these patients MGO causes cardiac fibroblasts to differentiate into myofibroblasts which is often associated with heart failure (Yuen *et al.* 2010). Also, the modification and consequent stiffness and fibrosis of the collagen matrix associated with the formation and accumulation of AGEs should be taken into consideration when it comes to the treatment of diabetic ulcers with MGO products. There is however no evidence to suggest that MGO will have negative effect if used to treat wounds other than ulcers in diabetic patients (i.e. burn wounds). More studies are needed in order to determine if MGO will result in fibrosis in such a wound or have a systemic effect at peripheral site.

In vitro, high concentrations of MGO activate RAW 264.7 cells and this is an important process as macrophages migrate to the site of injury during the second stage of wound healing (Velnar *et al.* 2009). This can provide a secondary bactericidal effect from activation of immune cells as well as direct killing of bacteria as shown in chapter 4.

The Caco-2 cells became more spheroid-like which is a morphology that has been described for tumour cells stem cell like characteristics. This is reason for concern however MGO has been shown to inhibit the ability of cancer cells to migrate through collagen that has been MGO treated. There have been a number of studies that suggest MGO has anticancer

properties. Bartling *et al.* (2009) discovered that an accumulation of AGE modified collagen from rat tails reduces the ability of cancer cells to migrate through the tissue.

Similarly Paul and Bailey (1999) found that increasing concentrations of MGO caused a decrease in the spreading and adherence of cancer cells (fibrosarcomas and osteosarcomas) to the collagen matrix.

5.5.1 Methylglyoxal in other studies

Many studies have verified that honeys have antimicrobial properties and can help accelerate the healing of a wound. Most of these studies are related to burn wounds however and not much evidence exists to support its effectiveness on other types of wounds (Majtan 2011). MGO has been evaluated for toxicity in previous studies including the evaluation of the effects of MGO in different cell lines, concentrations and exposure times. The results are summarised in Table 5.1. These are compared to the present study.

Table 5.1: Comparison of different studies on the toxic effect of MGO

Cell type	Exposure Time (hr)	Concentration (mM)	Toxicity range (mM)	Assay	References
Human buccal cells	1	1 – 100	10 – 100	MTT	(Vaca *et al.* 1997)
RINm5F insulin secreting cells	6	0.1 – 10	10	Hoechst 33342	(Sheader *et al.* 2001)
Bovine retinal pericytes	6	0.2–0.8	0.6 –0.8	MTT	(Kim *et al.* 2004)
PDGF-receptor activity in rabbit femoral smooth muscle cells	16	0 – 1.0	0.1	MTT Kinase activity Western blotting	(Cantero *et al.* 2007)
Fibrosarcoma (HT1080) Osteosarcoma (MG63)	20	0.1 – 100	10 – 100	MTT	(Paul and Bailey 1999)
Mouse Phoechromocytoma (PC12) Aldehyde reductase overexpressing PC12 (PC12-ALR-14)	24	1 – 100	5 – 10	Methylene Blue	(Suzuki *et al.* 1997)
Rat Schwannoma RT4 U-87 glioma cells	24	0.05 – 2	0.5 – 2	MTT	(Lee *et al.* 2009)
Immortalized rat Schwann cells	48	0 – 1.0	50% of control at 0.5 mM 15% increase in apoptosis of at 1.0 mM	MTS Hoechst 33342	(Ota *et al.* 2007)
RAW 264.7	48	0.0003 - 324.7	32.5 – 324.7	MTT : CV	Present study
SC-1	48	0.0003 - 324.7	32.5 – 324.7	MTT : CV	Present study
Caco-2	48	0.0003 - 324.7	3.5 – 324.7	MTT : CV	Present study

Two factors that contribute to toxicity is concentration and exposure time. The higher the concentration and the longer the exposure time the greater the toxicity. In addition the sensitivity of the assay used to measure the end point also influences the results. For

example the MTT assay is more sensitive than the methods such as CV, Methylene Blue and Hoechst 33342 staining methods used to determine cell number.

In Table 5.1, it is shown that the most sensitive cell lines are primary cell cultures of bovine retinal pericytes that showed toxicity of 50% at 0.6 mM after only 6 hours of exposure (Kim *et al.* 2004). Primary cell cultures are normally more sensitive than cells from an immortalised cell line.

The U87 glioma and TR4 schwannoma cells were also found to be MGO sensitive following 24 hrs exposure using the MTT assay. The U87 glioma cells are human glioblastoma or astrocytoma cells taken from the brain tissue (ATCC 2014) and the RT4 cells are rat neuronal Schwannoma cells of the peripheral nervous system (ATCC 2014). In general neurological tissue is more sensitive to the effects of toxins.

The least sensitive cell line was the fibrosarcoma and osteosarcoma cell lines where toxicity was observed at 10 mM after 20 hrs of exposure. Both cell lines are derived from support tissue (ATCC 2014) and MG63 are osteosarcoma cells taken from human bone tissue (ATCC 2014). Sarcomas are mesenchymal in origin and may be more resilient to toxins due to their malignant nature.

Platelet derived growth factor (PDGF), important in smooth muscle proliferation as well as the healing of diabetic foot ulcers, plastic surgery and bone fractures, shows reduced receptor activity following 16 hr exposure to 0 -0.1 mM MGO (Table 5.1) (Cantero *et al.* 2007). This study used low levels of MGO in comparison to certain other studies suggesting that exposure to low MGO levels can cause changes in biochemical pathways prior to changes in cellular morphology associated with exposure to high MGO levels.

In contrast to the above mentioned studies, Jia *et al.* (2012) demonstrated that MGO exposure resulted in an increase in proliferation and progression through the cell cycle of adipocyte like cells 3T3-L1 with an increase in activation sites phosphor-Atk1 (S473) and phosphor-Atk1 (T308) in ATK1-kinase. The major difference between this study and the previously mentioned studies is that this study used levels of MGO that were at a more physiological level (0 – 50 µM) where as the other studies used higher doses. In agreement with other studies this study also observed a decrease in proliferation when the MGO doses were increased. This suggests a biphasic response to MGO exposure where low levels stimulate growth but higher levels result in apoptosiss (Jia *et al.* 2012) as was also found in the present study. A hormetic effect was observed at lower concentrations from 0.0003 - 0.0325 mM (0.3 – 32.5 µM). This range covers the physiological MGO concentrations of

healthy as well as diabetic individuals; 1.4 – 3.3 µM for healthy individuals and 3.6 – 5.9 µM for diabetic patients respectively (Chang *et al.* 2011).

5.5.2 Cellular toxicity in comparison to bacterial MIC

The concentration of MGO in UMF 10, 15, 20 and 25 is ≥ 263, ≥ 514, ≥ 829 and ≥ 1200 mg/kg respectively (Table 2.2, Chapter 2). This is equivalent to 3.65, 7.13, 11.50 and 16.65 mM respectively which is not toxic.

According to the results from chapter 3 the MGO contents of various southern Africa honeys ranged from 692.59 – 1261.23 mg/kg (9.61 – 17.5 mM) (Figure 3.11, Chapter 3), indicated by yellow block in the table below. Also indicated below is the effect of MGO on the SC-1, RAW 264.7 and the Caco-2 cell lines where in Table 5.2, H indicates hormesis, N normal growth and T toxicity. The corresponding effect that these concentrations had on bacteria is indicated on the same table (blue block) in order to compare if the concentrations that are able to kill or inhibit bacteria are harmful to cells.

Table 5.2: MGO concentrations tested on cells and their corresponding effect seen on bacteria

Cell/Bacteria type	Concentration (mM)						
	0.0003	**0.0032**	**0.0325**	**0.3247**	**3.2473**	**32.4729**	**324.7294**
MGO in honey						9.61 – 17.5	
Bacterial MIC					0.6 – 1.2		
RAW	H	H	H	H	H	N	T
Sc-1	H	H	H	N	N	N	T
Caco-2	H	H	H	H	H	**T**	T
S. aureus				**	*		
B. subtilis			**		*		
E. coli				**	*		
P. aeruginosa				**	*		

H = hormesis, N = normal, T = toxicity, yellow = MGO concentration found in honeys in this study, blue = MIC for bacteria.

* MIC (mM) for *S. aureus* (0.6 – 0.8), *B. subtilis* (1.0 – 1.2), *E. coli* (0.8 – 1.0), *P. aeruginosa* (1.0 – 1.2)

** IC_{50} (mM) for *S. aureus* (0.2 – 0.6), *B. subtilis* (0.01 – 1.0), *E. coli* (0.2 - 0.8), *P. aeruginosa* (0.2 – 1.0)

From this table it can be seen that within the concentration range (between 0.3247 and 3.2473 mM) where 100% bacterial inhibition starts occurring (indicated in blue) no cellular toxicity was observed. Within this range hormesis was observed for the RAW 264.7 cells

while the SC-1 cells exhibit normal growth. MGO caused toxicity in the Caco-2 cells in the upper region of this range where 33.79% Caco-2 cells had died at 32.4729 mM MGO.

5.5.3 Methylglyoxal toxicity and wound healing: Normal and diabetic patients

Wound healing occurs in 4 stages: 1) Coagulation and haematostasis is the first stage and happens immediately after injury. Its function is to protect the vascular system and keep it intact as well as to provide a matrix for new cells to migrate to. 2) The inflammatory phase provides an immune barrier against invading microorganisms. Firstly neutrophils invade the area of the wound and start to phagocytose microorganisms that may have entered during injury. Monocytes follow and differentiate into macrophages upon arrival at the wound. These cells continue with phagocytosis and secrete growth factors that activate keratinocytes, fibroblasts and endothelial cells for tissue remodelling. 3) The proliferative phase occurs when fibroblasts migrate from the surrounding tissue to the injured area and deposit new matrix. Fibroblasts proliferate and produce the extracellular matrix and then differentiate into myofibroblasts. The myofibroblasts extend pseudopodia to attach to fibronectin and actin in the matrix. 4) The remodelling stage is the final stage and may last up to several years. During this stage new epithelium is developed and scar tissue is formed (Velnar *et al.* 2009).

Findings of the present study have identified potential wound healing and beneficial effects of MGO including antibacterial activity, macrophage activation and myofibroblast formation. However the occurrence of toxicity at higher concentration is of concern, especially related with Manuka honey with a high UMF i.e. high MGO content.

Diabetic patients have elevated blood MGO levels of 3.6 – 5.9 µM as opposed to1.4 – 3.3 µM found in healthy individuals (Paul and Bailey 1999; Jia *et al.* 2006; Chang *et al.* 2011) and these patients with raised MGO levels may provide important information on the long term cellular effects of MGO. MGO is a highly reactive molecule that reacts with Lys, Arg and Cys residues, forming cross-links in long-lived proteins such as collagen. This cross-linking results in the irreversible formation of AGEs within the collagen matrix which disrupts the normal physiological functioning and matrix formation (Sassi-Gaha *et al.* 2010; Majtan 2011). Cross-linking within collagen fibres may also result in loss of elasticity (Majtan 2011). Song *et al.* (2008) reported that the cross-linking resulting from AGE accumulation inhibits keratinocyte migration in high glucose concentrations (Song *et al.* 2008; Majtan 2011). This may be due to the stiffness from reduced elasticity which impairs movement through the collagen matrix of diabetics. According to a study by Niu *et al.* (2012) accumulation of AGEs increase the activity of neutrophils in diabetic ulcers. This may contribute to the occurrence of chronic inflammation in diabetic patients.

In a study done by Chong *et al.* (2007) it was found that MGO exposure reduced the binding and subsequent phagocytotsis of collagen when human gingival fibroblast cells from both healthy patients and patients with gingivitis. It is important for collagen to be phagocytosed in order to maintain homeostasis otherwise fibrosis occurs.

Diabetic cardiomyopathy is a common cause of heart failure in diabetic patients associated with ventricular malfunction. The cause of this is still unknown although it is believed that it may be partially due to collagen stiffness in the heart (Oguri *et al.* 2014). Cardiac fibroblasts normally secrete collagen type I and II as well as growth factors, cytokines, lipid mediators and they influence the cell-matrix and cell-cell interactions (Sassi-Gaha *et al.* 2010; Oguri *et al.* 2014). Homeostasis of these functions and the tight regulation of migration, proliferation, differentiation and secretion is essential for proper functioning of the heart (Yuen *et al.* 2010).

It is believed that AGEs are involved in collagen cross-linking. This modification of collagen causes the collagen to become stiff and more contracted (Sassi-Gaha *et al.* 2010; Oguri *et al.* 2014). In a study by Sassi-Gaha *et al.* (2010) they found that MGO-modified collagen stimulates an increase in secretion of collagen type I by the fibroblasts as well as an increase in size of the collagen fibres. The stiffness and tension was also greater in MGO-modified collagen. The fibroblasts cultured on the modified collagen also showed less adherence the matrix. In accordance to their study Yuen *et al.* (2010) observed similar results when they cultured fibroblasts on MGO-treated collagen. The fibroblasts had a decreased adherence to the matrix but a stronger adherence to one another. When viewed using SEM the cells grew in clusters as opposed to spreading out evenly throughout the matrix. Intercellular adhesion encourages differentiation into myofibroblasts. They also found that the MGO induced the expression of proteins that are associated with myofibroblast formation from fibroblasts. More myofibroblasts encourage the collagen to become more contacted and stiffer. Two thirds of heart ventricle consists of fibroblasts. Differentiation of fibroblasts into myofibroblasts strongly up regulate heart failure. Oguri *et al.* (2014) discovered that MGO stimulates Ca^{2+} influx into human cardiac fibroblasts. Increased intracellular Ca^{2+} promotes the progression of the cells from the G1/G0 phase to the S and G2/M-phase as well as promoting fibroblast differentiation.

A common occurrence in diabetic patients is the occurrence of foot ulcers and the treatment of such a wound can become costly. Dressings impregnated with silver are often used since these help with the control of bacterial infection. However, some bacteria have been reported to have become resistant to these products. Other products need to be found and researchers are looking more and more into natural products as they are abundant,

therefore less costly, and also have many antimicrobial properties to which bacteria are not resistant (Majtan 2011).

Although medical honey products containing MGO have been found to aid in the healing process of wounds in otherwise healthy patients, caution should be used in the treatment of diabetic ulcers with MGO containing honey and wound healing products (Majtan 2011). There are several reasons for this. Firstly, diabetic patients have already elevated MGO blood levels (Paul and Bailey 1999) although it is unknown if topical administration alters these levels. MGO is highly reactive and easily reacts with certain amino acid side chains forming cross-links within the structure of a protein such as collagen which results in the formation of AGEs. Cross-linking causes stiffness and loss of elasticity (Sassi-Gaha *et al.* 2010). In addition to this it causes impaired migration of keratinocytes through the collagen matrix (Song *et al.* 2008) as well as impairing collagen phagocytosis (Chong *et al.* 2007). The stiffness and impaired phagocytosis contributes the fibrosis occurring in the wound. In addition to this, as reported by Nui *et al.* (2012) MGO also activates neutrophils which may lead to chronic inflammation.

As also previously mentioned increased levels of MGO in the blood and the accumulation of AGEs in the heart muscle may contribute to the development of diabetic cardiomyopathy. No studies were found providing insight into the effects of MGO should it be used to treat a wound other than ulcers in diabetics (for example the use of MGO containing products to treat a burn wound in a diabetic patient) There is also no evidence suggesting that MGO can enter the blood stream if used externally and get transported to the heart to contribute to cardiomyopathy. Further studies will need to be done in order to shed some light on this.

5.6 Conclusion

At low concentrations MGO has a hormesis effect while at higher levels toxicity is observed. Morphological characteristics associated with differentiation are observed that may have a beneficial effect in wound healing. MGO levels in southern Africa honey are not cytotoxic and at bacterial MIC no cellular toxicity is observed.

Chapter 6: Concluding discussion

6.1 Rationale for the study

The wound healing process is a complex process that occurs in four stages namely haemostasis and coagulation, inflammation, proliferation and the remodelling phase (Velnar *et al.* 2009). If this process is disrupted, the wound many not close or heal properly and complications can arise (Mavric *et al.* 2008; Velnar *et al.* 2009). In a chronic wound this process has been disrupted due to the infection that has occurred. In order for such a wound to heal the infection needs to be eradicated first before regrowth can be re-stimulated (Mavric *et al.* 2008). Another area of concern is the occurrence of nosocomial, postsurgical infections. Patients that have a compromised immunity or that are on immune suppressing medication are especially vulnerable to such an infection while in hospital (Rubin 1993; Mangram *et al.* 1999). Such infections need to be prevented before occurrence as it can complicate and delay the healing process.

A well known method of treatment in the healing of wounds is via the use of Manuka honey. This honey has been found to be effective against pathogens that grow in wounds including bacteria that have become resistant to certain drugs such as Methicillin-resistant *S. aureus*. The antibacterial activity of Manuka honey is due to several characteristics of the honey as well as compounds present in the honey that all contribute to its effect. The main compound responsible for this activity however, is MGO (Kim *et al.* 2004; Mavric *et al.* 2008; Stewart *et al.* 2014). Different grades of Manuka are available according to the Unique Manuka Factor (UMF) of the honey which is an indication of the amount of MGO present in the honey (Mavric *et al.* 2008). Manuka honey is derived from *Leptospermum scoparium* blossoms indigenous to New Zealand (Stewart *et al.* 2014) which means that any Manuka products used in South Africa have to be imported and therefore is costly.

To address this limitation, the aims of this study were to develop a rapid and inexpensive colorimetric method for the quantification of MGO in southern Africa honey. Then to evaluate the antibacterial and cellular effects of MGO *in vitro* and to determine whether MGO levels as found in southern Africa honey kills bacteria without causing cellular damage.

6.2 Summary of results

Existing methods for MGO quantification could not be used due to protein and polyphenol interference and cost. To overcome this problem a new colorimetric method for the quantification of MGO was developed. According to this method the MGO content of UMF 15

Manuka honey was between 557.01 and 590.28 mg/kg, similar to 514 mg/kg reported by the Unique Manuka Factor Honey Association (UMFHA 2015). The honey samples evaluated were found to contain from 692.59 – 1261.23 mg/kg MGO, as determined using the new assay, which is comparable to or higher than the MGO levels of the UMF 15 Manuka used in this study.

It was determined that MGO had antibacterial effects and the MIC in Gram positive *B. subtilis* and *P. aeruginosa* was 0.4 – 1.2 mM and for Gram negative *S. aureus* and *E. coli* was 0.8 – 1.2 mM MGO. Morphological evaluation revealed that at 1 mM MGO the formation of fimbriae and flagellae was inhibited and at 2.0 mM lysis occurred. Therefore MGO levels as found in southern Africa honey kills bacteria.

Three cell lines used in this study were exposed to 0.0003 – 324.7294 mM MGO for 48 hrs. At the MIC range that inhibited bacterial growth (from 0.4 – 1.2 mM) RAW 264.7 mouse macrophages and Caco-2 colon carcinoma cells showed signs of hormesis and the SC-1 fibroblast cell line exhibited normal growth. At a concentration > 32.4729 mM toxicity was observed.

Morphological evaluation showed no morphological changes in any of the cell lines at MIC of MGO. At a concentration of 324.7294 mM MGO the RAW 264.7 mouse macrophages showed signs of activation and differentiation similar to those observed by Saxena *et al.* (2003) when RAW 264.7 cells were exposed to LPS. The Caco-2 cells became more compacted and spheroid in shape which is associated with stem cell-like characteristics (Yan *et al.* 2013). At the highest concentration of MGO (324.7294 mM), SC-1 fibroblasts grew in whorls with few large cells amongst the others cells in cell culture, possibly due to differentiation into myofibroblasts as described by (Oguri *et al.* 2014).

6.3 Implications of this study

The implications of the first part of this study are that the honey samples from southern Africa that were evaluated contain MGO levels worthy of further development into wound healing products. The honey samples with lower MGO content can also potentially be used as a wound healing product as these low concentrations still fall within the MIC range for the bacteria evaluated and was generally not cytotoxic to the cell lines evaluated.

In this study it was found that MGO prevents the formation of flagella and fimbrae and at high concentrations cause lysis. This is important for two reasons: Bacteria require flagella and fimbrae in order to be able to migrate towards, attach to the surface and invade the host and also in order to be able to secrete virulent factors into the host (Sherlock *et al.* 2010). In

addition, the formation of a biofilm also requires bacteria to form fimbrae and flagellae. Without these structures bacteria are immobile as well as unable to attach to the surface or invade a host. Afimbriate, aflagellate bacteria are less virulent and their ability to form biofilms would also be impaired (Ragione *et al.* 2000; Ramos *et al.* 2004; Post *et al.* 2007; James *et al.* 2008).

At the MIC for MGO (0.3247 – 3.2473 mM) hormesis occurs in the Caco-2 and RAW 264.7 and normal growth in SC-1 cell lines. This would mean that MGO can potentially be used as a bactericidal agent which also stimulates cellular growth. The fact that MGO caused RAW 264.7 cells to become more like dendritic cells in appearance suggests that MGO could possibly be used to induce secondary antibacterial response by activating local immune cells in addition to its direct killing effect. SC-1 fibroblasts become more differentiated and form extensions and filopodia. According to Bartling *et al.* (2009) these structures are essential for cellular migration in wounds required for tissue repair. Differentiation into myofibroblasts assists with the contraction phase of wound healing and closure.

There is however also some concern with regards to the use of MGO containing products in diabetic patients since these patients already have an elevated MGO level in their blood (Paul and Bailey 1999; Bartling *et al.* 2009). Elevated MGO and AGE production has been associated with the formation of cross-links within the tissue structure and resultant stiffness and resistance to remodelling (Bierhaus *et al.* 1998; Singh *et al.* 2001). This loss of elasticity and build-up of sclerotic tissue has been associated with several pathological conditions and is closely associated with diabetic complications (Bierhaus *et al.* 1998; Uchida 2000; Singh *et al.* 2001; Stitt 2001). Therefore, although MGO has been found *in vitro* to promote wound healing at low concentrations caution should be taken when treating diabetic patients.

Another cause for concern is the morphological changes observed on Caco-2 cells towards a more spheroid-like form. Yan *et al.* (2013) also observed that the spheroid shaped human lung cancer cells highly express stem cell markers Oct4 and Sox2 suggesting that they have become stem cell-like. This stem cell like morphology is essential for tumour initiation, maintenance, metastasis as well as drug resistance. Since similar changes were observed in the Caco-2 colon cancer cells it may be wise to consider that exposure to MGO may also be tumerogenic at high concentrations.

In conclusion the MGO positive local honey samples may be a plausible method of treatment for stimulating wound healing as well as the prevention and eradication of bacterial infections in surface wounds with the exception of diabetic patients and patients with skin cancers as high levels of MGO may pose a possible threat to these patients.

6.4 Limitations of the study

The developed colorimetric method was not validated using a different method such as HPLC analysis. Another limitation is that MGO levels were only determined in 12 honey samples.

In bacteria MGO affects the formation of flagella and fimbrae, however it is not certain as to whether this effect is directly on the protein assembly of the fimbrae and flagella or if it is as a result of an inhibition of the metabolic pathways within the bacteria inhibiting its ability to form these extensions. No drug resistant bacteria were evaluated in this study and the findings of this study cannot be extrapolated to all bacteria.

Another limitation to this study was that mouse (RAW 264.7 and SC-1) and a human cancer cell line (Caco-2) was used. No skin associated cell lines or primary cultures were used. This means that the conclusions that were drawn does not necessary reflect all aspects of wound healing.

6.5 Future perspectives

Possible future perspectives for this study are as follows:

With regards to honey samples, the colorimetric method of MGO determination needs to be validated using a sensitive technique such as HPLC. In addition, honey samples from more regions can be screened for MGO content in order to get an indication of MGO content from different biomes in South Africa. Also, since the effectiveness of honey seems to be dependent on the overall composition of the honey and not just a single component another possible future study could be to evaluate the contribution to antibacterial activity and the promotion of wound healing of other components such as polyphenols, H_2O_2 and bee defensin.

To determine how MGO inhibits fimbriae and flagella formation, the effects MGO on associated gene expression can be determined using reverse transcription PCR. Proteomics could be used in order to determine changes in protein composition after MGO exposure and possibly changes in protein structure due to AGE formation. Biofilm formation in wounds is notoriously difficult to eradicate. It will be interesting to determine the effect of MGO on bacterial biofilm formation and associated gene expression.

The cellular effects of MGO can be further evaluated using primary skin cell cultures. Aspects such as the effect of MGO on the migration, proliferation and differentiation of fibroblasts and epithelial cells can be determined. Animal studies using pigs can also be

used to determine how different MGO concentrations or honey samples affect the healing of superficial wounds. Using a diabetic mouse or rat model the effect of superficial application of MGO to wounds on MGO blood levels can be evaluated to elucidate the risk in using MGO based wound healing products in diabetic patients.

Chapter 7: Reference list

Abdullah, M. G., Anderson, M. C., Anderson, M. J., *et al.* (2015). Bacillus subtilis. Encyclopedia Britanica, Encyclopedia Britanica Inc.

Adams, C., Manley-Harris, M. and Molan, P. (2009). The origin of methylglyoxal in New Zealand Manuka (Leptospermum scoparium) honey. *Carbohydr Res* **344**(8): doi: 10.1016/j.carres.2009.1003.1020.

Adams, C. J., Boult, C. H., Deadman, B. J., *et al.* (2008). Isolation by HPLC and characterisation of the bioactive fraction of New Zealand Manuka (*Leptospermum scoparium*) honey. *Carbohydr Res* **343**(4): 651 - 659.

Allen, K., Molan, P. and Reid, G. (1991). A survey of the antibacterial activity of some New Zealand honeys. *J. Pharm. Pharmacol* **43**(12): 817 - 822.

ATCC (2014) Caco-2 [Caco2] (ATCC® HTB-37™) (Last updated: 2014). Retrieved 10 October, 2015, from http://www.atcc.org/Products/All/HTB-37.aspx.

ATCC (2014) HT-1080 [HT1080] (ATCC® CCL-121™) (Last updated: 2014). Retrieved 13 OCtober, 2015, from http://www.atcc.org/products/all/CCL-121.aspx.

ATCC (2014) MG-63 (ATCC® CRL-1427™) (Last updated: 2014). Retrieved 13 October, 2015, from http://www.atcc.org/products/all/CRL-1427.aspx.

ATCC (2014) RAW 264.7 (ATCC® TIB-71™) (Last updated: 2014). Retrieved 10 October, 2015, from http://www.atcc.org/products/all/TIB-71.aspx.

ATCC (2014) RT4-D6P2T (ATCC® CRL-2768™) (Last updated: 2014). Retrieved 13 October, 2015, from http://www.atcc.org/products/all/CRL-2768.aspx.

ATCC (2014) SC-1 (ATCC® CRL-1404™) (Last updated: 2014). Retrieved 10 October, 2015, from http://www.atcc.org/Products/All/CRL-1404.aspx.

ATCC (2014) U-87 MG (ATCC® HTB-14™) (Last updated: 2014). Retrieved 13 October, 2015, from http://www.atcc.org/products/all/HTB-14.aspx.

Atrott, J., Haberlau, S. and Henle, T. (2012). Studies on the formation of methylglyoxal from dihydroxyacetone in Manuka (Leptospermum scoparium) honey. *Carbohydr Res* **361**(1): 7 - 11.

Bartling, B., Desole, M., Rohrbach, S., *et al.* (2009). Age-associated changes of extracellular matrix collagen impair lung cancer cell migration. *FASEB J* **23**(5): 1510 - 1520.

Bierhaus, A., Hofmann, M. A., Ziegler, R., *et al.* (1998). AGEs and their interaction with AGE-receptors in vascular disease and diabetes mellitus. I. The AGE concept. *Cardiovascular Res* **37**(3): 586 - 600.

Booth, I. R., Ferguson, G. P., Miller, S., *et al.* (2003). Bacterial production of methylglyoxal: a survival strategy or death by misadventure? *Biochem Soc Trans* **31**(6): 1406 - 1408.

Briske-Anderson, M. J., Finley, J. W. and Newman, S. M. (1997). The influence of culture time and passage number on the morphological and physiological development of Caco-2 cells. *Exp Biol Med* **214**(3): 248 - 257.

Burt, S. A., Zee, R. v. d., Koets, A. P., *et al.* (2007). Carvacrol induces heat shock protein 60 and inhibits synthesis of flagellin in Escherichia coli O157: H7. *Appl Environ Microbiol* **73**(14): 4484 - 4490.

Calabrese, E. and Baldwin, L. (2002). Defining hormesis. *Hum Exp Toxicol* **21**(2): 91 - 97.

Cantero, A., Portero-Otín, M., Ayala, V., *et al.* (2007). Methylglyoxal induces advanced glycation end product (AGEs) formation and dysfunction of PDGF receptor-beta: implications for diabetic atherosclerosis. *FASEB J* **21**(12): 3096 - 3106.

CDC (2013) Pseudomonas aeruginosa in Healthcare Settings (Last updated: 2013). Retrieved 17 September, 2015, from http://www.cdc.gov/hai/organisms/pseudomonas.html.

CDC (2014) *E.coli* (*Escherichia coli*) (Last updated: 2014). Retrieved 17 September, 2015, from http://www.cdc.gov/ecoli/general/index.html.

Cedergreen, N. (2010). Predicting hormesis in mixtures. *Integr Enviro Assess Manage* **6**(2): 310 - 311.

Chang, T., Wang, R., Olson, D. J. H., *et al.* (2011). Modification of Akt1 by methylglyoxal promotes the proliferation of vascular smooth muscle cells. *FASEB J* **25**(5): 1746 - 1757.

Chong, S., Lee, W., Arora, P., *et al.* (2007). Methylglyoxal inhibits the binding step of collagen phagocytosis. *J Biol Chem* **282**(11): 8510 - 8520.

Daglia, M., Ferrari, D., Collina, S., *et al.* (2013). Influence of in Vitro Simulated Gastroduodenal Digestion on Methylglyoxal Concentration of Manuka (Lectospermum scoparium) Honey. *J. Agric. Food Chem* **61**(9): 2140 - 2145.

deBoer, A. S. and Diderichsen, B. (1991). On the safety of Bacillus subtilis and B. amyloliquefaciens: a review. *Appl Microbiol Biotechnol* **36**(1): 1 - 4.

Emsen, I. M. (2006). A different and safe method of split thickness skin graft fixation: Medical honey application. *Burns* **33**(6): 782 - 787.

Eyer, P., Worek, F., Kiderlen, D.*, et al.* (2003). Molar absorption coefficients for the reduced Ellman reagent: reassessment. *Anal Bichem* **312**(2): 224 - 227.

Ferguson, G., Tötemeyer, S., MacLean, M.*, et al.* (1998). Methylglyoxal production in bacteria: suicide or survival? *Arch Microbiol* **170**(4): 209 - 218.

Foster, T. (1996). Staphylococcus. In: Medical Microbiology. Chapter 12. Edited by: Baron. Galveston, The University of Texas Medical Branch.

Frei, M. (2015). Cell viability and proliferation. *BioFiles* **6**(5): 17 - 21.

Gao, J. J., Zuvanich, E. G., Xue, Q.*, et al.* (1999). Cutting edge: bacterial DNA and LPS act in synergy in inducing nitric oxide production in RAW 264.7 macrophages. *J Immunol* **163**(8): 4095 - 4099.

Gu, Y., Fu, J., Lo, P.-K.*, et al.* (2011). The effect of B27 supplement on promoting in vitro propagation of Her2/neu-transformed mammary tumorspheres. *J Biotech Res* **3**: 7 - 18.

Guttenplan, S. B. and Kearns, D. B. (2013). Regulation of flagellar motility during biofilm formation. *Microbiol Rev* **37**(6): 849 - 871.

Han, Y., Randell, E., Vasdev, S.*, et al.* (2007). Plasma methylglyoxal and glyoxal are elevated and related to early membrane alteration in young, complication-free patients with Type 1 diabetes. *Mol Cell Biochem* **305**(1): 123 - 131.

Henriques, A. F., Jenkins, R. E., Burton, N. F.*, et al.* (2010). The intracellular effects of Manuka honey on Staphylococcus aureus. *Eur J Clin Microbiol Infect Dis* **29**(1): 45 - 50.

Hipkiss, A. R. (2007). Dietary restriction, glycolysis, hormesis and ageing. *Biogerontology* **8**: 221 - 224.

Irish, J., Blair, S. and Carter, D. A. (2011). The antibacterial activity of honey derived from Australian flora. *PLoS ONE* **6**(3): e18229.

Jagt, D. L. V. and Hunsaker, L. A. (2003). Methylglyoxal metabolism and diabetic complications: roles of aldose reductase, glyoxalase-I, betaine aldehyde dehydrogenase and 2-oxoaldehyde dehydrogenase. *Chem Biol Interact* **143 - 144**: 341 - 351.

James, G. A., Swogger, E., Wolcott, R.*, et al.* (2008). Biofilms in chronic wounds. *Wound Rep Reg* **16**(1): 37 - 44.

Jensen, T. M., Vistisen, D., Fleming, T., *et al.* (2015). Impact of intensive treatment on serum methylglyoxal levels among individuals with screen-detected type 2 diabetes: the ADDITION-Denmark study. . *Acta Diabetol* **52**(5): 929 - 936.

Jervis-Bardy, J. and Tan, L. (2011). Methylglyoxal-infused honey mimics the anti-Staphylococcus aureus biofilm activity of Manuka honey: Potential Implication in Chronic Rhinosinusitis. *Laryngoscope* **121**(5): 1104 - 1107.

Ji, L. L., Gomez-Cabrera, M.-C. and Vina, J. (2006). Exercise and hormesis. *Ann NY Acad Sci* **1067**(1): 425 - 435.

Jia, X., Chang, T., Wilson, T. W., *et al.* (2012). Methylglyoxal mediates adipocyte proliferation by Increasing phosphorylation of Akt1. *PLoSOne* **7**(5): e0036610.

Jia, X., Olson, D. J. H., Ross, A. R. S., *et al.* (2006). Structural and functional changes in human insulin induced by methylglyoxal. *The FASEB Journal* **20**(9): 1555 - 1557.

Kilty, S., Duval, M., Chan, F., *et al.* (2011). Methylglyoxal: (active agent of Manuka honey) in vitro activity against bacterial biofilms. *Int Forum Allergy Rhinol* **1**(5): 348 - 350.

Kim, J., Son, J.-W., Lee, J.-A., *et al.* (2004). Methylglyoxal induces apoptosis mediated by reactive oxygen species in bovine retinal pericytes. *J Korean Med Sci* **19**(7): 95 - 100.

Klemm, P. (1985). Fimbrial Adhesins of *Escherichia coli*. *Rev Infect Dis* **7**(8): 321 - 340.

Kouda, K. and Iki, M. (2010). Beneficial effects of mild stress (hormetic effects): Dietary restriction and health. *J Phys Anthropol* **29**(4): 127 - 132.

Kwakman, P., Velde, A. t., Boer, L. d., *et al.* (2010). How honey kills bacteria. *FASEB J* **24**(7): 2575 - 2582.

Lee, D. K., Jang, S., Kim, M. J., *et al.* (2008). Anti-proliferative effects of Bifidobacterium adolescentis SPM0212 extract on human colon cancer cell lines. *BMC Cancer* **8**(310): doi:10.1186/1471-2407-1188-1310.

Lee, H. K., Seo, I. A., Suh, D. J., *et al.* (2009). A novel mechanism of methyglyoxal cytotoxicity in neuroglial cells. *J Neurochem* **108**(1): 273 - 284.

Li, X., Xu, Y., Chen, Y., *et al.* (2013). SOX2 promotes tumor metastasis by stimulating epithelial-to-mesenchymal transition via regulation of WNT/b-catenin signal network. *Cancer Lett* **336**(2): 379 - 389.

Lister, P. D., Wolter, D. J. and Hanson, N. D. (2009). Antibacterial-resistant pseudomonas aeruginosa: Clinical impact and complex regulation of chromosomally encoded resistance mechanisms. *Clin. Microbiol. Rev* **22**(4): 582 - 610.

Lo, T., Westwood, M., McLellan, A.*, et al.* (1994). Binding and modification of proteins by methylglyoxal under physiological conditions. A kinetic and mechanistic study with N alpha-acetylarginine, N alpha-acetylcysteine, and N alpha-acetyllysine, and bovine serum albumin. *J Biol Chem* **269**(51): 32299 - 32305.

Majtan, J. (2011). Methylglyoxal - A potential risk factor of Manuka honey in healing of diabetic ulcers. *Evid Based Complement Alternat Med* **2011**: doi:10.1093/ecam/neq1013.

Mandal, A. (2012) What is Staphylococcus Aureus? (Last updated: 2012). Retrieved 17 September, 2015, from http://www.news-medical.net/health/What-is-Staphylococcus-Aureus.aspx.

Mangram, A. J., Horan, T. C., Pearson, M. L.*, et al.* (1999). Guideline for prevention of surgical site infection. *Am J Infect Control* **27**(2): 97 - 134.

Masip, L., Veeravalli, K. and Georgiou, G. (2006). The many faces of glutathione in bacteria. *Antioxid Redox Signal* **8**(5 - 6): 753 - 762.

Mattson, M. P. (2008). Hormesis defined. *Ageing Research Reviews* **7**(1): 1 - 7.

Mavric, E., Wittmann, S., Barth, G.*, et al.* (2008). Identification and quantification of methylglyoxal as the dominant antibacterial constituent of Manuka (*Leptospermum scoparium*) honeys from New Zealand. *Mol Nutr Food Res* **52**(4): 483 - 489.

Münch, G., Thome, J., Foley, P.*, et al.* (1997). Advanced glycation endproducts in ageing and Alzheimer's disease. *Brain Res Rev* **23**(1-2): 134 - 143.

Nakajima, Y., KanaeMukai, Nasruddin*, et al.* (2013). Evaluation of the effects of honey on acute-phase deep burn wounds. *Evid Based Complement Alternat Med* **2013**: doi: 10.1155/2013/784959.

Nekrassova, O., White, P., Threlfell, S.*, et al.* (2002). An electrochemical adaptation of Ellman's test. *Analyst* **127**(6): 797 - 802.

Niu, T., Miao, M., Dong, W.*, et al.* (2012). Effects of advanced glycation end products and its receptor on oxidative stress in diabetic wounds. *CJB* **28**(1): 32 - 35.

Nomi, Y., Aizawa, H., Kurata, T.*, et al.* (2009). Glutathione reacts with glyoxal at the N-terminal. *Biosci Biotechnol Biochem* **73**(11): 2408 - 2411.

NZ-ManukaNatural (2015) What is UMF? (Last updated: 2015). *The UMF® Quality Trademark*. Retrieved 23 October, 2015, from http://www.nzmanukanatural.com/what-is-umf.

Oguri, G., Nakajima, T., Yamamoto, Y.*, et al.* (2014). Effects of methylglyoxal on human cardiac fibroblast: roles of transient receptor potential ankyrin 1 (TRPA1) channels. *Am J Physiol* **307**(9): 1339 - 1352.

Ota, K., Nakamura, J., Li, W.*, et al.* (2007). Metformin prevents methylglyoxal-induced apoptosis of mouse Schwann cells. *Biochem Biophys Res Commun* **357**(1): 270 - 275.

Pankey, G. and Sabath, L. (2003). Clinical relevance of bacteriostatic versus bactericidal mechanisms of action in the treatment of gram-positive bacterial infections. *Clin Infect Dis* **38**(6): 864 - 870.

Paul, R. G. and Bailey, A. J. (1999). The effect of advanced glycation end-product formation upon cell-matrix interactions. *Int J Biochem Cell Biol* **31**(6): 653 - 660.

Pavlovic-Djuranovica, S., Kunb, J. F. J., Schultza, J. E.*, et al.* (2006). Dihydroxyacetone and methylglyoxal as permeants of the Plasmodium aquaglyceroporin inhibit parasite proliferation. *Biochim. Biophys. Acta* **1758**(8): 1012 - 1017.

Phillips, S. and Thornalley, P. (1993). The formation of methylglyoxal from triose phosphates. Investigation using a specific assay for methylglyoxal. *Eur J Biochem* **212**(1): 101 - 105.

Pieper (2009). Honey-based dressings and wound care. *J Wound Ostomy Continence Nurs* **36**(1): 60 - 66.

Pietrangelo, A. (2012) *E. coli* Infection (Last updated: 2012). Retrieved 17 September, 2015, from http://www.healthline.com/health/e-coli-infection#Overview1.

Post, J., Hiller, N., Nistico, L.*, et al.* (2007). The role of biofilms in otolaryngologic infections: update 2007. *Curr Opin Otolaryngol Head Neck Surg* **15**(5): 347 - 351.

Rachman, H., Kim, N., Ulrichs, T.*, et al.* (2006). Critical role of methylglyoxal and AGE in mycobacteria-induced macrophage apoptosis and activation. *PLoS ONE* **1**(1): DOI: 10.1371/journal.pone.0000029.

Ragione, R. M. L., Sayers, A. R. and Woodward, M. J. (2000). The role of fimbriae and flagella in the colonization, invasion and persistence of *Escherichia coli* O78:K80 in the day-old-chick model. . *Epidemiol Infect* **124**(3): 351 - 363.

Ramos, H. C., Rumbo, M. and Sirard, J.-C. (2004). Bacterial flagellins: mediators of pathogenicity and host immune responses in mucosa. *Trends Microbiol* **12**(11): 509 - 517.

Ranzato, E., Martinotti, S. and Burlando, B. (2012). Epithelial mesenchymal transition traits in honey-driven keratinocyte wound healing: Comparison among different honeys. *Wound Repair Regen* **20**(5): 778 - 785.

Roberts, A. E. L., Maddocks, S. E. and Cooper, R. A. (2014). Manuka honey reduces the motility of Pseudomonas aeruginosa by suppression of flagella-associated genes. *J Antimicrob Chemother* **70**(3): 716 - 725.

Rosca, M. G., Mustata, T. G., Kinter, M. T.*, et al.* (2005). Glycation of mitochondrial proteins from diabetic rat kidney is associated with excess superoxide formation. *Am J Physiol Renal Physiol* **289**(2): F420 - F430.

Rossiter, K., Cooper, A., Voegeli, D.*, et al.* (2010). Honey promotes angiogeneic activity in the rat aortic ring assay. *J Wound Care* **19**(10): 442 - 446.

Rubin, R. H. (1993). Fungal and bacterial infections in the immunocompromised host. *Eur J Clin Mierobi Infect Dis* **12**(1): 42 - 48.

Russell, K., Molan, P., Wilkins, A.*, et al.* (1990). Identification of some antibacterial constituents of New Zealand Manuka honey. *J Agric Food Chem* **38**(1): 10 - 13.

Sasaki, N., Fukatsu, R., Tsuzuki, K.*, et al.* (1998). Advanced glycation end products in Alzheimer's disease and other neurodegenerative diseases. *Am J Pathol* **153**(4): 1149 - 1155.

Sassi-Gaha, S., Loughlin, D. T., Kappler, F.*, et al.* (2010). Two dicarbonyl compounds, 3-deoxyglucosone and methylglyoxal, differentially modulate dermal fibroblasts. *Matrix Biol* **29**(2): 127 - 134.

Saxena, R. K., Vallyathan, V. and Lewis, D. M. (2003). Evidence for lipopolysaccharide induced differentiation of RAW264. 7 murine macrophage cell line into dendritic like cells. *J Biosci* **28**(1): 129 - 134.

Schalkwijk, C. G. (2015). Vascular AGE-ing by methylglyoxal: the past, the present and the future. *Diabetologia* **58**(8): 1715 - 1719.

Schmid, F.-X. (2001). Biological macromolecules: UV-visible spectrophotometry. *Encyclopedia of life sciences*: DOI: 10.1038/npg.els.0003142.

Schwentker, A., Vodovotz, Y., Weller, R.*, et al.* (2001). Nitric oxide and wound repair: role of cytokines? *Nitric Oxide* **7**(1): 1 - 10.

Serem, J. and Bester, M. J. (2012). Physicochemical properties, antioxidant activity and cellular protective effects of honeys from southern Africa. *Food Chem* **133**(4): 1544 - 1550.

Sheader, E. A., Benson, R. S. P. and Best, L. (2001). Cytotoxic action of methylglyoxal on insulin-secreting cells. *Biochem Pharmacol* **61**(11): 1381 - 1386.

Shekhter, A. B., Serezhenkov, V. A., Rudenko, T. G., *et al.* (2005). Beneficial effect of gaseous nitric oxide on the healing of skin wounds. *Nitric Oxide* **12**(4): 210 - 219.

Sherlock, O., Dolan, A., Athman, R., *et al.* (2010). Comparison of the antimicrobial activity of Ulmo honey from Chile and Manuka honey against methicillin-resistant *Staphylococcus aureus*, *Escherichia coli* and *Pseudomonas aeruginosa*. *BMC Complement Altern Med* **10**(47): doi: 10.1186/1472-6882-1110-1147.

Singh, R., Barden, A., Mori, T., *et al.* (2001). Advanced glycation end-products: a review. *Diabetologia* **2**(129 - 146).

Smith, M. A., Taneda, S., Richey, P. L., *et al.* (1994). Advanced Maillard reaction end products are associated with Alzheimer disease pathology. *Neurobiology* **91**(12): 5710 - 5714.

Smitha, I. K., Vierhellera, T. L. and Thorne, C. A. (1988). Assay of glutathione reductase in crude tissue homogenates using 5,5′-dithiobis(2-nitrobenzoic acid) *Anal Bichem* **175**(2): 408 - 413.

Song, Z., Wang, R., Yu, D., *et al.* (2008). Impact of advanced glycosylation end products-modified human serum albumin on migration of epidermal keratinocytes: an in vitro experiment. *Natl Med J Chin* **88**(38): 2690 - 2694.

Stewart, J. A., McGrane, O. L. and Wedmore, I. S. (2014). Wound care in the wilderness: Is there evidence for honey? *Wilderness Environ Med* **25**(1): 103 - 110.

Stitt, A. W. (2001). Advanced glycation: an important pathological event in diabetic and age related ocular disease. *Br J Ophthalmol* **85**(6): 746 - 753.

Sukedo, N., Clugstone, S. L., Daub, E., *et al.* (2004). Distinct classes of glyoxalase I: metal specificity of the Yersinia pestis, Pseudomonas aeruginosa and Neisseria meningitidis enzymes. *Biochem J.* **15**(384): 111 - 117.

Suzuki, K., Koh, Y. H., Mizuno, H., *et al.* (1997). Overexpression of aldehyde reductase protects PC12 cells from the cytotoxicity of methylglyoxal or 3-deoxyglucosone. *J. Biochem* **123**(2): 353 - 357.

Talukdar, D., Chaudhuri, B. S., Ray, M., *et al.* (2009). Critical evaluation of toxic versus beneficial effects of methylglyoxal. *Biochemistry* **74**(10): 1059 - 1069.

Tam, N. K. M., Uyen, N. Q., Hong, H. A., *et al.* (2006). The intestinal life cycle of Bacillus subtilis and close relatives. *J Bacteriol* **188**(7): 2692 - 2700.

Tanji, N., Markowitz, G. S., Fu, C., *et al.* (2000). Expression of advanced glycation end products and their cellular receptor RAGE in diabetic nephropathy and nondiabetic renal disease. *JASN* **11**(9): 1656 - 1666.

Thornalley, P. J. (1996). Pharmacology of methylglyoxal: formation, modification of proteins and nucleic acids, and enzymatic detoxification-A role in pathogenesis and antiproliferative chemotherapy. *Gen Pharmacol* **27**(4): 565 - 573.

Todar, K. (2008) Pseudomonas aeruginosa (Last updated: 2008). Retrieved Septernber 17, 2015, from http://textbookofbacteriology.net/pseudomonas.html.

Tötemeyer, S., Booth, N., Nichols, W., *et al.* (1998). From famine to feast: the role of methylglyoxal production in Escherichia coli. *Mol Microbiol* **27**(3): 553 - 562.

Uchida, K. (2000). Role of reactive aldehyde in cardiovascular diseases. *Free Radical Bio Med* **28**(12): 1685 - 1696.

UMFHA (2015) Unique Manuka Factor Honey Association (Last updated: 2015). *Grading System*. Retrieved 02 September, 2015, from http://www.umf.org.nz/grading-system.

Vaca, C. E., Nilsson, J. A., Fang, J.-L., *et al.* (1997). Formation of DNA adducts in human buccal epithelial cells exposed to acetaldehyde and methylglyoxal in vitro. *Chem Biol Interact* **108**(3): 197 - 208.

Velnar, T., Bailey, T. and Smrkolj, V. (2009). The wound healing process: an overview of the cellular and molecular mechanisms. *J Int Med Res* **37**(5): 1528 - 1542.

Verzijl, N., DeGroot, J., Zaken, C. B., *et al.* (2002). Crosslinking by advanced glycation end products increases the stiffness of the collagen network in human articular cartilage: A possible mechanism through which age is a risk factor for osteoarthritis. *Arthritis Rheum* **46**(1): 114 - 123.

Wahdan, H. (1998). Causes of the antimicrobial activity of honey. *Infection* **26**(1): 26 - 31.

Wang, Y. and Ho, C.-T. (2012). Flavour chemistry of methylglyoxal and glyoxal. *Chem Soc Rev* **41**(11): 4140 - 4149.

Weigel, K. U., Opitz, T. and Henle, T. (2004). Studies on the occurrence and formation of 1,2-dicarbonyls in honey. *Eur Food Res Technol* **218**(2): 147 - 151.

Wild, R., Ooi, L., Srikanth, V.*, et al.* (2012). A quick, convenient and economical method for the reliable determination of methylglyoxal in millimolar concentrations: the N-acetyl-l-cysteine assay. *Anal Bioanal Chem* **403**(9): 2577 - 2581.

Yadav, S., Singla-Pareek, S., Ray, M.*, et al.* (2005). Methylglyoxal levels in plants under salinity stress are dependent on glyoxalase I and glutathione. *Biochem Biophys Res Commun* **337**(1): 61 - 67.

Yan, X., Lou, H., Zhou, X.*, et al.* (2013). Identification of CD90 as a marker for lung cancer stem cells in A549 and H446 cell lines *Oncol Rep* **30**(6): 2733 - 2740.

Yuen, A., Laschinger, C., Talior, I.*, et al.* (2010). Methylglyoxal-modified collagen promotes myofibroblast differentiation. *Matrix Biol* **29**(6): 537 - 548.